

***Enhancing the oxygen supply  
to whole-cell oxygenase  
bioconversions***

Sarah Fish

A thesis submitted for the degree of  
Doctor of Engineering  
to  
University of London

May 2006

Department of Biochemical Engineering  
University College London  
Torrington Place  
London  
WC1E 7JE

UMI Number: U592773

All rights reserved

INFORMATION TO ALL USERS

The quality of this reproduction is dependent upon the quality of the copy submitted.

In the unlikely event that the author did not send a complete manuscript and there are missing pages, these will be noted. Also, if material had to be removed, a note will indicate the deletion.



UMI U592773

Published by ProQuest LLC 2013. Copyright in the Dissertation held by the Author.  
Microform Edition © ProQuest LLC.

All rights reserved. This work is protected against  
unauthorized copying under Title 17, United States Code.



ProQuest LLC  
789 East Eisenhower Parkway  
P.O. Box 1346  
Ann Arbor, MI 48106-1346

## **Acknowledgements**

I would like to thank my supervisor John Woodley and advisor Gary Lye for their help and advice throughout the project.

Thanks to Ian and Billy for all their assistance and patience in the pilot plant.

Thanks to everyone who has helped me in or out of the lab, especially: Pedro, Helen, Jean, Heckarl, Clive, and Jerry.

Special thanks to Tina, Claudia and Alfred for their friendship and support.

This thesis is dedicated to my parents for all their love and support.

## Abstract

The aim of this work was to investigate the effect of oxygen limitation on whole-cell oxygenases, and to determine how the physiochemical properties of oils affect their ability to enhance the oxygen transfer rate. Whole-cell oxygenase biocatalysts require oxygen as a substrate for the reaction and for the electron transport chain. The productivity of these bioconversions is therefore influenced by the maximum oxygen transfer rate of the fermenter. Organic solvents are commonly used in oxygenase bioconversions to alleviate substrate or product limitation, and they can also increase the oxygen transfer rate to the aqueous phase.

The model system was the bioconversion of bicycloheptenone to oxabicyclooctenone using a recombinant *E.coli* biocatalyst overexpressing cyclohexanone monooxygenase (CHMO). Above a critical biomass concentration the oxygen transfer rate determined the maximum activity. When oxygen was not limited, the electron transport chain used twice as much oxygen as the CHMO. When it was limited, the CHMO and the electron transport chain competed for the oxygen - the CHMO used approximately 20% whatever the severity of the limitation.

The oxygen transfer rate to the aqueous phase increased up to 2.5 fold depending on the physical properties and the volume fraction of the oil phase. The oxygen transfer rate only increased if the oil drops were small enough - the magnitude was determined by the oxygen solubility of the oil. There was no correlation between the spreading coefficient and the oxygen transfer rate. A model that predicted the enhancement in the oxygen transfer rate caused by the addition of oil was in good agreement with the experimental results. The specific activity of an oxygen limited CHMO bioconversion was increased up to 2.25 fold using perfluorotributylamine.

# Contents

Section		Page
	<b>Acknowledgements</b>	<b>2</b>
	<b>Abstract</b>	<b>3</b>
	<b>Contents</b>	<b>4</b>
	<b>List of Tables</b>	<b>10</b>
	<b>List of Figures</b>	<b>11</b>
	<b>Abbreviations</b>	<b>14</b>
	<b>Nomenclature</b>	<b>15</b>
<b>1.0</b>	<b>Introduction</b>	<b>17</b>
<b>1.1</b>	<b>Biocatalysis</b>	<b>17</b>
<b>1.2</b>	<b>Oxygenases</b>	<b>17</b>
1.2.1	Description of the oxygenases	17
1.2.2	Oxygen consumption by whole-cell oxygenases	18
1.2.2.1	NADH production	18
1.2.2.2	NADPH production	18
1.2.2.3	Oxygen limitation in <i>E.coli</i>	20
1.2.2.4	Cofactor recycling in oxygenase processes	21
1.2.3	Industrial potential of oxygenases	21
1.2.4	Process development of oxygenase processes	21
1.2.4.1	Biological techniques	22
1.2.4.2	Processing techniques	22
1.2.4.3	Two liquid-phase bioconversions	23
1.2.5	Process examples from industry	24
<b>1.3</b>	<b>Baeyer – Villiger monooxygenases (BVMOs)</b>	<b>26</b>
1.3.1	Baeyer – Villiger reaction	26
1.3.1.1	Advantages of BVMOs	26
1.3.2	Cyclohexanone monooxygenase (CHMO)	27
1.3.2.1	Development of a CHMO biocatalyst	27
1.3.2.1.1	Biocatalyst type	28
1.3.2.1.2	Substrate and product inhibition	28

1.3.2.1.3	Oxygen limitation	29
<b>1.4</b>	<b>Oxygen Supply</b>	<b>30</b>
1.4.1	Oxygen transfer in stirred tank reactors	30
1.4.2	Mass transfer and diffusion theory	31
1.4.2.1	Two-film theory	31
1.4.2.2	Gas – liquid mass transfer	32
1.4.3	Methods to increase the oxygen transfer rate	33
1.4.3.1	Impeller speed	33
1.4.3.2	Air flow rate	34
1.4.3.3	Partial pressure	34
1.4.3.4	Water – immiscible liquids	35
<b>1.5</b>	<b>Water – immiscible liquids</b>	<b>35</b>
1.5.1	Background	35
1.5.2	Mechanism of gas mass transfer enhancement	35
1.5.2.1	Effect on the mass transfer coefficient ( $k_L$ )	37
1.5.2.2	Effect of oil on the gas-liquid interfacial area ( $a$ )	37
1.5.2.3	Effect of the oils on the driving force ( $C^*$ )	37
1.5.2.3.1	Bubble mechanism	38
1.5.2.3.2	Shuttle mechanism	40
1.5.3	Models	41
1.5.3.1	Description of homogenous model for the shuttle mechanism	43
<b>1.6</b>	<b>Project Objectives</b>	<b>46</b>
<b>2.0</b>	<b>Materials and Methods</b>	<b>48</b>
<b>2.1</b>	<b>Materials</b>	<b>48</b>
2.1.1	Chemicals	48
2.1.2	Microorganism	48
<b>2.2</b>	<b>Analytical techniques</b>	<b>48</b>
2.2.1	Substrate and product quantification by gas chromatography (GC)	48
2.2.1.1	Preparation of samples	48
2.2.1.2	Quantification by gas chromatography	48

2.2.1.2.1	Cyclohexanone and caprolactone	49
2.2.1.2.2	Bicycloheptenone	49
2.2.1.3	Quantification of the GC response	49
2.2.2	Biomass concentration	49
2.2.2.1	Dry cell weight (dcw) measurement	49
2.2.2.2	Optical density (OD) measurement	49
2.2.3	Intracellular CHMO activity	50
2.2.4	Glycerol assay	50
2.2.5	Exit – gas measurement	51
<b>2.3</b>	<b>Routine cultivation and storage of <i>E.coli</i></b>	<b>51</b>
<b>2.4</b>	<b>Fermentations</b>	<b>51</b>
2.4.1	Growth media	51
2.4.2	Inoculum preparation	52
2.4.3	Shake flask fermentations	52
2.4.4	7l fermentations	52
2.4.4.1	Fermentation equipment	52
2.4.4.2	Fermentation operation	53
<b>2.5</b>	<b>Shake flask bioconversions</b>	<b>53</b>
2.5.1	Whole-cell activity assay	53
2.5.1.1	Effect of substrate and product concentration on the activity.	53
2.5.1.1.1	Cyclohexanone and $\epsilon$ - caprolactone	53
2.5.1.1.2	Bicycloheptenone and oxabicyclooctenone	54
<b>2.6</b>	<b>2l fermenter bioconversions</b>	<b>54</b>
2.6.1	Description of the 2l fermenter	54
2.6.2	Bioconversion procedure	55
<b>2.7</b>	<b>Determination of the critical oxygen concentration</b>	<b>55</b>
<b>2.8</b>	<b>Effect of the oils on the OUR</b>	<b>56</b>
<b>2.9</b>	<b>Physical properties of oils</b>	<b>57</b>
2.9.1	Density	57
2.9.2	Surface and interfacial tensions	57
2.9.3	Spreading coefficients	58

2.9.4	Viscosity	58
2.9.4.1	Viscosity measurements	58
2.9.4.2	Average viscosity	59
2.9.5	Oxygen solubility	60
2.9.5.1	Average oxygen concentration	60
2.9.5.2	Oxygen diffusivity	60
2.9.5.3	Oxygen permeability	61
<b>2.10</b>	<b>Power - input</b>	<b>61</b>
<b>2.11</b>	<b>Sauter mean droplet diameter</b>	<b>61</b>
<b>2.12</b>	<b>Volumetric mass transfer coefficient (<math>k_{La}</math>)</b>	<b>62</b>
2.12.1	$k_{La}$ measurement	62
2.12.2	Data analysis	62
<b>2.13</b>	<b>2l fermenter bioconversions with FC-40</b>	<b>64</b>
2.13.1	Experiment design	64
2.13.2	Bioconversion procedure	64
<b>2.14</b>	<b>Solubility and partition coefficients</b>	<b>65</b>
2.14.1	Solubility in FC-40	65
2.14.2	Partition coefficients between phosphate buffer and ethyl acetate	65
<b>3.0</b>	<b>Production of the <i>E.coli</i> biocatalyst and characterisation of the bioconversion kinetics</b>	<b>67</b>
<b>3.1</b>	<b>Introduction</b>	<b>67</b>
<b>3.2</b>	<b>Results and Discussion</b>	<b>68</b>
3.2.1	Production of the <i>E.coli</i> biocatalyst in shake flasks	68
3.2.2	Production of <i>E.coli</i> biocatalyst in a 7l fermenter	69
3.2.3	Bioconversions	69
3.2.3.1	Whole-cell activity	69
3.2.3.2	Stability of the biocatalyst	70
3.2.3.3	Substrate and product inhibition	76
<b>3.3</b>	<b>Conclusions</b>	<b>79</b>



<b>4.0</b>	<b>Oxygen consumption of the biocatalyst</b>	<b>81</b>
<b>4.1</b>	<b>Introduction</b>	<b>81</b>
<b>4.2</b>	<b>Results and Discussion</b>	<b>82</b>
4.2.1	2l fermenter bioconversions	82
4.2.1.1	Bioconversions at 700 rpm	82
4.2.1.2	Bioconversions at 900 rpm	82
4.2.2	Oxygen consumption during the bioconversions	87
4.2.3	NADPH production	92
4.2.4	Implications for whole-cell oxygenase processes	93
<b>4.3</b>	<b>Conclusions</b>	<b>96</b>
<b>5.0</b>	<b>Enhancement of the oxygen transfer rate by the addition of the oils</b>	<b>97</b>
<b>5.1</b>	<b>Introduction</b>	<b>97</b>
<b>5.2</b>	<b>Results and Discussion</b>	<b>98</b>
5.2.1	Selection of oils	98
5.2.2	Experiment design	99
5.2.3	Effect of the oils on the oxygen uptake rate	100
5.2.3.1	Effect of the oils on the $k_{L}a$	103
5.2.3.1.1	Effect of the viscosity on the $k_{L}a$	109
5.2.3.2	Effect of the oils on the saturation concentration $C^*$	110
5.2.3.2.1	Spreading coefficient	110
5.2.3.2.2	Oxygen solubility	111
5.2.3.2.3	Viscosity	111
5.2.3.2.4	Diffusivity and permeability	111
5.2.3.2.5	Drop size	112
5.2.3.2.6	Impeller speed	115
5.2.4	Assessment of $E_{shuttle}$ model	117
5.2.5	Implications for whole-cell oxygenase processes	124
<b>5.3</b>	<b>Conclusions</b>	<b>126</b>

<b>6.0</b>	<b>Enhancement of oxygen transfer rate of whole-cell bioconversions</b>	<b>127</b>
<b>6.1</b>	<b>Introduction</b>	<b>127</b>
<b>6.2</b>	<b>Results and Discussion</b>	<b>128</b>
6.2.1	Outline of experiments	128
6.2.2	Bioconversions with FC-40	128
6.2.3	Comparison of experimental and predicted results	131
6.2.4	Application to whole-cell bioconversions	133
<b>6.3</b>	<b>Conclusions</b>	<b>135</b>
<b>7.0</b>	<b>Discussion and Conclusions</b>	<b>136</b>
<b>7.1</b>	<b>Discussion</b>	<b>136</b>
<b>7.2</b>	<b>Conclusions</b>	<b>138</b>
<b>7.3</b>	<b>Future Work</b>	<b>139</b>
<b>8.0</b>	<b>References</b>	<b>141</b>
<b>Appendix 1</b>	<b>Calibration curves</b>	<b>162</b>
<b>Appendix 2</b>	<b>Glycerol concentration</b>	<b>164</b>
<b>Appendix 3</b>	<b>Eng.D. requirements: business</b>	<b>166</b>
<b>Appendix 4</b>	<b>Eng.D. requirements: validation</b>	<b>167</b>

## List of Tables

- Table 1.1. Typical characteristics of oxygenases that limit their industrial application.
- Table 1.2. Examples of industrial oxygenase bioconversions and the techniques used during their process development.
- Table 1.3. Constraints that influence the design of CHMO processes.
- Table 1.4. Properties that influence the oxygen transfer rate.
- Table 1.5. Examples of oils used in biological systems to enhance the oxygen transfer rate.
- Table 2.1. Composition of growth media used in all fermentations.
- Table 2.2. Volume of oil added at each volume fraction.
- Table 2.3. Composition of the fermenter during bioconversions with FC-40.
- Table 5.1. The oxygen solubility and viscosity of the oils.
- Table 5.2. Average oxygen solubility of the dispersions.
- Table 5.3. Average viscosity of the dispersions at each volume fraction.
- Table 5.4. Spreading coefficients of the oils with different aqueous phases.
- Table 5.5. The oxygen solubility, diffusivity and permeability of the oils.

## List of Figures

- Figure 1.1. Generic reaction scheme for cofactor dependent oxygenases.
- Figure 1.2. NAD(P)H regeneration in glycolysis, TCA cycle, oxidative phosphorylation and the pentose phosphate pathway.
- Figure 1.3. Routes for glucose catabolism by *E.coli* under different oxygen concentrations (From Uden, 1994).
- Figure 1.4. Baeyer-Villiger reactions of aliphatic and cyclic ketone substrates.
- Figure 1.5. Oxygen transfer from inside an air bubble to inside a cell.
- Figure 1.6. Schematic of two-film theory.
- Figure 1.7. Schematic of the bubble covering mechanism
- Figure 1.8. Schematic of the shuttle mechanism
- Figure 1.9. Schematic of concentration gradient at the gas – liquid interface with time according to the shuttle model of Bruining *et al.* (1986).
- Figure 3.1. Reaction schemes for the two substrates. A. cyclohexanone. B. bicycloheptenone.
- Figure 3.2. The growth kinetics and intracellular CHMO activity of *E.coli* during growth in 1l shake flasks.
- Figure 3.3. The biomass concentration, glycerol concentration, and specific intracellular CHMO activity during the growth of *E.coli* in a 7l fermenter.
- Figure 3.4. Exit-gas and DOT during a 7l fermentation.
- Figure 3.5. Reaction profiles during the bioconversion of A cyclohexanone and B bicycloheptenone to their respective products.
- Figure 3.6. Stability of the whole-cell biocatalyst stored at 4°C after harvest.
- Figure 3.7. The effect of the initial cyclohexanone and  $\epsilon$  – caprolactone concentration on the specific activity.
- Figure 3.8. The effect of the initial bicycloheptenone and its lactone products on the specific activity.
- Figure 4.1. Reaction profile during the bioconversion of bicycloheptenone to its oxabicyclooctenone in a 2l fermenter.
- Figure 4.2. OUR and CER profiles corresponding to the bioconversion in Figure 4.1.

- Figure 4.3. The effect of biomass concentration on the activity and OUR during bioconversions in 2l fermenter with an impeller speed of 700 rpm.
- Figure 4.4. The effect of biomass concentration on the activity and OUR during bioconversions in 2l fermenter with an impeller speed of 900 rpm.
- Figure 4.5. The effect of biomass concentration on the OUR and CER of biocatalyst during bioconversions in a 2l fermenter at 700 rpm.
- Figure 4.6. The effect of biomass concentration on the OUR and CER of biocatalyst during bioconversions in a 2l fermenter at 900 rpm.
- Figure 4.7. The effect of the DOT on the specific OUR of the biocatalyst.
- Figure 4.8. The effect of the specific OUR of the biocatalyst during the bioconversion on the specific activity.
- Figure 5.1. The effect of an oil on the OUR of the biocatalyst.
- Figure 5.2. The effect of the oil volume fraction on the OUR enhancement factors ( $E_{OUR}$ ) on a total volume basis.
- Figure 5.3. The effect of the oil volume fraction on the  $k_{La}$  enhancement factors ( $E_{kLa}$ ).
- Figure 5.4. Predicted Sauter mean diameters of the oils at 700 rpm and 1vvm.
- Figure 5.5. The effect of the 5cS and 50cS silicone oil volume fraction on the OUR enhancement factors ( $E_{OUR}$ ) on a total volume basis.
- Figure 5.6. Percentage difference between experimental and  $E_{shuttle}$  model predicted OUR enhancement factors ( $E_{OUR}$ ) at different volume fractions.
- Figure 5.7. Percentage difference between experimental and  $E_{shuttle}$  model predicted enhancement factors ( $E_{OUR}$ ) at different volume fractions.
- Figure 5.8. The effect of the oil volume fraction OUR enhancement factors ( $E_{OUR}$ ) on an aqueous phase basis.
- Figure 6.1. Reaction profile for bioconversion using FC-40 at a volume fraction of 0.05 in a 2 l fermenter.
- Figure 6.2. The effect of FC-40 volume fraction on the specific activity and OUR during bioconversions carried out in a 2l fermenter.

- Figure 6.3. Comparison of experimental and predicted OUR enhancement factors ( $E_{OUR}$ ) for 2l bioconversions on an aqueous phase basis.
- Figure 6.4. The effect of the oil volume fraction on the OUR (aqueous phases basis) – predicted and experimental.
- Figure A.1. Calibration curves for substrates and products. A – cyclohexanone and caprolactone. B. Bicycloheptenone and oxabicyclooctenone.
- Figure A.2. Calibration curve correlating the optical density with the dry cell weight.
- Figure A.3. The effect of glycerol concentration on the specific activity of the biocatalyst in a 1 l shake flask.
- Figure A.4. The effect of the glycerol concentration on the OUR of  $1g_{dcw} l^{-1}$  of the biocatalyst in a 2l fermenter.

## Abbreviations

ATP	adenosine triphosphate
BSA	bovine serum albumin
BVMO	Baeyer-Villiger monooxygenase
CHMO	cyclohexanone monooxygenase
dcw	dry cell weight
DOT	dissolved oxygen tension
FAD	flavine adenine dinucleotide
FID	flame ionisation detector
GC	gas chromatography
IPTG	isopropyl $\beta$ -D-thiogalacto pyranoside
ISPR	<i>in-situ</i> product removal
m	solubility ratio
NAD	nicotinamide adenine dinucleotide (oxidised)
NADH	nicotinamide adenine dinucleotide (reduced)
NADP	nicotinamide adenine dinucleotide phosphate (oxidised)
NADPH	nicotinamide adenine dinucleotide phosphate (reduced)
NIR	near infrared spectroscopy
PPG	polypropylene glycol
rpm	revolutions per minute
RQ	respiratory quotient
STR	stirred tank reactor
TCA	tricarboxylic acid
Tris	Tris-(hydroxymethyl) aminomethane

## Nomenclature

a	gas – liquid interfacial area ( $\text{m}^{-1}$ )
C	oxygen concentration ( $\text{mmol l}^{-1}$ )
C*	saturation concentration of oxygen ( $\text{mmol l}^{-1}$ )
C* <sub>oil</sub>	saturation concentration of the oil ( $\text{mmol l}^{-1}$ )
C <sub>ave</sub>	average oxygen concentration ( $\text{mmol l}^{-1}$ )
C <sub>e</sub>	electrode oxygen concentration ( $\text{mmol l}^{-1}$ )
C <sub>L</sub>	normalised oxygen concentration ( $\text{mmol l}^{-1}$ )
CER	carbon dioxide evolution rate ( $\text{mmol l}^{-1}\text{hr}^{-1}$ ; $\text{U l}^{-1}$ )
d <sub>32</sub>	Sauter mean drop diameter ( $\mu\text{m}$ )
D <sub>AB</sub>	diffusion coefficient of solute A in solvent B ( $\text{m}^2 \text{s}^{-1}$ )
D	impeller diameter (m)
E	enhancement factor
F	force (N)
g <sub>dcw</sub>	grams of dry cell weight (g)
H	Henry's Law constant ( $\text{atmm}^{-3}\text{kg}^{-1}$ )
k <sub>cat</sub>	catalytic constant ( $\text{s}^{-1}$ )
k <sub>L</sub>	mass transfer coefficient ( $\text{m s}^{-1}$ )
k <sub>L</sub> a	volumetric mass transfer coefficient ( $\text{s}^{-1}$ )
k <sub>m</sub>	Michaelis-Menten parameter ( $\text{gl}^{-1}$ )
MW	molecular weight
N	rate of mass transfer ( $\text{mmol l}^{-1}\text{s}^{-1}$ )
N <sub>i</sub>	impeller rotational speed $\text{s}^{-1}$
OTR	oxygen transfer rate ( $\text{mmol l}^{-1}\text{hr}^{-1}$ )
OUR	oxygen uptake rate ( $\text{mmol l}^{-1}\text{hr}^{-1}$ ; $\text{U l}^{-1}$ )
P	power (W)
P <sub>O2</sub>	oxygen permeability ( $\text{mol m}^{-1} \text{s}^{-1}$ )
p <sub>O2</sub>	partial pressure of oxygen (atm)
p <sub>T</sub>	total gas pressure (atm)
R	distance between load cell and the centre of the tank (m)
S	spreading coefficient of oil on water ( $\text{kg s}^{-2}$ )
T	temperature (K)



U	units of enzyme activity ( $\mu\text{mol min}^{-1}$ )
$We_T$	Weber tank number ( $= \rho_c N^2 D^3 / \sigma$ )
V	molar volume at normal boiling temperature
vvm	vessel volumes per minute
v/v	volume per unit volume
$Y_{O_2}$	mole fraction of oxygen in air

## Greek Symbols

$\gamma$	shear rate ( $\text{s}^{-1}$ )
$\Delta$	difference
$\mu$	viscosity (Pa.s)
$\rho$	density ( $\text{kg m}^{-3}$ )
$\sigma$	interfacial tension ( $\text{kg s}^{-2}$ )
$\tau_p$	DOT probe response time (s)
$\tau$	shear stress ( $\text{N m}^{-2}$ ) per unit torque
$\zeta$	torque (Nm)
$\Phi$	volume fraction
$\varphi$	association factor for water (for Wilke-Chang correlation)

## Subscripts

aq	aqueous phase
A	solute A
B	solute B
c	continuous phase
d	dispersed phase
G	gas phase
$G_i$	gas phase interface
L	liquid phase
$L_i$	Liquid phase interface
OG	surface tension of oil
OW	Interfacial tension between aqueous phase and oil
WG	surface tension of aqueous phase

# 1.0 Introduction

## 1.1 Biocatalysis

Biocatalysts are enzymes or cells that can be used for the production of organic compounds. The use of biocatalysts for the synthesis of chemicals offers a number of advantages over chemical routes. Enzymes offer excellent chemo-, regio- and stereoselectivity, produce little or no by-products, can replace several chemical steps, and are more environmentally friendly than chemical methods. To date, at least 140 bioconversion processes have been implemented at industrial scale in the pharmaceutical, food, agricultural, cosmetics and polymer industries (Liese and Fihlo, 1999; Straathof *et al.*, 2002).

## 1.2 Oxygenases

### 1.2.1 Description of the oxygenases

Oxygenases introduce oxygen from molecular oxygen into their substrates. Monooxygenases introduce one oxygen atom into their substrate and dioxygenases introduce two. Figure 1.1 shows reactions schemes for NAD(P)H dependent monooxygenases and dioxygenases. There are oxygenases that do not require NAD(P)H (Fetzner, 2002), but they are not the focus of this thesis.

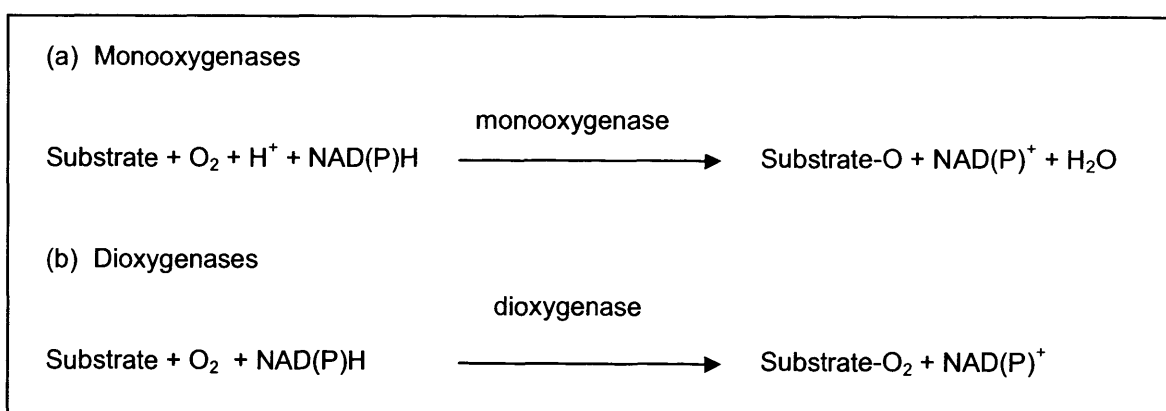


**Figure 1.1.** Generic reaction schemes for cofactor dependent oxygenases.

### 1.2.2 Oxygen consumption by whole-cell oxygenases

Whole-cell oxygenases require oxygen as a substrate for the reaction and for NAD(P)H regeneration. In this section, the function and regeneration of NAD(P)H in *E.coli* are discussed.

#### 1.2.2.1 NADH production

NADH has two major functions in biological systems. First, it is a source of electrons for the production of adenosine triphosphate (ATP) during oxidative phosphorylation. ATP stores free energy that is required by organisms for growth and maintenance. Secondly, it is a source of reducing power for reactions.

NADH is generated by catabolic pathways, which oxidize organic molecules to produce ATP. Electrons from organic molecules are transferred in the form of hydrogen atoms to  $\text{NAD}^+$  to produce NADH. Two catabolic pathways generate NADH: glycolysis and the tricarboxylic acid (TCA) cycle. During glycolysis glucose is oxidized to pyruvate, and two NADH are produced. During the TCA cycle the pyruvate is then completely oxidised to carbon dioxide, and six NADH are produced. Glucose is generally used as an energy source for *E.coli* fermentations, but sometimes glycerol is used.

The NADH produced during glycolysis and the TCA cycle is used as an electron donor during oxidative phosphorylation. Electrons are transferred from NADH to oxygen by a series of electron carriers called the electron transport chain. Oxygen is reduced to water in the final step of the electron transport chain by cytochrome oxidase.

#### 1.2.2.2 NADPH production

NADPH is used as reducing power for biosynthesis. In *E.coli*, NADPH can be produced via several routes (Csonka and Fraenkel, 1977): the pentose phosphate pathway, isocitrate dehydrogenase in the TCA cycle, and the action of various dehydrogenases. One of the major functions of the pentose phosphate pathway is to supply NADPH for biosynthesis: it is produced in the

first two steps of the pathway via glucose – 6- phosphate dehydrogenase and gluconate-6-phosphate dehydrogenase. The pentose phosphate pathway is cyclic and can be fed back into the glycolytic pathway to produce pyruvate. Although NADPH regeneration is not directly linked to oxygen consumption, if the flux through the electron transport chain is decreased the flux through other metabolic pathways can also decrease.

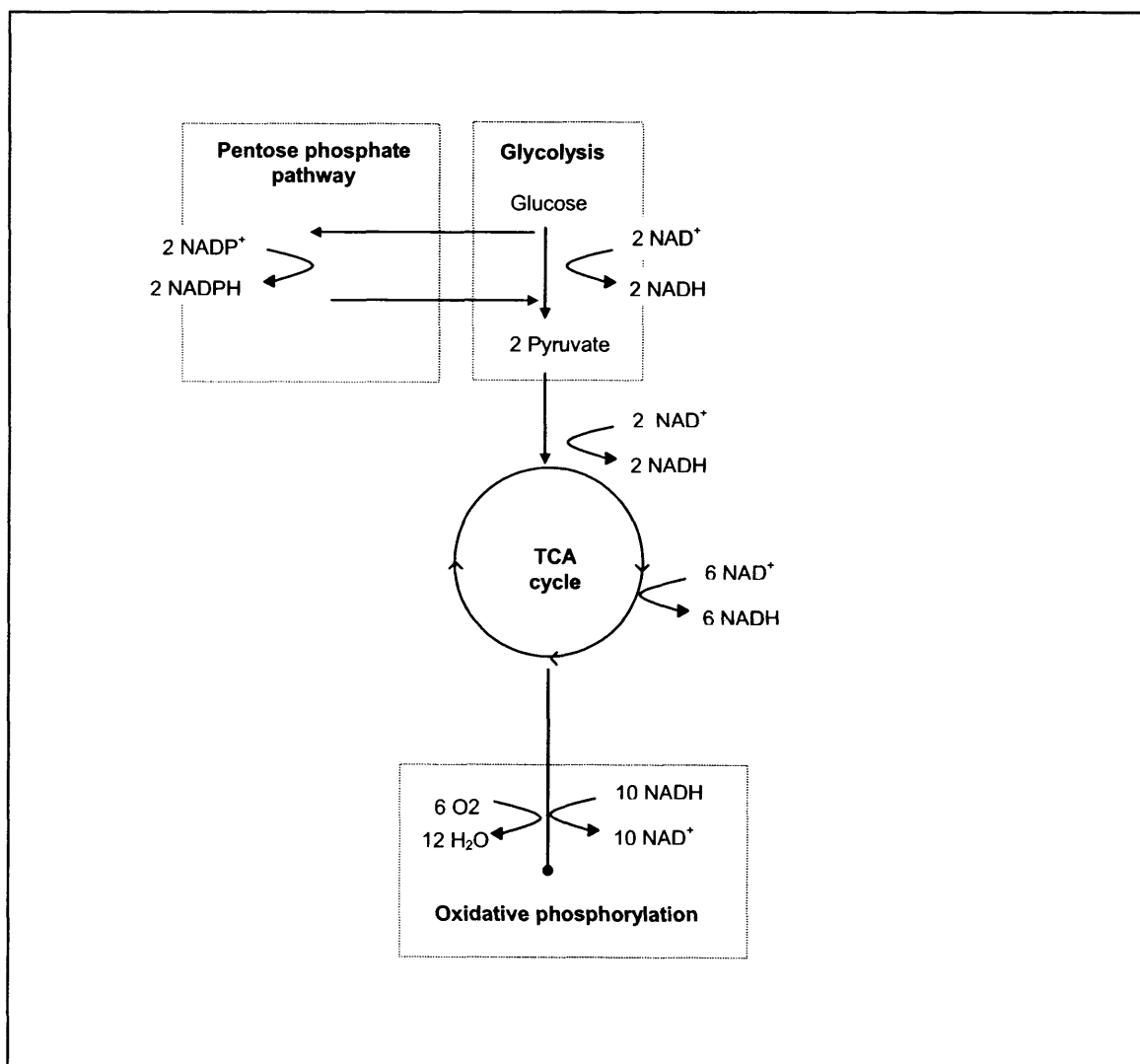


**Figure 1.2.** NAD(P)H regeneration in glycolysis, TCA cycle, oxidative phosphorylation and the pentose phosphate pathway.

### 1.2.2.3 Oxygen limitation in *E.coli*

*E.coli* controls the synthesis of the respiratory enzymes in response to the oxygen concentration. If the oxygen concentration is very low, *E.coli* can recycle NADH, and produce ATP by anaerobic respiration or by mixed-acid fermentation (Gunsalus, 1992; Uden, 1994).

During anaerobic respiration alternative electron acceptors such as nitrate, fumarate, or dimethylsulfoxide are used. Mixed-acid fermentation, where pyruvate acts as the final electron acceptor, is used if no alternative electron acceptors are available. Mixed-acid fermentation results in the production of compounds such as acetate, formate and succinate. Figure 1.3 shows three possible routes for glucose catabolism.

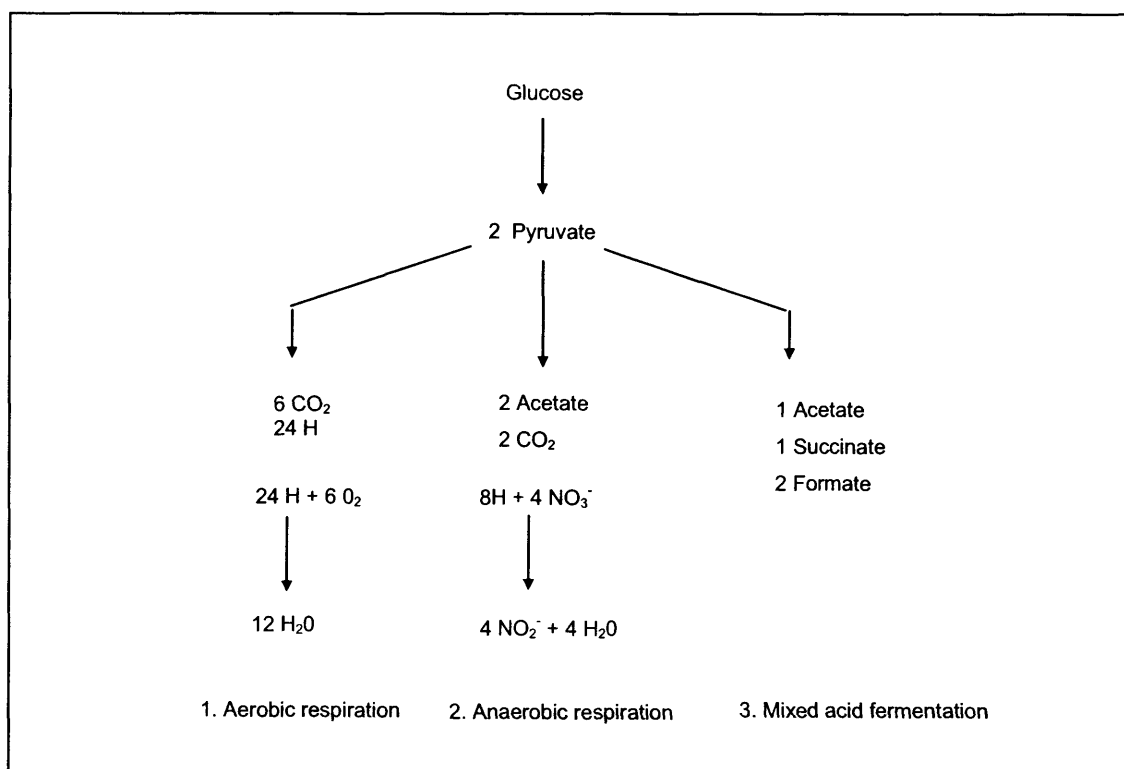


**Figure 1.3.** Routes for glucose catabolism by *E.coli* under different oxygen concentrations (From Uden, 1994).

#### **1.2.2.4 Cofactor recycling in oxygenase processes**

The activity of oxygenases with high  $k_{cat}$  values could be limited by the NAD(P)H regeneration rate of the host (Duetz *et al.*, 2001; van Beilen *et al.*, 2003). Several authors have found that the activity of whole-cell oxygenases gradually decreases as the cells reach stationary phase (Wubbolts *et al.*, 1996; Walton and Steward, 2002; Buhler *et al.*, 2002,2003). This might be because the NAD(P)H regeneration rate decreases with the metabolic rate of the cells. Growing cells might have higher NAD(P)H regeneration rates because they have high metabolic activities, but on the other hand the NAD(P)H demand of the oxygenase could have a detrimental effect on the growth rate and viability of the host.

#### **1.2.3 Industrial potential of oxygenases**

Oxygenases play a key role in the aerobic degradation of both natural and xenobiotic compounds in bacteria. Hence, bacteria contain a diverse range of oxygenases with high regio- and stereoselectivity. Oxygenases offer higher regio-, stereo-, and chemo- selectivity, many can catalyse reactions that have no chemical alternative, and they are often more environmentally friendly than chemical oxidative processes that often use non-specific, toxic and expensive reagents (Duetz *et al.*, 2001; Li *et al.*, 2002; Cirino and Arnold, 2002). Among the reaction types catalysed by oxygenases are hydroxylations, epoxidations, sulfoxidations, and dealkylations (May, 1999).

#### **1.2.4 Process development of oxygenase processes**

The aim of process design is to use processing and biological techniques to minimise any detrimental effect the biological or chemical properties of a bioconversion have on the cost or safety of a process (Burton *et al.*, 2002; Lye *et al.*, 2002). Parameters that influence the costs of a process include the volumetric productivity, product concentration, yield on substrate, turnover number, half-life and biocatalyst consumption.

Lilly and Woodley (1996) developed a systematic approach to process design whereby the properties that constrain the bioconversion can be split into four

categories. These categories are shown in Table 1.1 along with constraints that have been identified as typical for oxygenase processes (Buhler and Schmid, 2004). One of the key constraints for oxygenase processes is the requirement for NAD(P)H: it is expensive and difficult to recycle, and consequently these bioconversions are generally carried out using whole-cells.

#### **1.2.4.1 Biological techniques**

Biological techniques are generally used to alleviate constraints that are associated with biocatalyst and reaction properties. Biological techniques include host selection, media optimisation (Reddy *et al.*, 1999; Buhler *et al.*, 2003), and various genetic engineering techniques.

The over-expression of oxygenase genes in non-native hosts has been the most useful genetic engineering technique. It has been used to increase the specific activity (Buhler *et al.*, 2002) to avoid product degradation by the native host (Wubbolts *et al.*, 1996), to avoid using a pathogenic host (Doig *et al.*, 2001), and to avoid a difficult fermentation process (Panke *et al.*, 2002). The over-expression of other genes has been used to alter hosts so that they have improved substrate uptake (Schneider *et al.*, 1998) and increased organic solvent tolerance (Aono, 1998).

Metabolic engineering has been used to prevent product degradation (Hack *et al.*, 1994), and to prevent the synthesis of unwanted metabolites or increase the precursor supply (Berry *et al.*, 2002). Enzyme engineering has been used to improve the enzyme activity, specificity and the stability by either site directed mutagenesis (Nickerson *et al.*, 1997; Graham – Lorence *et al.*, 1997) or directed evolution (Meyer *et al.*, 2002).

#### **1.2.4.2 Processing techniques**

Processing techniques are generally used to alleviate constraints associated with substrate and product properties, and in particular substrate and product toxicity and inhibition. Techniques include fed-batch addition of substrates (Gbewonyo *et al.*, 1991; Held *et al.*, 1999; Hack *et al.*, 2000; Doig *et al.*, 2002a),

feed-back control systems to monitor the substrate and product concentration (Carragher *et al.*, 2001; Hack *et al.*, 2000; Bird *et al.*, 2002), and in-situ product removal (ISPR).

ISPR methods selectively remove the product from the aqueous phase and can also act as a reservoir for the substrate (Woodley and Lilly, 1990; Lye and Woodley, 1999; Stark and von Stockar, 2003). The two most common ISPR methods are the use of a second liquid phase (separation based on solubility) and the use of solid resins (separation based on charge and hydrophobicity). The use of a second liquid phase will be discussed in more detail in the next section.

<b>Biocatalyst properties</b>	<b>Reaction properties</b>
<b>Oxygenases</b> Unstable Require NAD(P)H Uncoupling  <b>Host</b> Product degradation Pathogenicity Heterologous expression	Low $k_{cat}$ Oxygen consumption
<b>Substrate/product properties</b>	<b>Biocatalyst-substrate-product</b>
Low water solubility Explosion hazard	Substrate / product toxicity Substrate uptake Overoxidation

**Table 1.1.** Typical characteristics of oxygenases that limit their industrial application.

### 1.2.3.3 Two liquid-phase bioconversions

Organic solvents have been used successfully for many whole-cell oxygenase bioconversions to overcome substrate and product inhibition and low water



solubility (Schmid *et al.*, 1998a; Held *et al.*, 1999; Mathys *et al.*, 1999; Husken *et al.*, 2001; Buhler *et al.*, 2002; Panke *et al.*, 2002; Buhler *et al.*, 2003a; Buhler *et al.*, 2003b). The organic solvent acts as a reservoir for the substrate and product, whilst the reaction takes place in the aqueous phase. The choice of organic solvent depends on the properties of the solvent and its interaction with the biocatalyst, substrate and product (Lye and Woodley, 1999). Two important factors that need to be considered when selecting a suitable organic solvent are the distribution coefficient and the biocompatibility.

Organic solvents separate compounds from the aqueous phase based on solubility. The distribution coefficient is the ratio of the solute concentration in the aqueous and organic phase at equilibrium. It is a measure of the affinity of the organic solvent for the substrate and product.

Organic solvents can be toxic to cells. A parameter called log P is used to indicate the toxicity of an organic solvent. It is defined as the logarithm of the partition coefficient of a solvent in a water-octanol two-phase system (Laane *et al.*, 1987). The more hydrophobic a solvent is the higher the log P value, and the less likely it is to damage the biocatalyst.

The design of a two-liquid phase reactor requires consideration of the reaction kinetics, the rate of mass transfer, and downstream processing (Woodley and Lilly, 1992). A key design factor is the phase ratio, which is the fraction of the total reaction volume occupied by the organic solvent. It influences the rate of mass transfer of reactants and products between the two phases, and the ease of down stream processing (Woodley and Lilly, 1990).

#### **1.2.5. Process examples from industry**

There are relatively few industrial oxygenase processes because of the constraints described in the previous sections. Table 1.2 shows some examples of industrial oxygenase processes, and lists the techniques used during process development.

Product and biocatalyst	Process development	References
6- $\beta$ -hydroxymethyl-simvastatin  Suspended whole-cells of a <i>Nocardia</i> species.	Fed – batch addition of substrate	Gbewonyo <i>et al.</i> , 1991
(R)-(4-hydroxy)phenoxypropionic acid  Resting whole-cells of <i>Beauveria bassiana</i>	Extensive screening of microorganisms  Strain improvement via random mutagenesis for increased reaction specificity and substrate tolerance	Dingler <i>et al.</i> , 1996
5 – methyl-2-pyrazinecarboxylic acid  Growing <i>P.putida</i> mt 2.	Used strain unable to further degrade heteroaromatic carboxylic acids.  Fed-batch addition of carbon source p-xylene and substrate.	Kiener, 1995
trans – 4-hydroxy-L-proline  Recombinant engineered growing <i>E.coli</i>	Overexpression of two genes involved in L-proline synthesis and introduced mutation so the strain could not degrade L-proline.	Shibasaki <i>et al.</i> , 2000a 2000b
Indigo  Recombinant and engineered growing <i>E.coli</i>	Overexpression of naphthalene dioxygenase  Modifications of metabolic pathways	Berry <i>et al.</i> , 2002
2-quinolinecarboxylic acid  <i>P.putida</i>	Substrate feed Screened inducers for low flammability	Wong <i>et al.</i> , 2002

**Table 1.2.** Examples of industrial oxygenase bioconversions and the techniques used during their process development.

## 1.3 Baeyer – Villiger monoxygenases (BVMOs)

### 1.3.1 Baeyer – Villiger reaction

A diverse range of microorganisms have been found to produce enzymes, known as BVMOs, that are capable of performing Baeyer-Villiger reactions with a high regio- and stereoselectivity on a broad range of substrates (Willetts, 1997). In addition to carrying out the Baeyer – Villiger reaction, BVMOs are also capable of carrying out the electrophilic oxygenation of various heteroatoms. BVMOs use a flavin coenzyme as an organic cofactor and either NADH or NADPH as the reductant (Willetts, 1997). The Baeyer-Villiger reaction involves the insertion of an oxygen atom into a cyclic or non-cyclic ketone to generate an ester or a lactone as illustrated in Figure 1.4 (Baeyer and Villiger, 1899). The chiral Baeyer – Villiger oxidation of cyclic ketones produces asymmetric lactones, which are valuable precursors in enantioselective synthesis.

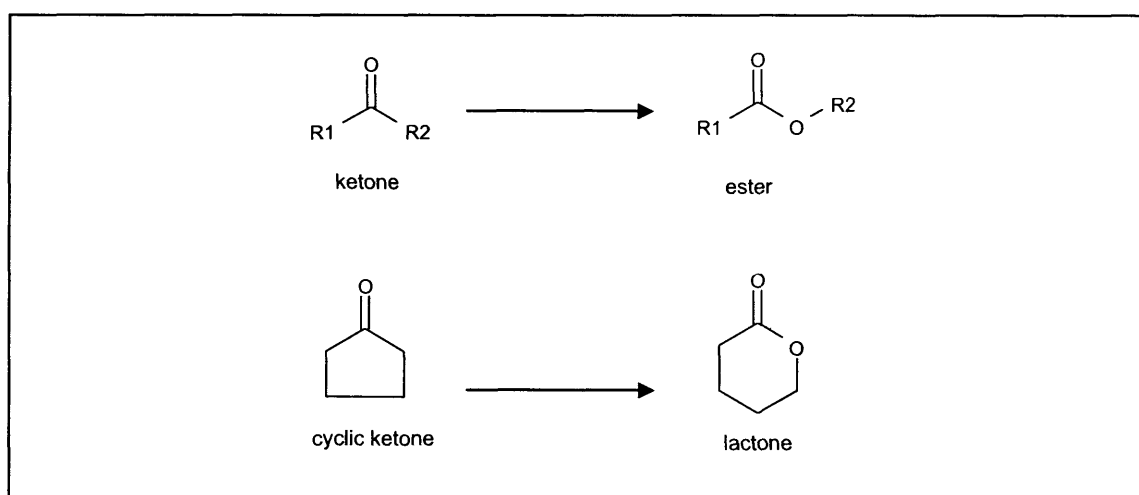


**Figure 1.4.** Baeyer-Villiger reactions of aliphatic and cyclic ketone substrates.

#### 1.3.1.1. Advantages of BVMOs

Peracid or peroxide catalysts such as *m*-chloroperoxybenzoic acid or hydrogen peroxide can be used for Baeyer-Villiger reactions. However, they also oxidize other functional groups and so it might be necessary to use protection-deprotection steps to obtain the desired compound (Renz and Meunier, 1999). Organometallic oxidants have been used to obtain enantioselectivity (Bolm *et al.*, 1997); however, the ee values achieved were low compared with Baeyer-

Villiger monooxygenases, and the catalysts are expensive and environmentally unfriendly.

### 1.3.2 Cyclohexanone monooxygenase (CHMO)

CHMO from *Acinetobacter calcoaceticus* is the best characterised BVMO. It allows microorganisms to grow on cyclohexanol or cyclohexanone (Donoghue and Trudgill, 1975). CHMO catalyses a key step in the metabolism of these compounds by converting cyclohexanone to  $\epsilon$ -caprolactone, which can be catabolised further because *A. calcoaceticus* contains a lactonase that subsequently opens up the lactone ring. The resulting compound can be metabolised to adipate, from which acetyl-coA can be generated (Donoghue and Trudgill, 1975). The CHMO isolated from *A. calcoaceticus* was found to be an NADPH dependent, flavin adenine dinucleotide (FAD) binding, single chain BVMO (Donoghue *et al.*, 1976). It has been shown to oxidise more than 80 different ketones (Mihovilovic *et al.*, 2002; Stewart, 1998).

#### 1.3.2.1 Development of a CHMO catalyst

Several constraints that influence the design of a process using CHMO from *Acinetobacter calcoaceticus* have been identified (Alphand *et al.*, 2003), and are listed in Table.1.3. The biological and processing techniques that have been used to overcome some of these limitations are discussed in the following sections.

Constraint	Reference
NADPH cofactor	Donoghue <i>et al.</i> , 1976
Stability	Zambianchi <i>et al.</i> , 2002
Lactonase activity ( <i>Acinetobacter</i> )	Donoghue and Trudgill, 1975; Alphand <i>et al.</i> , 1990
Pathogenicity ( <i>Acinetobacter</i> )	
Substrate uptake ( <i>E.coli</i> )	Doig <i>et al.</i> , 2002a
Substrate / product toxicity ( <i>E.coli</i> )	Doig <i>et al.</i> , 2003; Simpson <i>et al.</i> , 2001; Lander, 2001.
Oxygen consumption	Hilker <i>et al.</i> , 2004; Baldwin and Woodley, 2005; Doig <i>et al.</i> , 2002b; Zambianchi <i>et al.</i> , 2004

**Table 1.3.** Constraints that influence the design of CHMO processes.

### 1.3.2.1.1 Biocatalyst type

The use of isolated CHMO avoids many problems associated with using a whole-cell biocatalyst: e.g. substrate and product toxicity, limited substrate uptake rates and complicated downstream processing. Isolated CHMO has been used with cofactor recycle systems (Abril, 1989; Rissom, 1997; Hogan and Woodley, 2000). However, the costs of NADPH, the recycling system, and purifying the enzyme make the use of isolated CHMO at large-scale unviable. Another disadvantage associated with isolated CHMO is its stability: Zambianchi *et al.* (2002), found that half life of isolated CHMO from *Acinetobacter calcoaceticus* was 1 day, or 2.5 days when it was immobilised.

There are several disadvantages associated with using *Acinetobacter calcoaceticus* for industrial bioconversions. It has to be grown on a toxic carbon source such as cyclohexanol to induce the expression of CHMO (Donoghue and Trudgill, 1975), it is a class 2 pathogen, which is undesirable for industrial production, and it contains a lactone hydrolase that can cause product degradation (Donoghue and Trudgill, 1975; Alphand *et al.*, 1990).

These problems have been overcome by overexpressing CHMO in non-native hosts such as *S.cerevisiae* (Stewart *et al.*, 1996; Kayser *et al.*, 1998) and *E.coli* (Chen, 1988; Chen *et al.*, 1999; Doig *et al.*, 2001). The activity of the *E.coli* biocatalysts was limited by the rate of substrate uptake (Doig *et al.*, 2003; Walton and Stewart, 2004).

### 1.3.2.1.2 Substrate and product inhibition

The substrates and products of CHMO bioconversions have been shown to inhibit the whole-cell activity (Lander, 2001; Simpson *et al.*, 2001; Doig *et al.*, 2003; Zambianchi *et al.*, 2004). Most of the work regarding substrate and product inhibition has been carried out using bicycloheptenone and its lactone products.

Substrate inhibition has been avoided by using feeding strategies to keep the substrate concentration below inhibitory levels. Doig *et al.* (2002a) added

bicycloheptenone in a fed-batch mode at 1.5 and 55 l scales. Bird *et al.* (2002) refined the fed-batch process by developing a feed back control system which used near infrared spectroscopy (NIR) to monitor the ketone and lactone concentration. Hilker *et al.* (2004a;2004b) controlled the bicycloheptenone concentration by pre-saturating a resin with the substrate so that it would be slowly released during the course of the bioconversion. Zambianchi *et al.*, (2004) pre-saturated a resin with the substrate 1,3 diathiane because it had a very low water solubility.

Solid resins have also been used to alleviate lactone inhibition. Lander (2001) used a resin in a column external to the fermenter, and obtained an 85% increase in the final product concentration. Hilker *et al.* (2004a, 2004b) used the resin as a reservoir for the substrate and the product, and increased the final lactone concentration five fold. Zambianchi *et al.* (2004) used a similar methodology with 1,3 diathiane and its products.

#### **1.3.2.1.3 Oxygen limitation**

Results from shake-flask and microwell bioconversions indicate that above a critical biomass concentration the specific activity begins to decrease - this is probably due to oxygen limitation (Simpson *et al.*, 2001; Doig *et al.*, 2002b; Zambianchi *et al.*, 2004; Baldwin and Woodley, 2005). Hilker *et al.* (2004a) found that the whole-cell activity in a bubble column was higher than in a stirred tank reactor because it had a higher oxygen transfer rate.

## 1.4 Oxygen Supply

### 1.4.1 Oxygen transfer in stirred tank reactors

Stirred tank reactors are the most commonly used vessel for aerobic culture. Oxygen is supplied to the microorganism by sparging air bubbles underneath the impellers. The impellers then disperse the gas throughout the vessel. Oxygen molecules must overcome a series of transport resistances as they move from inside the air bubbles to the inside of the microorganism (Doran, 1999). These mass transfer steps are outlined in Figure 1.5.

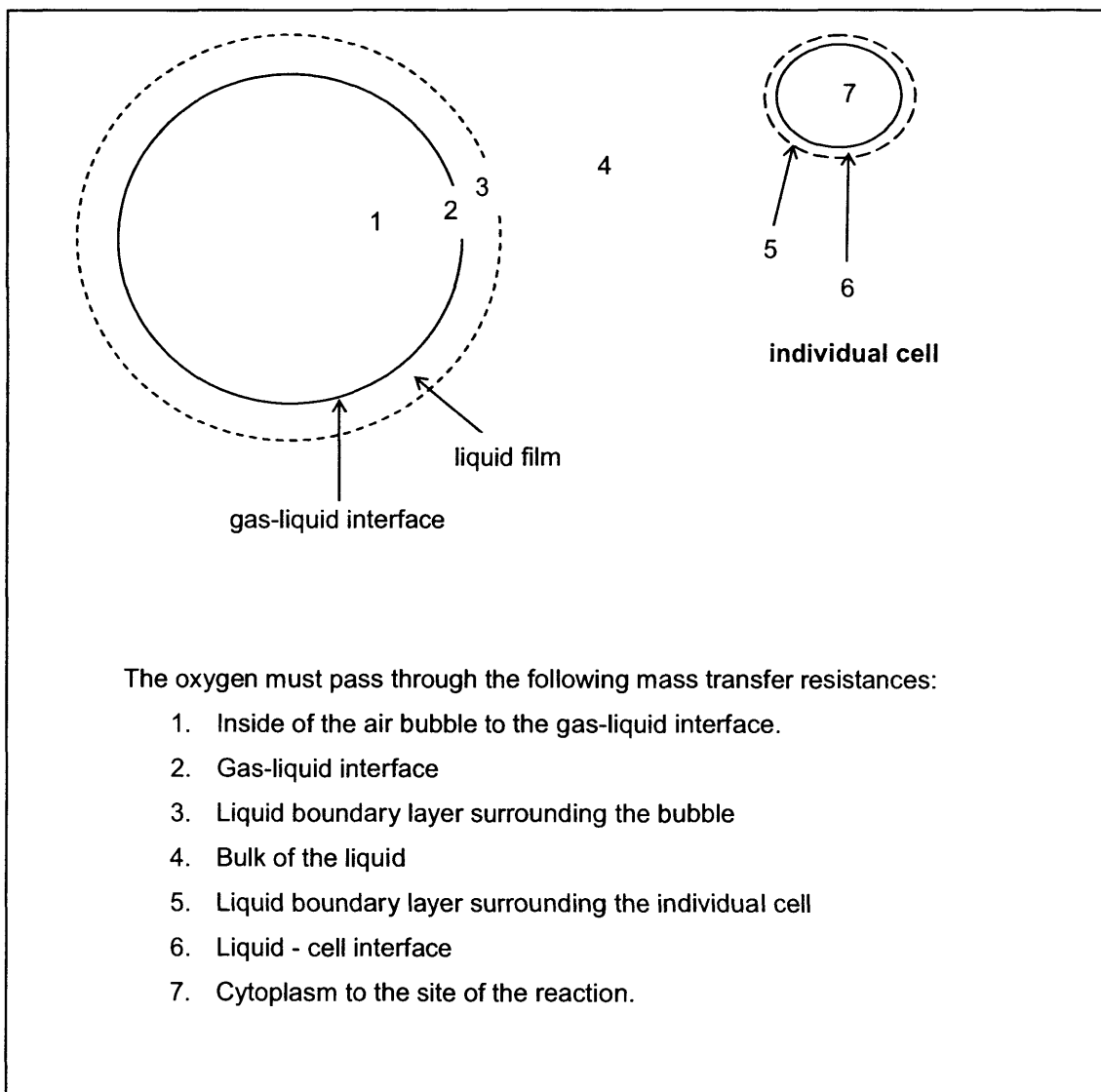


**Figure 1.5.** Oxygen transfer from inside an air bubble to inside a cell

### 1.4.2 Mass transfer and diffusion theory

Oxygen transfer in fermenters is driven by an oxygen concentration gradient that exists between the air bubbles and the fermentation broth. Fick's law of diffusion states that the rate of mass transfer is proportional to the concentration gradient (the driving force for mass transfer) and the area available for transfer to take place:

$$N = k a \Delta C \quad (1.1)$$

where,  $N$  is the rate of mass transfer of the component,  $a$  is the area available for mass transfer,  $\Delta C$  is the concentration gradient, and  $k$  is the mass transfer coefficient. The mass transfer coefficient is determined by physical properties such as shear forces and also fluid properties such as diffusivity and viscosity.

#### 1.4.2.1 Two-film theory

The two-film theory is used as a model for mass transfer between two phases. It assumes that local fluid velocities approach zero at the interface and consequently a film of stagnant fluid called a boundary layer forms on either side of the phase interface (Coulson and Richardson, 1990). Mass transfer through the boundary layer is thought to be by diffusion, and it is the main resistance to mass transfer. Figure 1.6 depicts the path of oxygen from the bulk gas phase to the boundary layer on the gas side, across the interface, across the boundary layer on the liquid side and then to the bulk liquid.

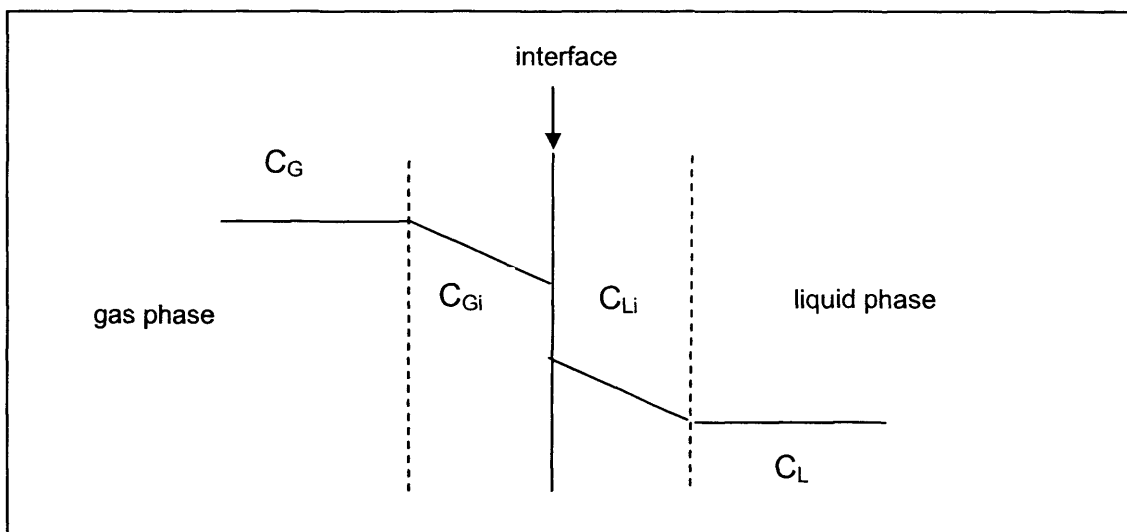


**Figure. 1.6** Schematic of two-film theory.



### 1.4.2.2 Gas – liquid mass transfer

The rate of oxygen transfer through each fluid can be expressed as follows (Doran, 1999):

$$N_G = k_{Ga} (C_G - C_{Gi}) \quad (1.2)$$

or

$$N_L = k_{La} (C_{Li} - C_L) \quad (1.3)$$

where,  $N_G$  and  $N_L$  are the rate of oxygen transfer through the gas boundary layer and liquid boundary layer respectively,  $k_{Ga}$  and  $k_{La}$  are the gas phase and liquid phase mass transfer coefficient respectively,  $C_G$  and  $C_L$  are the oxygen concentration in the bulk gas and liquid phase respectively, and  $C_{Gi}$  and  $C_{Li}$  are the oxygen concentration in the gas and liquid interface respectively.

For process design calculations, these equations are impractical because it is not possible to measure the oxygen concentration at the interface. However, these parameters can be eliminated from the equations if it is assumed that  $C_{Gi}$  and  $C_{Li}$  are in equilibrium and that there is negligible resistance to transport at the interface. The boundary layer concentrations can be related by a distribution factor ( $m$ ), which represents the ratio between the oxygen solubility in the two phases.

$$C_{Gi} = m C_{Li} \quad (1.4)$$

By using this relationship and rearranging the following equation is obtained:

$$N_L = k_{La} (C^* - C_L) \quad (1.5)$$

Because oxygen is poorly soluble in an aqueous solution the liquid phase mass transfer dominates therefore the resistance to mass transfer is dominated by the  $k_{La}$ . The value  $C^*$  is the liquid phase concentration in equilibrium with the gas phases. In practical terms this means the saturation concentration of oxygen in the aqueous phase.

### 1.4.3 Methods to increase the oxygen transfer rate

The rate of oxygen transfer in fermentation broths is influenced by several physical and chemical properties that affect either the mass transfer coefficient ( $k_L$ ), the interfacial area ( $a$ ), or the saturation concentration ( $C^*$ ). Table 1.4 lists these properties. Changing these properties can either increase or decrease the oxygen transfer rate; however, some of these properties cannot be altered systematically to increase the oxygen transfer rate e.g. the media composition and the interfacial tension. The properties in bold print can be systematically changed in order to increase the oxygen transfer rate, and are discussed in the following sections.

Parameter	Properties
Mass transfer coefficient ( $k_L$ )	Viscosity <b>Power input</b> Media composition Temperature
Interfacial area ( $a$ )	Interfacial tension <b>Gas hold-up</b> <b>Power input</b>
Driving force ( $C^*$ )	Temperature Media composition <b>Partial pressure of oxygen</b>

**Table 1.4** Properties that influence the oxygen transfer rate

#### 1.4.3.1 Impeller speed

The impeller speed determines the power input, which in turn influences the mass transfer coefficient ( $k_L$ ) and the interfacial area ( $a$ ). At higher power inputs the turbulence in the boundary layer surrounding the air bubbles is greater and therefore there is less resistance to mass transfer – thus the mass transfer coefficient increases. The interfacial area is increased because small bubbles have a higher surface area and also a slower rise velocity, which means they stay in the liquid longer allowing more time for the oxygen to transfer to the

aqueous phase. However, if the impeller speed is increased too much, the shear forces will cause the microorganism to disintegrate, and the higher power input required can make the process economically unfeasible (Nienow, 1998).

#### 1.4.3.2 Air flow rate

The air flow rate determines the volume of gas in the reactor (gas hold-up), which influences the interfacial area. The airflow rate has a minor effect on the oxygen transfer rate compared to the impeller speed, and if it is increased too much the air will not be dispersed by the impellers but instead will flow up the impeller shaft.

#### 1.4.3.3 Partial pressure

There is a linear relationship between the oxygen partial pressure and the aqueous phase oxygen concentration. The equilibrium relationship obeys Henry's Law:

$$p_{O_2} = p_T y_{O_2} = H C^* \quad (1.6)$$

where,  $p_{O_2}$  is the partial pressure of oxygen,  $p_T$  is the gas pressure,  $y_{O_2}$  is the mole fraction of oxygen in the gas,  $H$  is the Henry's Law constant, and  $C^*$  is the saturation concentration of oxygen in the aqueous phase.

If the total pressure of the gas is increased the driving force will be greater (Matsui *et al.*, 1989). However, for bioconversions that use flammable organic solvents and substrates, an increase in the pressure can increase the risk of an explosion.

If the volume fraction of oxygen in the air entering the reactor is increased the driving force for mass transfer will increase. The use of pure oxygen and oxygen-enriched air will increase the oxygen transfer rate (Castan *et al.*, 2002). However, it can be an explosion hazard, particularly if the reactor contents are flammable as they often are in oxygenase bioconversions (Schmid *et al.*, 1999).

A technology exists that allows the direct injection of pure oxygen bubbles with diameters as small as 0.1 mm into the reactor in addition to air that is provided in the normal way (Cheng, 1998;1999). A much smaller volume of oxygen is required to achieve the same oxygen transfer rate than the air. Oxygen bubbles are injected separately from the air to prevent the two coalescing. If coalescence were to occur the effect of the additional oxygen would not be as great. The system was used industrially in antibiotic production, and the oxygen transfer rate was doubled (Noorman, 2004). The system produces oxygen relatively inexpensively using an adsorption process.

#### **1.4.3.4 Water-immiscible liquids**

The use of water immiscible liquids that have an oxygen solubility higher than water will be discussed in the next section.

### **1.5 Water- immiscible liquids**

#### **1.5.1 Background**

The addition of water immiscible liquids to an aqueous – gaseous system is known to enhance the rate of gas mass transfer to the aqueous phase. Table 1.5 lists studies that have used water immiscible liquids in biological systems. In this thesis water immiscible liquids will be called oils. The following reviews the literature regarding the enhancement in gas mass transfer obtained in both chemical and biological processes. These studies have either investigated the effect of the oils on the volumetric mass transfer  $k_L a$  or on the enhancement of the oxygen transfer rate into the aqueous phase.

#### **1.5.2 Mechanism of gas mass transfer enhancement**

The main resistance to gas transfer from a gas bubble to an aqueous phase is in the liquid boundary layer at the gas – liquid interface. Oils might increase the gas transfer rate to the aqueous phase by three mechanisms: by increasing the mass transfer coefficient ( $k_L$ ); increasing the gas-liquid interfacial area ( $a$ ); or increasing the driving force ( $C^*$ ) by absorbing gas at or near the interface and transferring it to the bulk aqueous phase.

Ref	Oil and volume fraction	Comments
Ates <i>et al.</i> , 2002	silicone oil 0.02 – 0.15	Increase in citric acid production by <i>Aspergillus niger</i> .
Damiano and Wang, 1985	perfluoromethyldecalin 0.1 – 0.2	Increased biomass concentration during <i>Escherichia coli</i> fermentation.
Elibol and Mavituna, 1996	perfluorodecalin 0.1 – 0.5	Increased acitinorhodin (antibiotic) production by <i>Streptomyces coelicolor</i>
Elibol, 2001	perfluorodecalin 0.1	Increased acitinorhodin (antibiotic) production by <i>Streptomyces coelicolor</i> 1.4 fold increase in oxygen uptake rate
Leonhardt <i>et al.</i> , 1985	silicone oil 0.05 – 0.25	Increase in L-amino acid oxidase activity by <i>Providencia sp.</i>
Jia <i>et al.</i> , 1999	soybean oil 0.02 – 0.1	Increase in DOT Increase in tetracycline production by <i>Streptomyces aureofaciens</i>
Elibol and Ozer, 2000	perfluorodecalin 0.1	Increased lipase production by <i>Rhizopus arrhizus</i>
Menge <i>et al.</i> , 2001	perfluorodecalin 0.1 – 0.4	Increased alkaloid production by <i>Claviceps purpurea</i>
Rols and Goma, 1991	soybean oil 0.01 – 0.3	Increase in oxygen uptake rate by <i>Aerobacter aerogenes</i>

**Table 1.5.** Examples of oils used in biological systems to enhance the oxygen transfer rate.

### 1.5.2.1 Effect of oil on the mass transfer coefficient ( $k_L$ )

There have been studies that have shown that the addition of oils has no effect on the  $k_L$  (Linek and Benes, 1976; Cents *et al.*, 2001; Lekhal *et al.*, 1997). However, other studies have indicated that the  $k_L$  can increase or decrease. Most have found that the  $k_L$  decreases at very low concentrations and then increases at higher concentrations (Eckenfelder and Barnhart, 1961; Yoshida *et al.*, 1970; Linek and Benes, 1976; Liu *et al.*, 1994; Morão *et al.*, 1999).

Oil drops could increase the mass transfer coefficient ( $k_L$ ) by increasing turbulence or mixing within the gas-aqueous boundary layer. However, no conclusive experimental evidence has been produced to support this theory (Dumont and Delmas, 2003). The oils can also decrease the  $k_L$  by causing interfacial blockage and decreasing the surface mobility of the bubbles (Kawase and Moo-Young, 1990; Prins and van't Riet, 1987).

### 1.5.2.2 Effect of oil on the gas-liquid interfacial area ( $a$ )

Oils can increase the gas – liquid interfacial area ( $a$ ) by decreasing the surface tension and therefore decreasing either the bubble size or the rate of bubble coalescence. Das *et al.* (1985) found that as the organic phase fraction increases the interfacial area first increases, reaches a maximum and then decreases. Rols *et al.* (1990) used a photographic method to measure bubble size and found that the bubble Sauter mean diameter was reduced by approximately 15%, but MacMillan and Wang (1990) and Junker *et al.* (1990a) also used a photographic method and found no change in bubble size or gas hold-up.

### 1.5.2.3 Effect of the oils on the driving force

If an oil has a higher gas solubility than the aqueous phase, the average saturation concentration  $C^*$  for the dispersion will be higher, which means more oxygen can be removed from the gas phase. Two mechanisms have been proposed to describe how the oil absorbs oxygen from the gas phase: the bubble covering mechanism and the shuttle mechanism. Both require the oxygen solubility in the oil to be higher than the aqueous phase, and some

authors have suggested that the diffusivity of the gas is also important (McMillan and Wang, 1987; Junker *et al.*, 1990b).

### 1.5.2.3.1 Bubble mechanism

The bubble mechanism proposes that when a gas bubble and an oil droplet come into contact, the oil spreads around the bubble to form a gas – oil complex. The oil droplet then absorbs oxygen directly from the bubble, and then transfers the oxygen to the bulk continuous phase when the complex has broken up. The mechanism is depicted in Figure 1.7.

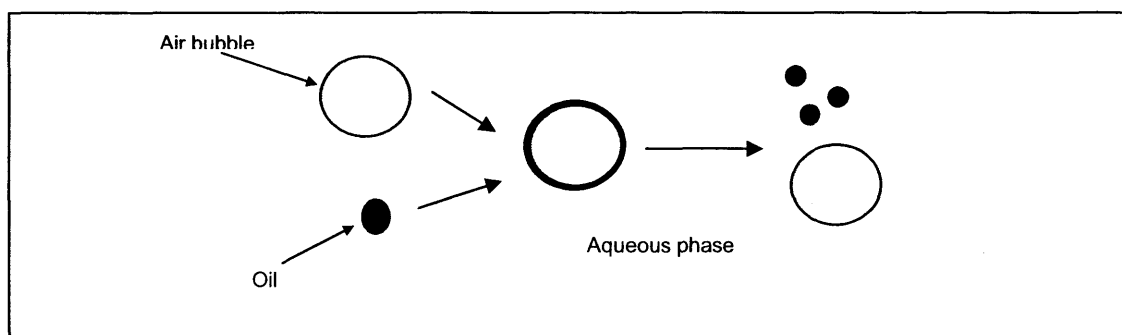


**Figure 1.7.** Schematic of the bubble covering mechanism.

This mechanism depends on the ability of the oil to spread around the gas bubble, which is thought to be determined by the spreading coefficient (Yoshida *et al.*, 1970). The spreading coefficient is defined as:

$$S_{OW} = \sigma_{WG} - (\sigma_{OG} + \sigma_{OW}) \quad (1.7)$$

Where,  $S_{OW}$  is the spreading coefficient of oil on water,  $\sigma_{WG}$  is the surface tension of the aqueous phase,  $\sigma_{OG}$  is the surface tension of the oil, and  $\sigma_{OW}$  is the interfacial tension between the aqueous phase and oil. If the spreading coefficient is positive the oil will spread and form a thin film around water, but if it is negative the oil will form a drop on the bubble surface. Yoshida *et al.* (1970) found that the addition of oils with negative spreading coefficients (kerosene and paraffin) caused the  $k_L a$  to decrease as the oil fraction increased, but had no effect on gas hold-up. Oils with positive spreading coefficients (toluene and

oleic acid) caused the  $k_L a$  to initially decrease and then increase with increasing oil fraction, and the gas hold-up also increased with oil fraction. Yoshida *et al.* (1970) concluded that if oil spread around a gas bubble, the surface tension would decrease, and therefore the specific interfacial area would also increase. Linek and Benes (1976) found that non – spreading n – alkanes did not change the  $k_L a$ , because they did not contact the air bubbles. Oleic acid (spreading) did contact the air bubbles and the  $k_L$  increased with the oil fraction.

Photographs taken of spreading and non-spreading oils during gas flotation show that oils with a positive spreading coefficient spread around the bubble, whilst the oils with negative spreading coefficients formed droplets on the side of the bubbles (Grattoni *et al.*, 2003). Rols and Goma (1989) produced photographs of n-dodecane and a perfluorochemical F66E droplets forming gas – oil complexes with a gas bubble. However, in those experiments the bubble and oil were forced to come into contact, and the time allowed for the bubble and oil to collide and form a complex was much greater than it would be in a stirred tank reactor where the oil droplets and bubbles are constantly moving.

Most authors calculate the spreading coefficient based on the surface and interfacial tensions of oil and water that have not been pre-saturated with each other. Brillman (1998) found that oils that had a positive spreading coefficient when the oil and the aqueous phase were not pre-saturated had negative spreading coefficients when the two phases were pre-saturated. This suggests that in a well mixed stirred tank fermenter the initial spreading coefficient is irrelevant and that the actual spreading coefficient appears to be negative for all systems. In dynamic experiments, Brillman (1998) found that complexes were formed irrespective of spreading coefficient. Oleic acid, which had a higher viscosity than the other oils, did not form a complex but instead formed a drop on the surface. Brillman (1998) and Moosai and Dawe (2003), suggest that the formation of a gas-oil complex is dependent not only on the spreading coefficient, but also the bubble and droplet size.



Castor oil drops have been shown to entrap air bubbles during simulated mycelial broths (Galindo *et al.*, 2000; Larralde-Corona *et al.*, 2002; Lucatero *et al.*, 2003; Pulido-Mayoral and Galindo, 2004). Depending on the volume fraction and the biomass concentration, between 20 – 60% of the air bubbles were trapped in the oil (Larralde-Corona *et al.*, 2002). However, the hydrodynamic conditions in these experiments were different from typical bacterial fermentations. Low power inputs were used, and the castor oil was very viscous (500 mPas); the result of which was that the Sauter mean diameters of the oil drops and the air bubbles were of a similar magnitude. The  $k_L a$  increased as the volume of air bubbles in the oil increase; however, further work is required to determine if this was due to an increase in the saturation concentration or the volumetric mass transfer coefficient (Pulido-Mayoral and Galindo, 2004).

#### 1.5.2.3.2 Shuttle mechanism

The shuttle mechanism proposes that oil droplets absorb oxygen in the gas-aqueous boundary layer, and then transfer the oxygen to the aqueous phase when they have returned to the bulk liquid (Figure 1.8). There is no direct evidence to prove the shuttle mechanism: the theory is based on experimental evidence that shows that the gas transfer rate is dependent on oil droplet size.

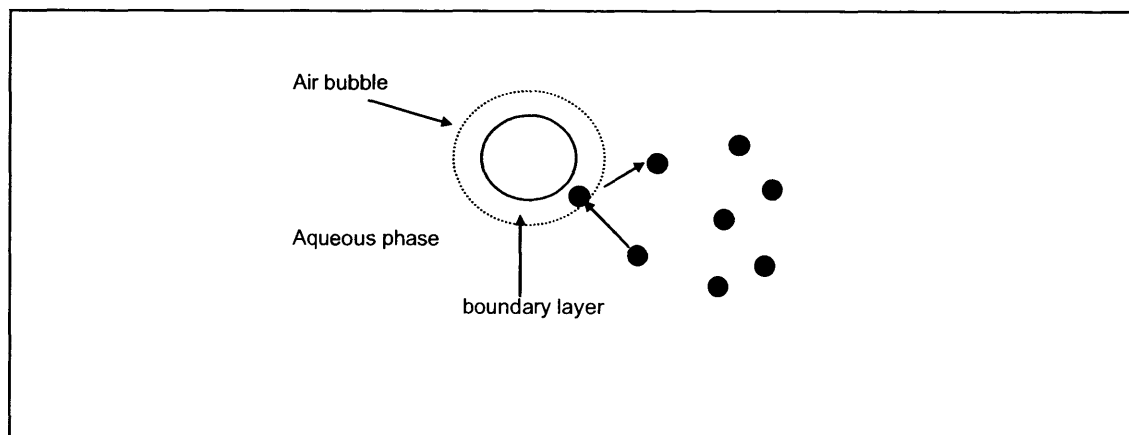


**Figure 1.8.** Schematic of the shuttle mechanism

Bruining *et al.* (1986) used emulsified cyclohexane and decane in a reactor with a flat gas – liquid interface, and found that the oxygen transfer rate only increased when the droplet diameters were the same size or smaller than the

film thickness. van der Meer *et al.* (1992) measured the  $k_L a$  during the growth of *Pseudomonas oleovorans* in the presence of neat and emulsified n-octane. The addition of 0-11%v/v n-octane had no effect on the  $k_L a$ , but the emulsified drops, which had smaller diameters, increased the oxygen transfer rate. Both Bruining *et al.* (1986) and van der Meer *et al.* (1992), concluded that the greatest increase in the oxygen transfer rate would occur when the drop size was small, and the oil volume fraction large. Nagy and Hadik (2003) used encapsulated silicone oils with different droplet diameters, and found that the oxygen transfer rate increased with decreasing particle size. However, once the oil droplets reached a small enough size there was no further increase in the oxygen transfer rate.

Solid particles that have a diameter smaller than the boundary layer thickness have also been shown to increase the oxygen transfer rate in stirred tank reactors and bubble columns (Beenackers and Swaaij, 1993).

### 1.5.3 Models

Many models have been developed to predict the enhancement factors obtained with oils (Brilman *et al.*, 2000). These models can be broadly categorised as either homogenous or heterogenous. Homogenous models are simpler than heterogenous models because they make the following assumptions:

- the fraction of oil is equally uniform in the gas – liquid phase film and the liquid bulk.
- ignore mass transfer in the dispersed droplets
- ignore geometrical effects such as the position of the oil droplets with respect to the interface and with respect to each other.
- assume gas diffuses perpendicular to the gas – liquid interface.

Bruining *et al.* (1986) developed a simple homogenous model based on the shuttle mechanism, which only requires the oxygen solubility of the oil to be known in order to predict the enhancement factor. Dumont and Delmas (2003) assessed the model using four different data sets from the literature and found

that it tended to underestimate the enhancement factor by 15 – 20 %. There may have been a discrepancy between the predicted and experimental results because the model does not take into account the effect of the oils on the  $k_{L,a}$ , and it also assumes that mass transfer only occurs perpendicular to the interface.

Littel *et al.* (1994) altered the model by assuming that a thin layer of oil surrounds the gas bubble. Nagy and Moser (1995) also altered the model to take into account the effects of liquid – liquid mass transfer and mass transfer within the drops. However, both of these altered models required parameters that could not be determined experimentally.

van Ede *et al.*, (1995) developed a homogenous model based on the bubble covering mechanism. It requires knowledge of the oxygen solubility and diffusivity in the oil, and it assumes that the fraction of oil in contact with the gas phase is the same as the volume fraction in the bulk. This model tended to overestimate the enhancement factor by 40 – 70% (Dumont and Delmas, 2003). van Ede *et al.* (1995) obtained a much better agreement between their experimental and predicted data when the model was altered to take into account the hold-up, drop diameter, and permeability of the oil. Although this model was in better agreement with the experimental data compared to the first, it did not give better agreement for the experimental data of other authors (Dumont and Delmas, 2003). The poor agreement between the experimental and predicted enhancement factor indicates that mass transfer enhancement does not occur via the bubble – covering mechanism.

Heterogeneous models take into account factors such as the location and the interaction between droplets in the boundary layer in the boundary layer the local geometry at the gas – liquid interface (Brilman *et al.*, 2000). Heterogeneous models have been developed to gain understanding about the mechanism of mass transfer enhancement. However, they are difficult to use because they require hydrodynamic and physical data that is difficult or

impossible to obtain experimentally. Therefore, for process design purposes homogenous models are of more practical use.

### 1.5.3.1 Description of homogenous model for the shuttle mechanism

The shuttle model of Bruining *et al.* (1986) assumes that the oil drops enter the boundary layer where they absorb oxygen, and are then returned to the bulk where oxygen is transferred from the oil to the bulk liquid phase.

The model makes the following assumptions:

solubility ratio between the oil and the aqueous phase is greater than 10

- no contact between the gas and the oil phase
- oil droplets are smaller than the boundary layer
- oil is homogeneously distributed throughout the aqueous phase
- mass transfer resistance within the oil can be resisted.

The model is based on the penetration theory of mass transfer. The theory assumes that the gas – water interface is covered with small stagnant fluid elements. The elements of fluid are brought to the interface where they are exposed to the gas phase for a defined interval of time. After a contact time of  $\tau$  the fluid elements return to the bulk phase, while new elements originating from the bulk take their place at the interface. Mass transfer is assumed to occur by unsteady state molecular diffusion.

Figure 1.9 shows a schematic of the model. The percentage saturation of the liquid against the distance from the gas - water interface is shown for two different exposure times. Initially only the surface layer contains solute and the concentration changes abruptly from 100 % to 0% at the interface. The graphs show the oxygen concentration at a depth of  $x$  for two different exposure times. If the exposure time is infinite and there is no reaction, the whole of the liquid will become saturated. It is assumed that the depth of the liquid element is infinite, which is reasonable if the time of exposure is sufficiently short for penetration to be confined to the surface layers.

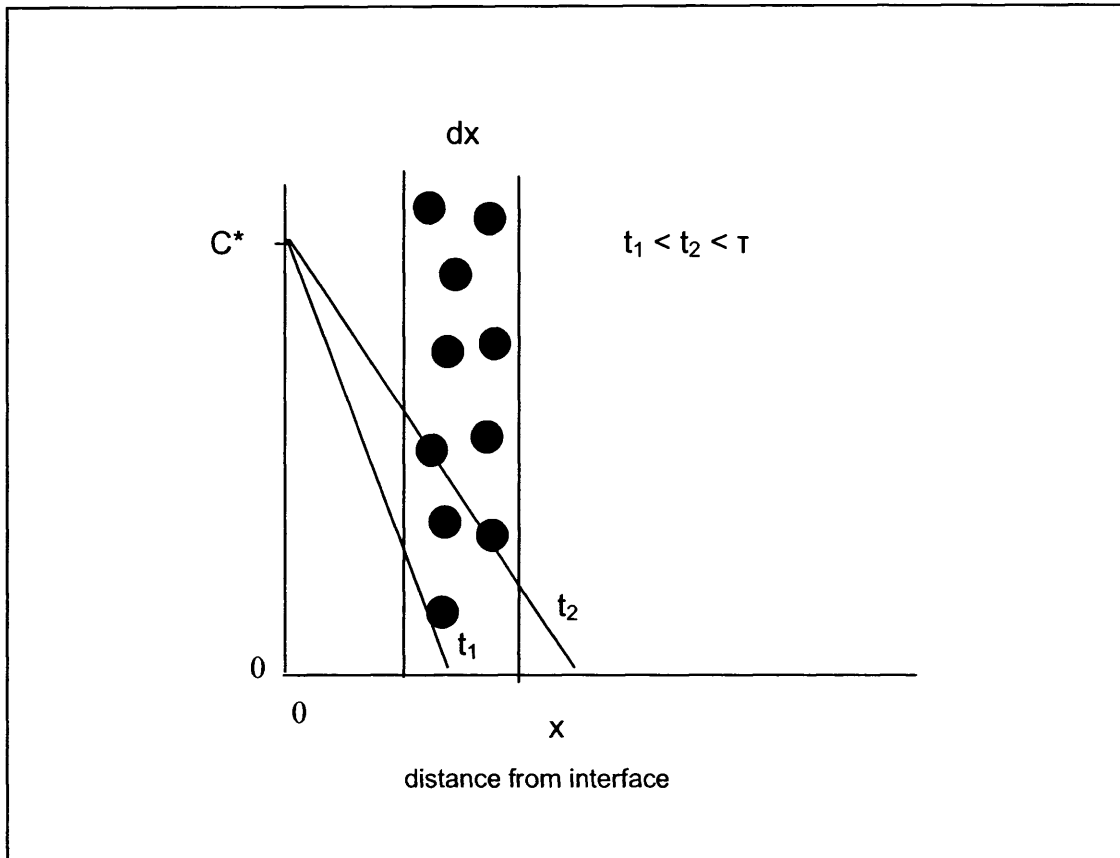


**Figure 1.9.** Schematic of concentration gradient at the gas – liquid interface with time according to the shuttle model of Bruining *et al.* (1986).

A mass balance over a slice  $dx$  of a liquid element in contact with the gas- water interface gives:

$$J = -D \frac{\delta c}{\delta x}(x+dx, t) + (1-\Phi) \frac{\delta c}{\delta t} dx + \Phi \frac{\delta(mc)}{\delta t} dx \quad (1.8)$$

where,  $J$  = is the mass flux of oxygen ( $\text{mol m}^{-2} \text{s}^{-1}$ ), and  $D$  is the diffusivity of oxygen ( $\text{m}^2 \text{s}^{-1}$ ),  $m$  is the solubility ratio, and  $c$  is the oxygen concentration ( $\text{mol l}^{-1}$ ). This reduces to the following differential equation, which represents the diffusion of oxygen away from the interface in the  $x$  direction.

$$D \frac{\delta^2 c}{\delta x^2} = (1-\Phi) \frac{\delta c}{\delta t} + \Phi \frac{\delta(mc)}{\delta t} \quad (1.9)$$

which in turn reduces to:

$$D \frac{\delta^2 c}{\delta x^2} = (1 + \Phi(m-1)) \frac{\delta c}{\delta t} \quad (1.10)$$

The following boundary conditions apply:

$$\begin{array}{lll} t = 0 & x > 0 & c = 0 \\ t > 0 & x = 0 & c = c^* \\ t > 0 & x = \infty & c = 0 \end{array}$$

The average flux of oxygen through the interface during the contact time  $t$  of a fluid element follows from:

$$N = \frac{1}{T} \int_0^T D \left( \frac{\delta c}{\delta x} \right)_{t,x=0} dt \quad (1.11)$$

The solution for this equation is:

$$N = 2 C^* \sqrt{\frac{D(1 + \Phi(m-1))}{\pi T}} \quad (1.12)$$

The enhancement factor is described as follows:

$$E_{\text{shuttle}} = \frac{\text{flux in the presence of droplets } \Phi \neq 0}{\text{flux in the absence of droplets } \Phi = 0} \quad (1.13)$$

Therefore the OUR enhancement factor by the shuttle mechanism can be described by:

$$E_{\text{shuttle}} = \sqrt{(1 + \Phi(m-1))} \quad (1.14)$$

## 1.6 Project Aims

There are three main aims of the project:

### 1. Investigate the effect of oxygen limitation on a whole-cell oxygenase bioconversion.

The specific activity of whole-cell oxygenases decreases when oxygen is limited. An understanding of the oxygen requirements of the electron transport chain and the oxygenase under aerobic conditions, and how the oxygen is split between the two when oxygen is limited will give an indication of which methods are most suitable for either preventing or alleviating oxygen limitation.

### 2. Investigate how the physiochemical properties of oils influence the oxygen transfer rate to the aqueous phase.

If organic solvents can be used to increase the oxygen transfer rate to the aqueous phase during whole-cell oxygenase bioconversions, it is of interest to know if this increase can be predicted from their physiochemical properties. This knowledge would assist in the selection of the optimum biocatalyst concentration and organic solvent volume fraction.

Oils with different oxygen solubilities, viscosities, and spreading coefficients will be used to determine the influence of these properties on the oxygen transfer rate to the aqueous phase at different volume fractions. The effect will be quantified by measuring the change in the OUR of an *E.coli* biocatalyst.

Oils are thought to increase the oxygen transfer rate by increasing the average saturation oxygen concentration i.e. increasing the driving force for mass transfer. If this is the case, the oxygen solubility of the oil should determine the increase in the oxygen transfer rate. However, the spreading coefficient and the viscosity of the oil can also influence the saturation concentration and the volumetric mass transfer coefficient. According to the bubble mechanism, oils can only increase the oxygen transfer rate if they can spread around the air bubbles, but there is no conclusive proof that this is correct. The viscosity of oils can affect the  $k_L a$ , the diffusivity of oxygen in the oil and the oil drop size. The

suitability of a homogenous model to predict the increase in the oxygen transfer rate will also be assessed.

**3. To show that oils can be used to alleviate oxygen limitation during whole-cell oxygenase bioconversions.**

The biocatalyst used throughout this work was a recombinant *E.coli* biocatalyst over-expressing cyclohexanone monooxygenase. An *E.coli* biocatalyst was selected because it is commonly used as a host for heterologous expression: it is easy to grow and the regulatory requirements are well understood.

The experimental work was split into four results chapters:

- The first chapter concerns the development of a standard fermentation for the production of the *E.coli* biocatalyst. The kinetics of the bioconversion was determined so that a standard bioconversion could be established.
- The second chapter investigated the oxygen consumption of the biocatalyst, and the effect of oxygen limitation on it.
- The third chapter investigated how the physical properties of the oils affect the oxygen transfer rate to the aqueous phase, and the suitability of a homogenous model to predict that.
- The fourth chapter demonstrated that the addition of an oil can increase the activity of an oxygen limited bioconversion.



## 2.0 Materials and Methods

### 2.1 Materials

#### 2.1.1 Chemicals

All materials were obtained from Sigma-Aldrich (Poole, Dorset, UK) except for: tryptone and (1S, 5R)-2-oxabicyclo[3.3.0]oct-6-en-3-one (Fluka, Poole, Dorset, UK); yeast extract and nutrient agar (Oxoid, Basingstoke, Hampshire, UK); Dow Corning 200 fluid 5cS and 50cS silicone oil (VWR, Poole, Dorset, UK). Bicyclo[3.2.0]hept-2-en-6-one and a 50:50 mixture of (1S, 5R)-2-oxabicyclo[3.3.0]oct-6-en-3-one and 1(R),5(S)3-oxabicyclo[3.3.0]oct-6-en-2-one was a gift from Roland Wolgemuth (Fluka, Poole, Dorset, UK)

#### 2.1.2 Microorganism

*E.coli* JM107 pQR210 was a gift from Dr John Ward (Department of Biochemistry and Molecular Biology, University College London).

### 2.2 Analytical techniques

#### 2.2.1 Substrate and product quantification by gas chromatography (GC)

##### 2.2.1.1 Preparation of samples

The samples were prepared by adding 400  $\mu$ l of the aqueous sample to an equal volume of ethyl acetate in a 1.5 ml Eppendorf tube. The liquids were vortex mixed for 30 seconds, and then centrifuged at 13000 rpm for 2 minutes (Biofuge 13, Heraeus Sepatech, Brentwood, Essex, UK). The ethyl acetate layer was then transferred to a vial and analysed.

##### 2.2.1.2 Quantification by gas chromatography (GC)

The substrates and products were analysed using a Perkin-Elmer autosystem XL-2 gas chromatograph (Perkin-Elmer, Connecticut, USA). 1  $\mu$ l samples were injected onto the column using an integrated autosampler. A flame ionisation detector (FID) detected compounds that exited the column. Data capture and analysis was achieved using Perkin-Elmer Nelson Turbochrom™ software.

#### **2.2.1.2.1 Cyclohexanone and caprolactone**

Cyclohexanone and  $\epsilon$ -caprolactone were analysed using an AT-1701 column (reverse phase silica, 30 m x 0.54 mm) (Alltech, Carnforth, Yorks, UK). The oven temperature was 100°C throughout.

#### **2.2.1.2.2 Bicycloheptenone and oxabicycloctenone**

Bicycloheptenone and its oxabicyclooctenone products were analysed using an AT-1701 column (reverse phase silica, 30 m x 0.54 mm) (Alltech, Carnforth, Yorks, UK). The oven temperature programme included an initial holding step at 100 °C for 5 minutes and then the temperature was ramped at 10 °C per minute until it reached 240°C.

#### **2.2.1.3 Quantification of the GC response**

External calibration curves were used to quantify the response of the FID for the substrates and products. Pure (1S,5R)-2-oxabicyclo[3.3.0]oct-6-en-3-one was used for the lactone standard. Typical calibration curves of concentration against peak area are shown in Appendix 1.

### **2.2.2 Biomass concentration**

#### **2.2.2.1 Dry cell weight (dcw) measurement**

Dry cell weights were measured by centrifuging (Biofuge 13, Heraeus Sepatech, Brentwood, Essex, UK) 1ml samples of culture at 13000rpm in pre-dried and pre-weighed Eppendorf tubes. The resulting cell pellet was resuspended in pH 7.0 50mM phosphate buffer, and then centrifuged for 4 minutes. The supernatant was removed and the Eppendorfs were placed in an oven at 100 °C until their weights were constant.

#### **2.2.2.2 Optical density (OD) measurement**

OD measurements were carried out at 600 nm ( $OD_{600}$ ) using a Uvikon 922 variable wavelength spectrophotometer (Kontron, Watford, UK). The cultures were diluted with RO water so that the OD was between 0.1-1 absorbance units. A calibration curve showing the correlation between the optical density

and the dry cell weight was prepared using samples from a growing shake flask culture and is shown in Appendix 1.

### 2.2.3 Intracellular CHMO activity

Intracellular CHMO enzyme activity was measured using the method of Doig *et al.* (2001). Samples of fermentation broth were centrifuged for 2 minutes at 13000 rpm (Biofuge 13, Heraeus Sepatech, Brentwood, Essex, UK) and the resulting cell pellet suspended in the reaction buffer (Tris-HCL buffer 50mM pH 9, bovine serum albumin 7.14 g l<sup>-1</sup>). The resuspended cells were sonicated on ice at an amplitude of 8  $\mu$ m of 5 cycles at 10 seconds on/ 10 seconds off (Soniprep 150 MSE, Sanyo,Crawley, Sussex, UK). The sample was then re-centrifuged for 2 minutes at 13000rpm to remove insoluble cell debris. The CHMO activity was calculated from the rate of NADPH utilisation upon the addition of cyclohexanone and NADPH to the CHMO sample. NADPH absorbs strongly at 340 nm ( $\epsilon = 6.22\text{ml } \mu\text{mol}^{-1}\text{cm}^{-1}$ ) and its consumption is stoichiometrically linked to product formation. In a final volume of 1ml the following reagents – expressed as final concentrations – were added to a 1.5 ml reaction cuvette: (Tris-HCL buffer 50mM pH 9, bovine serum albumin 7.14 g l<sup>-1</sup>, 0.161mM NADPH, 2mM cyclohexanone). The rate of NADPH consumption was measured at 340 nm and 37°C with a Kontron Uvikon 922 (Kontron, Watford, Herts, UK) variable wavelength spectrophotometer fitted with a thermostated cell.

### 2.2.4 Glycerol assay

The glycerol concentration was determined using glycerol enzymatic test kit of Boehringer-Mannheim Roche (R-Biopharm GmbH, Darmstadt, Germany). The assay linked the glycerol concentration to NADH oxidation via three enzyme catalysed reactions. First, glycerokinase catalysed the phosphorylation of glycerol by adenosine-5'-triphosphate (ATP) to L-glycerol-3-phosphate. Second, pyruvate kinase converted phosphoenolpyruvate to pyruvate and ATP. Third, L-lactate dehydrogenase reduced pyruvate to L-lactate with the concomitant conversion of NADH to NAD. NADH oxidation was followed spectrophotometrically by measuring the total difference in absorbance at 340 nm on completion of the above reactions using a Uvikon 922 variable

wavelength spectrophotometer (Kontron, Watford, Herts, UK). Samples were prepared by centrifuging cultures at 13000 rpm for 2 minutes (Biofuge 13, Heraeus Sepatech, Brentwood, Essex, UK) to remove the biomass. The supernatant was then used in the assay.

### 2.2.5 Exit – gas measurement

The exit gas was analysed by a mass spectrometer (Prima 600, VG Gas Analysis, Cheshire, UK).

## 2.3 Routine cultivation and storage of *E.coli*

Master stocks of *E.coli* were prepared by spreading 50µl of a cell suspension, which had been grown from an individual colony, on agar plates made from nutrient agar and containing 100 mg l<sup>-1</sup> ampicillin. The cells were grown in an incubator overnight at 37°C overnight, and then resuspended aseptically in 1ml of a sterilised 20 % (v/v) glycerol solution. The resuspended cells were pooled and then added to sterilised Eppendorf tubes and stored at -70°C.

## 2.4 Fermentations

### 2.4.1 Growth media

The *E.coli* was grown on the media components listed in Table 2.1. All of the media components, except for ampicillin, were sterilized together at 121°C for 20 minutes. The ampicillin was sterilized with 0.2 µm syringe filters and added to the media just before inoculation.

Component	Concentration gl <sup>-1</sup>
yeast extract	24
tryptone	12
glycerol	10
potassium phosphate monobasic	2.3
potassium phosphate dibasic	12.5
ampicillin	0.1

**Table 2.1.** Composition of growth media used in all fermentations.

### 2.4.2 Inoculum preparation

The inoculum for the fermentations was grown in 1l shake flasks that contained 150 ml of the growth media listed in Table 2.1. The pH was adjusted to 7.0 before sterilization. The flasks were inoculated with frozen stocks that were prepared as described in Section 2.3. The flasks were then placed overnight in an orbital shaker at 37°C and 200rpm (New Brunswick Scientific, Edison, NJ, USA).

### 2.4.3 Shake flask fermentations

Shake flask fermentations were carried out in 1l shake flasks with four diametrically opposed baffles. The shake flasks each contained 45 ml of growth media listed in Table 2.1. The pH was adjusted prior to sterilization with 3M H<sub>3</sub>PO<sub>4</sub>. The flasks were inoculated aseptically with 5ml of culture that was grown as described in Section 2.4.2. The cultures were grown in an orbital shaker at 37°C and 200rpm (New Brunswick Scientific, Edison, USA). In some experiments isopropyl-β-D-thiogalactopyranoside (IPTG) was added to the culture 210 minutes after inoculation. The IPTG was sterilized using a 0.2µm filter, and the final concentration in the shake flasks was 1mM.

### 2.4.4 7l fermentations

#### 2.4.4.1 Fermentation equipment

Fermentations were carried out in a Inceltech 7 l stirred tank fermenter with a 5 l working volume (Inceltech, Pangbourne, Berks., UK). The vessel was 40 cm high and 15 cm in diameter with an H:T ratio of 2.63. The pH was measured by a steam sterilisable Ingold pH probe (Ingold Messtechnik, Urdorf, Switzerland) and maintained by the metered addition of 3M NaOH and 3M H<sub>3</sub>PO<sub>4</sub>. The dissolved oxygen tension (DOT) was measured by a steam sterilizable polarographic oxygen electrode (Ingold Messtechnik, Urdorf, Switzerland). The fermenter was fitted with two six bladed rushton turbines and four diametrically opposed baffles. The temperature was controlled using a temperature probe and heating element (Bioprocess Engineering Services Ltd, Kent, UK). The vessel was aerated via a submerged sparger. The inlet and exit gases were

filtered through 0.2  $\mu\text{m}$  filters (Gelman Sciences, Ann Arbor, MI, USA). The impeller speed, aeration rate, pH, and DOT were logged and recorded using Bioview software (Adaptive Biosystems, Watford, Herts., UK).

#### **2.4.4.2 Fermentation operation**

The fermenter was filled with 4.55 l of the media listed in Table 2.1 and 1 mL polypropylene glycol 2000 (PPG), and then sterilized in place. After the media had cooled down the pH was adjusted to 7.0. Ampicillin was added to the fermenter through a 0.2  $\mu\text{m}$  filter immediately before inoculation. The fermenter was inoculated with 450 ml of culture grown as described in Section 2.4.2. The growth of the *E.coli* was followed by periodically measuring the OD<sub>600</sub> as described in Section 2.2.2.2. The operating conditions of the fermenter were as follows: agitation speed 900 rpm; temperature 37°C; aeration rate 1 VVM; pH 7.0.

## **2.5 Shake flask bioconversions**

### **2.5.1 Whole-cell activity assay**

The whole-cell activity of the *E.coli* biocatalyst was determined in 1l shake flasks using a 20 ml working volume. The biocatalyst was grown as described in Section 2.4.3. The biocatalyst was suspended in 50 mM phosphate buffer at pH 7.0 so that the final biocatalyst concentration was  $1\text{g}_{\text{dcw}}\text{l}^{-1}$ . Glycerol was added so that the final concentration was  $5\text{gl}^{-1}$ . The shake flask was then placed in an orbital shaker at 37°C and 200rpm for five minutes to pre-warm the biocatalyst suspension to 37°C. Concentrated stock solutions of the substrates were made and added to the flasks so that the final substrate concentration was  $1\text{gl}^{-1}$ . Each bioconversion lasted 20 minutes; samples were taken every four minutes and were analysed as described in Section 2.2.1. In subsequent shake flask conversions the biomass, glycerol, substrate and product concentrations were altered.

#### **2.5.1.1 Effect of substrate and product concentration on the activity**

##### **2.5.1.1.1 Cyclohexanone and $\epsilon$ -caprolactone**

The whole-cell assay described in Section 2.5.1 was used, but the initial cyclohexanone and  $\epsilon$  – caprolactone concentration was varied. The cyclohexanone concentration was varied between 0.25 and 8  $\text{gl}^{-1}$ . The  $\epsilon$  – caprolactone concentration was varied between 0 and 10  $\text{gl}^{-1}$ . Both the cyclohexanone and the  $\epsilon$  – caprolactone were dissolved in 50mM phosphate buffer (pH 7.0) to make a concentrated stock solution. The  $\epsilon$  – caprolactone was added to the shake flask just before the cyclohexanone was added to start the reaction.

### 2.5.1.1.2 Bicycloheptenone and oxabicyclooctenone

The whole-cell assay described in Section 2.5.1 was used, but the initial bicycloheptenone and oxabicyclooctenone concentration was varied. The bicycloheptenone concentration was varied between 0.25 and 4  $\text{gl}^{-1}$ . The oxabicyclooctenone concentration was varied between 0 and 8  $\text{gl}^{-1}$ . For the product inhibition experiments the bicycloheptenone concentration was 1 $\text{gl}^{-1}$ . The bioconversion produces the two stereoisomers in approximately equal proportions. To reflect this, a stock solution that contained a 50:50 mixture of the two stereoisomers was used. Both the substrates and the products were dissolved in 50mM phosphate buffer (pH 7.0) to make concentrated stock solutions. The combined lactones were added to the shake flask just before the bicycloheptenone was added to start the reaction.

## 2.6 2l Fermenter bioconversions

### 2.6.1 Description of the 2l fermenter

Bioconversions were carried out in a 2l fermenter with a 1.4l working volume. The vessel was 20.4 cm high and 12.2 cm in diameter. The pH was measured by a steam sterilisable pH probe (Mettler Toledo, Leicester, UK), and was maintained by the metered addition of 3M NaOH and 3M  $\text{H}_3\text{PO}_4$ . The dissolved oxygen tension (DOT) was measured by a steam sterilisable polarographic oxygen electrode (Ingold Messtechnik, Urdorf, Switzerland). The fermenter was fitted with two six bladed rushton turbines and four diametrically opposed baffles. The temperature was controlled using a temperature probe and heating element (Bioprocess Engineering Services Ltd, Kent, UK). The

vessel was aerated via a submerged sparger. The inlet and exit gases were filtered through 0.2  $\mu\text{m}$  filters (Gelman Sciences, Ann Arbor, MI, USA). The impeller speed, aeration rate, pH, and DOT were logged and recorded using Bioview software (Adaptive Biosystems, Watford, Herts, UK).

### 2.6.2 Bioconversion procedure

Bioconversions were carried out in the 2l fermenter with a 1.4l working volume described in Section 2.6.1. The *E.coli* biocatalyst was produced in a 7l fermenter as described in Section 2.4.4. Bioconversions were carried out at biomass concentrations ranging from 0.5 – 5  $\text{g}_{\text{dcw}}\text{l}^{-1}$ . The harvested *E.coli* was diluted to the appropriate concentration using spent media. The spent media was obtained by centrifuging a culture produced in a 7l fermenter as described in Section 2.5.3 at 4000 rpm for 30 minutes (Heraeus Megafuge, Heraeus Instruments Ltd, Brentwood, Essex, UK). The supernatant was then used to resuspend the biomass. Glycerol was added so that the final concentration was 5  $\text{g}\text{l}^{-1}$ .

The resuspended biomass was placed in the fermenter and heated to 37°C. The bioconversions were started by the addition of 1.4 g of bicycloheptenone so that the initial concentration in the fermenter was 1 $\text{g}\text{l}^{-1}$ . The bioconversions were carried out for 30 minutes. 2ml samples were taken every five minutes. The concentration of the substrate and product were determined as described in Section 2.2.1. The optical density was also measured so that any change in the biomass concentration could be accounted for when determining the specific OUR. The experiments were carried out using an impeller speed of either 700 or 900rpm and using an aeration rate of 1vvm. The pH was maintained at pH 7.0.

### 2.7 Determination of the critical oxygen concentration

The effect of the dissolved oxygen concentration on the specific OUR of the biomass was determined in the 2l fermenter described in Section 2.6.1. The biomass was grown in multiple 1l shake flasks with a 50ml working volume as described in Section 2.4.3. A final biomass concentration of 1 $\text{g}_{\text{dcw}}\text{l}^{-1}$  was



obtained by suspending the biomass in spent media. Glycerol was added so that the concentration was approximately  $5 \text{ g l}^{-1}$ . The experiments were carried out at  $37^\circ\text{C}$ . The DOT was set by the impeller speed, and the aeration rate was 1vvm. Fresh cells were used for each DOT. To ensure that the glycerol concentration did not effect the OUR of the biocatalyst, the OUR of  $1 \text{ g}_{\text{dcw}} \text{ l}^{-1}$  of the biocatalyst was measured at different glycerol concentrations. The DOT was maintained above zero so that oxygen was not limited, and the OUR was recorded for twenty minutes. Figure A.4 in Appendix 2 shows that the OUR was not effected by the initial glycerol concentration.

## 2.8 Effect of the oils on the OUR

To determine the effect of the oils on the oxygen uptake rate, the oils were added to a suspension of the biocatalyst. After the oils were added, the DOT could not increase above zero because the driving force would change - any increase in the oxygen uptake rate would be underestimated.

The maximum OUR using an impeller speed of 700 rpm and an aeration rate of 1vvm was  $47 \text{ mmol l}^{-1} \text{ h}^{-1}$ . The maximum specific OUR of the *E.coli* biocatalyst was  $20 \text{ mmol g}_{\text{dcw}} \text{ l}^{-1} \text{ h}^{-1}$ . If it is assumed that the highest enhancement factor will not exceed 3, the maximum OUR of the cells must be  $141 \text{ mmol l}^{-1} \text{ h}^{-1}$  or higher. If  $7 \text{ g}_{\text{dcw}} \text{ l}^{-1}$  *E.coli* JM107, which has a maximum OUR of  $20 \text{ mmol g}_{\text{dcw}}^{-1} \text{ l}^{-1} \text{ h}^{-1}$ , is used, the maximum OUR will be  $140 \text{ mmol l}^{-1} \text{ h}^{-1}$ .

The experiments were done in a 2l fermenter with a 1.4l working volume, which was described in Section 2.6.1. The *E.coli* biocatalyst was grown as described in Section 2.4.4.2 and harvested at a biomass concentration of  $7 \text{ g}_{\text{dcw}} \text{ l}^{-1}$ . 1.4 l of the biomass was placed in the 2l fermenter. Glycerol was added so that the final concentration was approximately  $5 \text{ g l}^{-1}$ . The biomass was pre-warmed to  $37^\circ\text{C}$ . The pH was controlled at pH 7.0 with 3M NaOH and 3M  $\text{H}_3\text{PO}_4$ .

Before the addition of oil, the OUR was recorded for fifteen minutes to ensure that it had reached a steady state. The appropriate volume of biomass was then removed from the fermenter and replaced with an equal volume of oil that had

been pre-saturated with air for half an hour before the experiment began. The OUR was recorded for 30 minutes after the addition of the oil to ensure that the oil droplets and air bubble diameters had reached equilibrium. The oil was added at four volume fractions: 0.01, 0.05, 0.1 and 0.2. The volume of oil required for each volume fraction is shown in Table 2. 2

Volume fraction ( $\Phi$ )	Volume of biomass removed (ml)
0.01	14
0.05	70
0.10	140
0.20	280

**Table 2.2.** Volume of oil added at each volume fraction.

## 2.9 Physical properties of oils

### 2.9.1 Density

Liquid density was determined by weighing 1 ml liquids volumes on a Mettler-Toledo AB54 mass balance (Leicester, UK). All measurements were performed in triplicate.

### 2.9.2 Surface and interfacial tensions

Surface and interfacial tensions were determined using a Kruss 10 tensiometer (Kruss, Palaiseau, France). The surface tension was measured using a Wilhelmy plate. Approximately 30ml of liquid was placed in a jacketed glass vessel. The liquid was pre-warmed to 37°C and maintained at that temperature by circulating warm water through the jacket of the glass vessel. The Wilhelmy plate was suspended vertically above the liquid by being attached to the tensiometer balance. The plate was then lowered onto the surface of the liquid so that about 1mm of the plate was immersed.

The interfacial tension was measured using the dynamic Wilhelmy method. The plate was lowered onto the surface of the heavy liquid that had been pre-warmed to 37°C and maintained at that temperature by circulating warm water through the jacket of the glass vessel. The light liquid, which had been pre-warmed to 37°C, was then poured over the heavy liquid until the whole plate was immersed in the light phase. The plate was then slowly lifted out of the interface between the two liquids by the balance. All measurements were performed in triplicate.

### 2.9.3 Spreading coefficient

The spreading coefficients were calculated from the following equation:

$$S_{OW} = \sigma_{WG} - (\sigma_{OG} + \sigma_{OW}) \quad (2.1)$$

Where,  $S_{OW}$  is the spreading coefficient of oil on water,  $\sigma_{WG}$  is the surface tension of the aqueous phase,  $\sigma_{OG}$  is the surface tension of the oil, and  $\sigma_{OW}$  is the interfacial tension between the aqueous phase and oil. Spreading coefficients were calculated for each of the oils on complex media and on complex media with  $7\text{gl}^{-1}$  *E.coli*.

### 2.9.4 Viscosity

#### 2.9.4.1 Viscosity measurements

The liquid viscosity was measured using a Contraves Rheomat 115 rheometer (Contraves AG, Zurich, Switzerland). The rheometer used the cup and bob to measure the viscosity. The liquids were pre-warmed to 37°C and then poured into the cup. The outer cylinder (cup) was stationary whilst the inner cylinder (bob) was rotated. The rheometer measured the braking torque exerted on the inner cylinder rotated in the dispersion. The braking torque is a function of the shear stress and the shear rate exerted on the inner cylinder, which are related to the apparent fluid viscosity by:

$$\mu = \frac{\tau\zeta}{\dot{\gamma}} \quad (2.2)$$

where  $\mu$  is the apparent viscosity,  $\tau$  is the shear stress per unit torque,  $\zeta$  is the torque read out from the rheometer control panel, and  $\gamma$  is the shear rate. To simplify calculations the manufacturers of the rheometer have put together a series of values,  $\eta$  (Equation 2.3) where:

$$\eta = \frac{\tau}{\gamma} \quad (2.3)$$

So the calculations reduce to Equation 2.4:

$$\mu = \eta\zeta \quad (2.4)$$

The shear stress at each rheometer setting is determined by multiplying the manufacturers value of shear stress per unit torque by the torque reading at each setting. The final values recorded were the average of three measurements. All measurements were performed in triplicate.

#### 2.9.4.2 Average viscosity

The relative viscosity of the dispersion at each volume fraction was estimated using the following equation:

$$\mu_m = \frac{\mu_c}{1-\phi} \left( 1 + \frac{1.5\phi\mu_d}{\mu_c + \mu_d} \right) \quad (2.5)$$

where,  $\mu_m$  is the relative viscosity,  $\mu_c$  is the viscosity of the continuous phase, and  $\mu_d$  is the viscosity of the dispersed phase. In principle this equation is only valid for dilute dispersions where the volume fraction is less than 0.15 (Guilinger *et al.*, 1988; Marcelis *et al.*, 2003). However, it was also used for a volume fraction of  $\Phi = 0.2$  because a more accurate calculation is not available.

## 2.9.5 Oxygen solubility

### 2.9.5.1 Average oxygen concentration

Oxygen solubility data was taken from the literature. The average oxygen solubility of the dispersions at each volume fraction was calculated using the following equation (MacMillan and Wang, 1990):

$$C_{ave} = (1 - \phi)C^* + \phi C_{oil}^* \quad (2.6)$$

where  $C_{ave}$  is the bulk average oxygen concentration,  $\phi$  is the volume fraction,  $C^*$  is the saturation concentration of the aqueous phase, and  $C_{oil}^*$  is the saturation concentration of the oil.

### 2.9.5.2 Oxygen diffusivity

The oxygen diffusivity of the aqueous phase was determined using the correlation of Wilke – Chang (Green, 1997):

$$D_{AB} = 7.4 \times 10^{-8} \cdot \frac{(\phi M_B)^{0.5} T}{\mu_B V_A^{0.6}} \quad (2.7)$$

where,  $D_{AB}$  is the diffusion coefficient of solute A in solvent B,  $\phi$  is the association factor for B (2.6 for water),  $M_B$  is the molecular weight of B,  $T$  is the temperature (K),  $\mu_B$  is the viscosity of B,  $V_A$  molar volume of solute A at its normal boiling temperature.

The Wilke-Chang correlation is not accurate for the determination of diffusivity in organic compounds. Therefore for the oils the Scheibel correlation was used (Green, 1997):

$$D = \frac{KT}{\mu_B V_A^{0.33}} \quad (2.8)$$

where,

$$K = 8.2 \times 10^{-8} \cdot \left[ 1 + \left( \frac{3V_B}{V_A} \right)^{2/3} \right] \quad (2.9)$$

where  $V_B$  is the molar volume of solute B at its normal boiling temperature.

### 2.9.5.3 Oxygen permeability

The oxygen permeability is the product of the oxygen solubility and diffusivity:

$$P_{O_2} = C^* D_{AB} \quad (2.10)$$

where,  $P_{O_2}$  is the permeability,  $C^*$  is the saturation oxygen concentration of the oil, and  $D_{AB}$  is the diffusivity of oxygen in the liquid.

### 2.10 Power input

The power input of the 2l fermenter was measured by placing the vessel on a turntable supported on an air layer (air bearing technique). When the impeller was switched on, the force,  $F$ , required to stop the rotation of the vessel on the air-bearing, was recorded with a load cell and the power input into the vessel was calculated according to:

$$P = 2\pi N R F \quad (2.11)$$

where,  $P$  is the power consumption,  $N$  is the impeller rotational speed,  $R$  is the distance between the load cell and the centre of the tank and  $F$  is the force.

### 2.11 Sauter mean drop diameter

The Sauter mean droplet sizes were estimated using two different correlations. The correlation of Godfrey and Crilic (1977) is applicable for oils with a viscosity below 10cS:

$$\frac{d_{32}}{D} = 0.058(1 + 3.6\phi)(We_T)^{-0.6} \quad (2.12)$$

where,  $d_{32}$  is Sauter mean drop diameter,  $D$  is the impeller diameter,  $N$  is the rotational speed of the impeller,  $\Phi$  is the volume fraction, and  $We_T$  is the Weber number in a mixing tank ( $= \rho N^2 D^3 / \sigma$ ).

The Nishikawa *et al.* (1987) correlation can be used for oils with higher viscosities:

$$\frac{d_{32}}{D} = 0.095 \cdot N^{-0.4} \cdot (We_T)^{-0.6} \cdot (1 + 2.5\phi^{2/3}) \left( \frac{\mu_d}{\mu_c} \right)^{0.2} \left( \frac{\mu_d}{\mu_c} \right)^{0.125} \quad (2.13)$$

$\mu_d$  is the viscosity of the dispersed phase,  $\mu_c$  is the viscosity of the continuous phase,  $\rho$  is the density of the continuous phase, and  $\sigma$  is interfacial tension.

## 2.12 Volumetric mass transfer coefficient ( $k_L a$ )

### 2.12.1 $k_L a$ measurement

The volumetric mass transfer coefficient was determined using the dynamic method (Dunn and Einsele, 1975). The  $k_L a$  was determined using the media listed in Table 2.1. The media was placed in the 2l fermenter and the contents pre-warmed to 37°C. The DOT was measured using a polarographic oxygen electrode (Ingold Messtechnik, Urdorf, Switzerland). The DOT was recorded using a Squirrel 2000 datalogger (Grant, Cambridge, UK). The media was sparged with nitrogen to deoxygenate the media. When the DOT reached zero, air was reintroduced and the DOT returned to 100%. The experiments were carried out using the oil volume fractions listed in Table 2.2.

### 2.12.2 Data analysis

The data was analysed using the method of Lamping *et al.* (2003). The rate of change of the oxygen concentration during the re-oxygenation step is:

$$\frac{dC}{dt} = k_L a (C^* - C) \quad (2.14)$$

where  $C$  is the oxygen concentration,  $C^*$  is the saturation oxygen concentration, and  $k_L a$  is the volumetric mass transfer coefficient. Assuming that the  $k_L a$  is constant with time equation can be integrated to give:

$$k_L a = \frac{1}{t} \cdot \ln\left(\frac{C^*}{C^* - C}\right) = \frac{1}{t} \cdot \ln\left(\frac{1}{C_L}\right) \quad (2.15)$$

where  $C_L$  is a normalised oxygen concentration defined by

$$C_L = \frac{C^* - C}{C} \quad (2.16)$$

The DOT probe did not respond instantaneously to the change in the dissolved oxygen tension in the fermenter. Therefore, the delay in the probe response had to be accounted for. The probe response time ( $\tau_p$ ) is defined as the time it takes the probe to reach 62.5% of its response reading when the probe has been moved from an environment with a DOT of 0% to 100%. The probe signal ( $C_e$ ) can be related to the real dissolved oxygen tension by a first order equation:

$$\frac{dC_e}{dt} = \frac{1}{\tau_p} (C - C_e) \quad (2.17)$$

The electrode response time was determined by quickly switching the electrode from a beaker of water with 0% DOT to a fermenter that had a DOT of 100%. The fermenter was operating at an impeller speed of 700 rpm and an aeration rate of 1vvm to match the hydrodynamic conditions of the fermenter that were used to determine the  $k_L a$ . The probe response time was 14 seconds.

Substituting for  $C_L$  in equation 2.15 and integrating gives:

$$C_p = \frac{1}{t_m - \tau_p} \cdot \left[ t_m \cdot \exp\left(\frac{-t}{t_m}\right) - \tau_p \cdot \exp\left(\frac{-t}{\tau_p}\right) \right] \quad (2.18)$$



The  $k_La$  was estimated using the Lineweaver – Marquart procedure, which utilizes the least squares non-linear regression.

## 2.13 2l Fermenter bioconversions with FC-40

### 2.13.1 Experimental design

The purpose of the bioconversions was to investigate the effect of FC-40 on the oxygen uptake rate at different volume fractions. So that the effects of FC-40 were not underestimated, the biocatalyst had to be oxygen limited enough so that the DOT did not increase above zero. At a volume fraction of 0.2, FC-40 increased the oxygen transfer rate to the aqueous phase 2.1 fold. The maximum oxygen transfer rate that can be achieved at 700 rpm and 1 vvm is:

$$47 \text{ mmol l}^{-1} \text{ h}^{-1} \times 2.1 = \mathbf{99 \text{ mmol l}^{-1} \text{ h}^{-1}}$$

The maximum potential OUR of a 1.12 l suspension with a biocatalyst concentration of  $4\text{g}_{\text{dcw}}\text{l}^{-1}$  is:

$$30 \text{ mmol g}_{\text{dcw}}^{-1} \text{ h}^{-1} \times 4\text{g}_{\text{dcw}}\text{l}^{-1} \times 1.12 \text{ l} = \mathbf{134 \text{ mmol l}^{-1} \text{ h}^{-1}}$$

Therefore, the biocatalyst concentration in the aqueous phase was  $4 \text{ g}_{\text{dcw}} \text{ l}^{-1}$  for all the experiments. Bioconversions were carried out using the volume fractions listed in Table 2.2.

### 2.13.2 Bioconversion procedure

Bioconversions were carried out in the 2l fermenter with a 1.4l working volume, described in Section 2.6.1. The biocatalyst was grown in a 7l fermenter as described in Section 2.4.4.2. Bioconversions were carried out at five different volume fractions: the volume of the aqueous phase and the FC-40 are listed in Table 2.3. The biocatalyst was harvested and diluted to the appropriate volume with spent media to the appropriate concentration, and then the appropriate volume of FC-40 was added. The fermenter was pre-warmed to 37°C.

Volume Fraction	Aqueous volume l	Oil volume l
0	1.400	0
0.01	1.386	0.014
0.05	1.330	0.070
0.10	1.260	0.140
0.20	1.120	0.280

**Table 2.3** Composition of the fermenter during bioconversions with FC-40.

To minimise any toxic effects of the substrate or product on the *E.coli* biocatalyst the initial concentration of the substrate in the aqueous phase was  $1\text{g l}^{-1}$ . The appropriate mass of substrate was weighed and then added to the fermenter using a Pasteur pipette. The bioconversions were carried out for 30 minutes. Samples were taken every five minutes. 2ml of the dispersion was removed through the sampling port and placed into an Eppendorf tube. The FC-40 and the aqueous phase were separated by centrifuging the Eppendorf for one minute at 13000 rpm. The aqueous phase was then analysed as described in Section 2.2.1.

## 2.14 Solubility and partition coefficients

### 2.14.1 Solubility in FC-40

The solubility of bicycloheptenone and oxabicyclooctenone in FC-40 were determined by adding excess quantities to 10ml FC-40. The bottles were sealed and agitated overnight at  $37^{\circ}\text{C}$ . FC-40 was partly soluble in ethyl acetate, so to determine the concentration in FC-40 a sample was taken and mixed with an equal volume of phosphate buffer. The aqueous phase was then analysed as described in Section 2.21.

### 2.14.2 Partition coefficients between phosphate buffer and ethyl acetate

Solutions of either bicycloheptenone or oxabicyclooctenone at a concentration of  $1\text{g l}^{-1}$  in phosphate buffer were prepared. An equal volume of FC-40 was

added, and the mixtures were then agitated overnight at 37°C. The aqueous phase concentration was then analysed as described in Section 2.2.1.

## 3.0 Production of the *E.coli* biocatalyst and characterisation of the bioconversion kinetics

### 3.1 Introduction

The first aim of this chapter was to develop a fermentation process to produce the *E.coli* biocatalyst. This was necessary because sufficient biocatalyst was needed for subsequent experiments that were carried out in a 2l fermenter. Therefore, a reliable fermentation process, which produced a consistent growth profile, biomass concentration, and CHMO activity, was required.

A fermentation process was first developed for a 1l shake flask with a 50ml working volume, and then for a 7l fermenter with a 5l working volume. They were developed by adapting the approach of *Doig et al.* (2001; 2002a), who demonstrated that a recombinant *E.coli* over-expressing CHMO could be produced at 1.5l and 300l scales, using a batch fermentation with complex media, and glycerol as a carbon source.

The second aim was to characterise the kinetics of the bioconversion of two ketone substrates to their respective products. The two reaction schemes that were used are shown in Figure 3.1. The first was the bioconversion of cyclohexanone and  $\epsilon$ -caprolactone. The second was the bioconversion of bicyclo[3.2.0]hept-2-en-6-one to (1S, 5R)-2-oxabicyclo[3.3.0]oct-6-en-3-one and 1(R),5(S)-3-oxabicyclo[3.3.0]oct-6-en-2-one.

The aim was first to determine the maximum specific activity that could be obtained, and second to determine which of the bioconversions causes the least inhibition of activity. In subsequent experiments, batch bioconversions were carried out to characterize the oxygen consumption, and it was therefore desirable to avoid both substrate and product inhibition as much as possible.

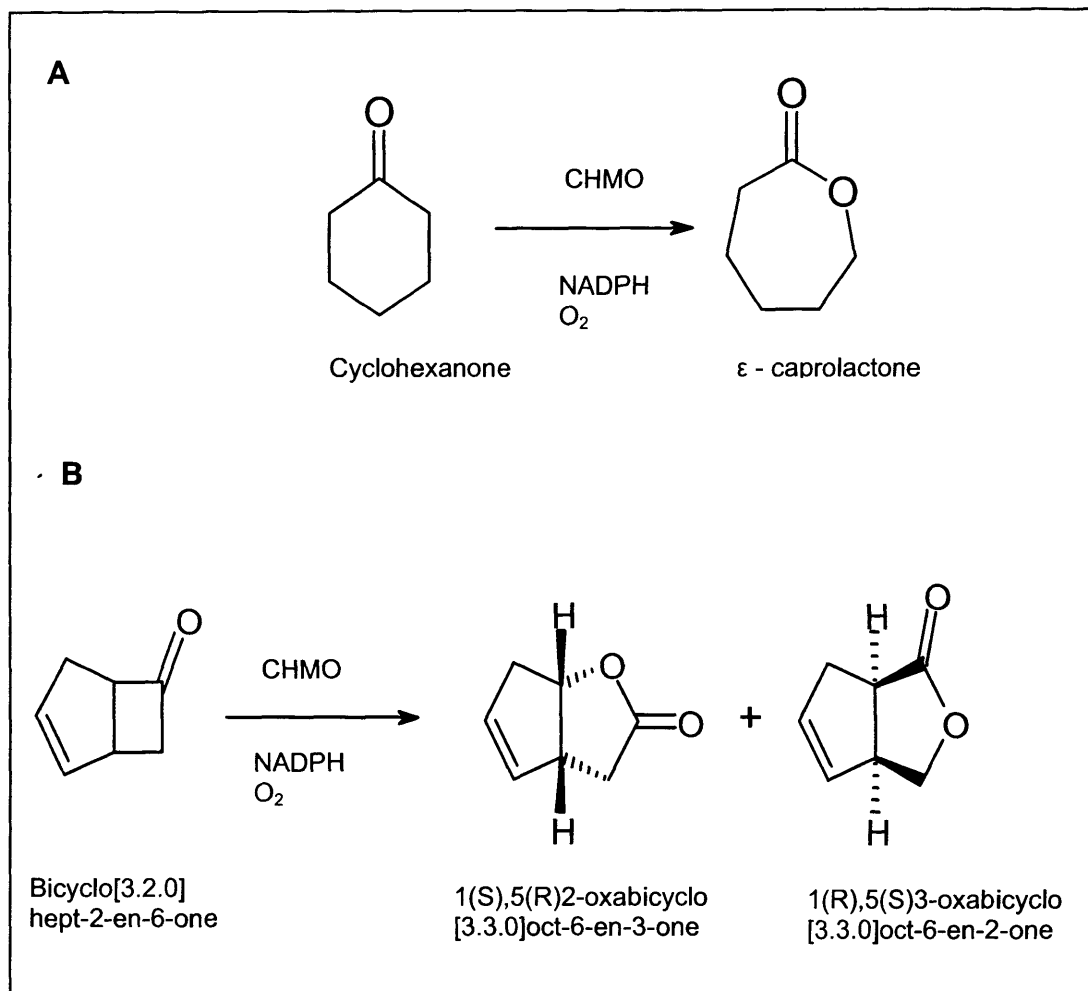


**Figure 3.1.** Reaction schemes for the two substrates. A. – cyclohexanone. B - bicyclo[3.2.0]hept-2-en-6-one.

## 3.2 Results and Discussion

### 3.2.1. Production of the *E.coli* biocatalyst in shake flasks

The *E.coli* was grown in 1l shake flasks as described in Section 2.4.3. The aim of the shake flasks experiments was to determine an appropriate time to add IPTG to induce the expression of CHMO. Figure 3.2 shows the biomass concentrations and the specific intracellular CHMO activities of growing *E.coli* cultures that did and did not have 1mM IPTG added at 210 minutes. The data points are the average of three repeats - error bars are omitted for clarity.

Induced and non-induced cultures both had specific growth rates of  $0.56 \text{ h}^{-1}$  and final biomass concentrations of  $9.8 \pm 0.2 \text{ g}_{\text{dcw}}\text{l}^{-1}$  and  $9.2 \pm 0.5 \text{ g}_{\text{dcw}}\text{l}^{-1}$  respectively. The final specific intracellular CHMO activities were  $272 \text{ U g}_{\text{dcw}}^{-1}$  for induced cultures, and  $254 \text{ U g}_{\text{dcw}}^{-1}$  for non-induced cultures. The addition of ITPG at 210 minutes did not cause a significant increase in intracellular activity in induced cultures compared to non-induced cultures. The CHMO activity increased with the biomass concentration, and seemed to be expressed constitutively. Because there was no significant difference in the activity obtained when ITPG was or was not added, it was not used in subsequent experiments.

### 3.2.2 Production of *E.coli* biocatalyst in a 7l fermenter

A 7l fermenter process was developed so that the biocatalyst could be produced in sufficient amounts for experiments in subsequent chapters. Figure 3.3 shows the biomass concentration, the glycerol concentration, and the specific intracellular CHMO activity during the growth of the *E.coli* biocatalyst in a 7l fermenter. The experiment is described in Section 2.4.4. The final biomass concentration for this fermentation was  $9.5 \text{ g}_{\text{dcw}}\text{l}^{-1}$ ; the maximum specific growth rate was  $0.7\text{h}^{-1}$ ; the apparent yield on glycerol was  $0.9 \text{ gg}_{\text{dcw}}^{-1}$ ; and the final intracellular CHMO activity was  $300 \text{ U g}_{\text{dcw}}^{-1}$ .

Figure 3.4 shows the DOT, OUR, CER and RQ values that correspond to the data in Figure 3.3. The DOT decreased from 90% at the start of the fermentation to a minimum of 1% at 150 minutes - at this time the OUR and CER reached their maximum values of 105 and 90  $\text{mmol l}^{-1}\text{h}^{-1}$  respectively. The growth rate and the glycerol consumption rate began to slow down at 150 minutes, which suggests that the growth of the *E.coli* was limited by the oxygen concentration.

### 3.2.3 Bioconversions

#### 3.2.3.1 Whole-cell activity

The whole-cell activity was determined as described in Section 2.5.1. Figure 3.5 shows typical reaction profiles for the bioconversion of cyclohexanone to  $\epsilon$  –

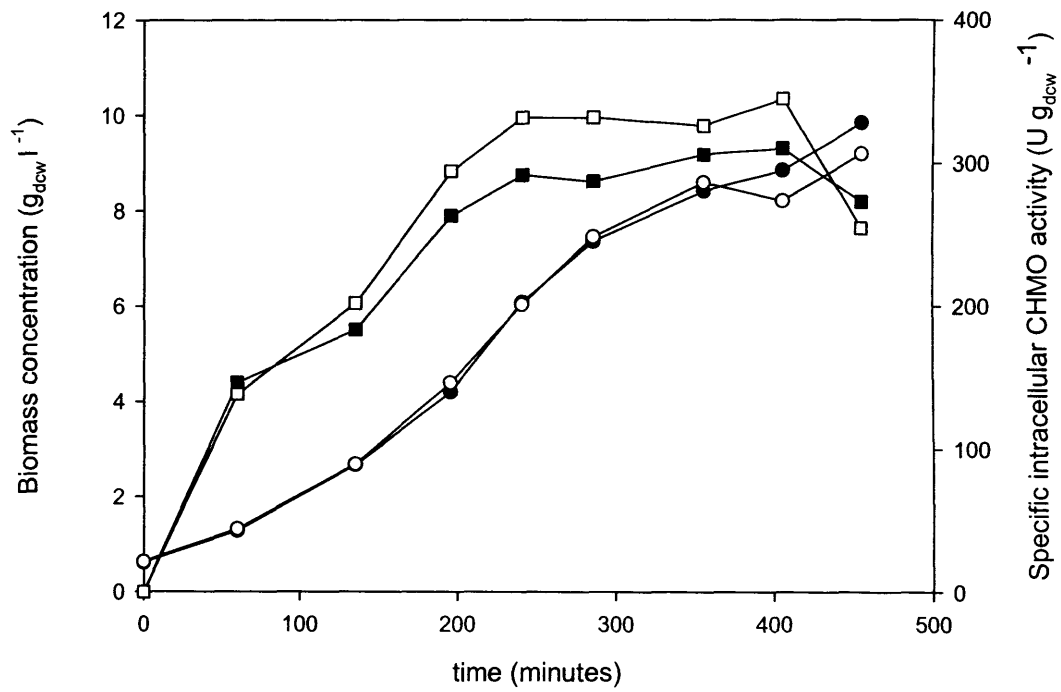
caprolactone and of bicycloheptenone to oxabicyclooctenone using initial substrate concentrations of  $1\text{g l}^{-1}$  and biomass concentrations of  $1\text{g}_{\text{dcw}}\text{l}^{-1}$ . The initial specific activity for the bioconversion of cyclohexanone was  $190\text{ U g}_{\text{dcw}}^{-1}$  and for bicycloheptenone it was  $105\text{ U g}_{\text{dcw}}^{-1}$ . The cyclohexanone bioconversion may have had a higher specific activity than the bicycloheptenone because it is the natural substrate.

The activity of the whole-cell bioconversion of cyclohexanone was approximately half of that of the isolated assay. Doig *et al.* (2003) found that the intracellular activity of a recombinant CHMO was higher than the whole-cell activity. The difference could not be entirely accounted for by differences in pH optima; therefore, the rate of substrate uptake may have limited the activity. Walton and Stewart (2002) also suggested that the transport of cyclohexanone across the cell membrane limited the whole-cell activity of a recombinant *E.coli* over-expressing CHMO. The difference in the specific activities obtained with cyclohexanone and bicycloheptenone might also be due in part to differences in their rate of uptake by the biocatalyst.

The glycerol concentration had no effect on the specific activity at concentrations between  $5 - 25\text{ g l}^{-1}$  (Appendix 2), which is consistent with the results of Doig *et al.* (2003) and Simpson *et al.* (2001).

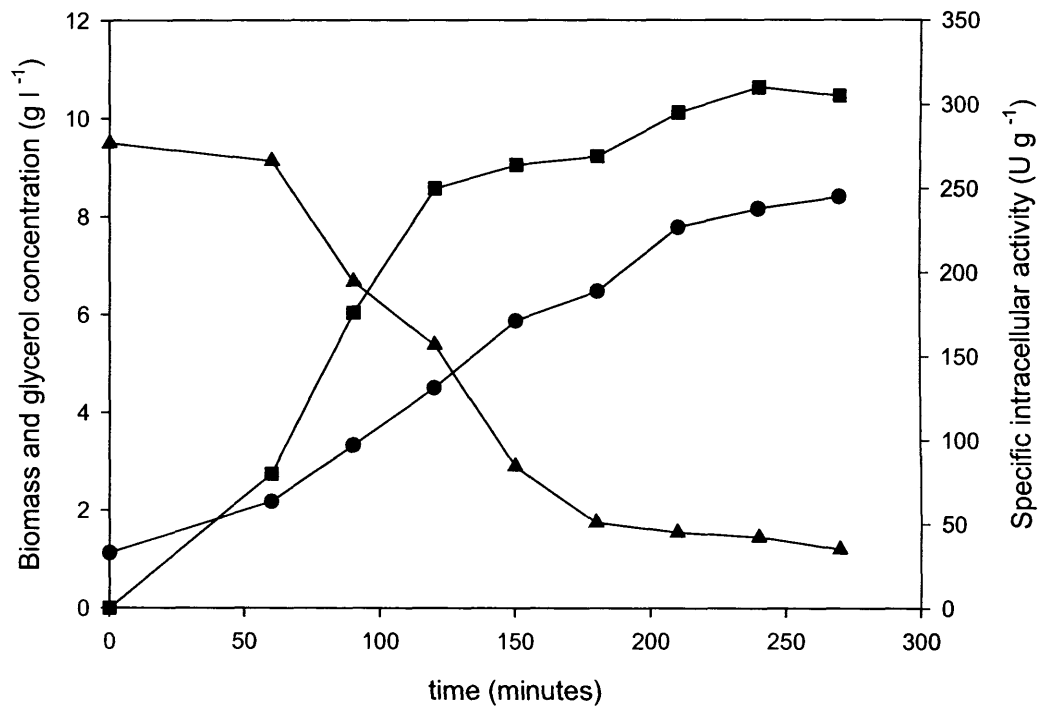
### 3.2.3.2 Stability of the biocatalyst

Figure 3.6 shows that there was no decrease in the whole – cell activity over the first 29.5 hours of harvest, but after 75 hours the whole – cell activity had dropped to 62 % of the original value. Therefore, all the bioconversions carried out with the biocatalyst had to be finished within 29.5 hours after harvest so that there was no decrease in the activity.



**Figure 3.2.** The growth kinetics and intracellular CHMO activity of *E.coli* during growth in 1l shake flasks. Biomass concentration: no IPTG (●); IPTG (○); specific intracellular CHMO activity: no ITPG (■) ITPG (□).





**Figure 3.3.** The biomass concentration, glycerol concentration, and specific intracellular CHMO activity during the growth of *E.coli* in a 7l fermenter. Biomass concentration (●), glycerol concentration (▲), specific intracellular CHMO concentration (■).

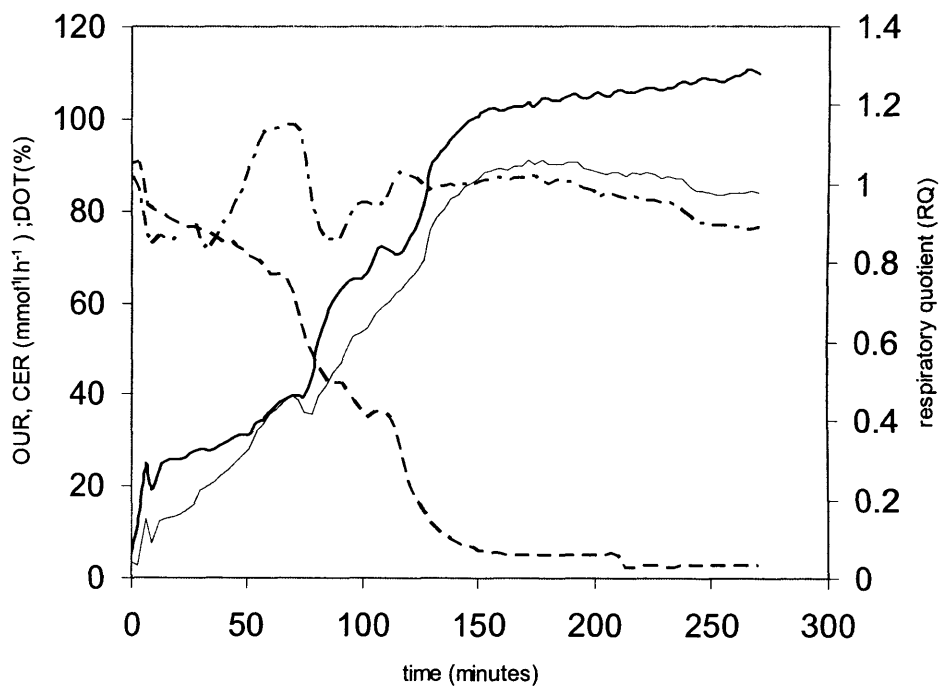


**Figure 3.4.** Exit-gas and DOT during a 7l fermentation. OUR (——), CER (-----), RQ (-·-·-), DOT(-·-·-).

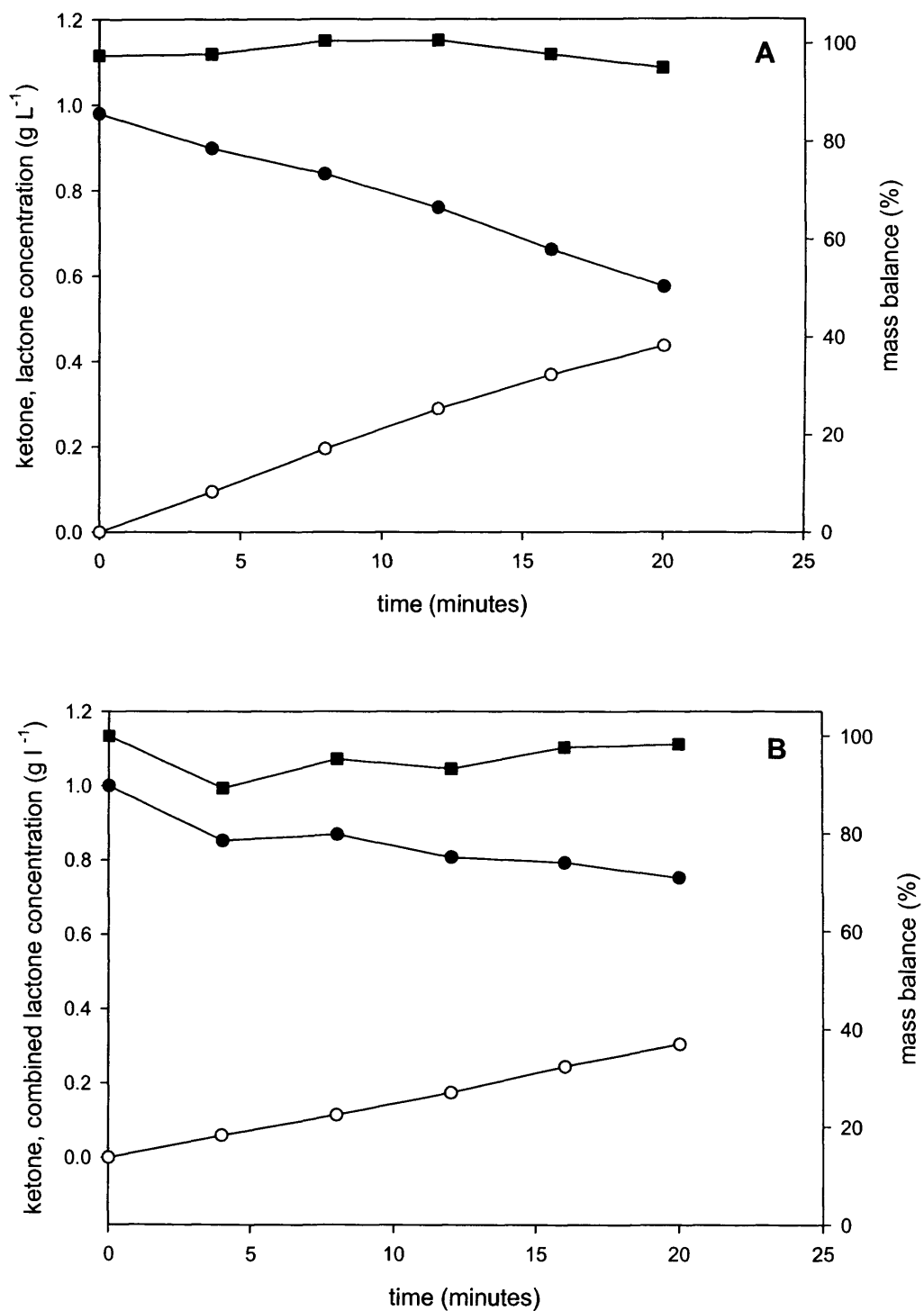


**Figure 3.5.** Reaction profiles during the bioconversion of A. cyclohexanone and B. bicycloheptenone to their respective products. Ketone (●), lactone (○), and mass balance (■).

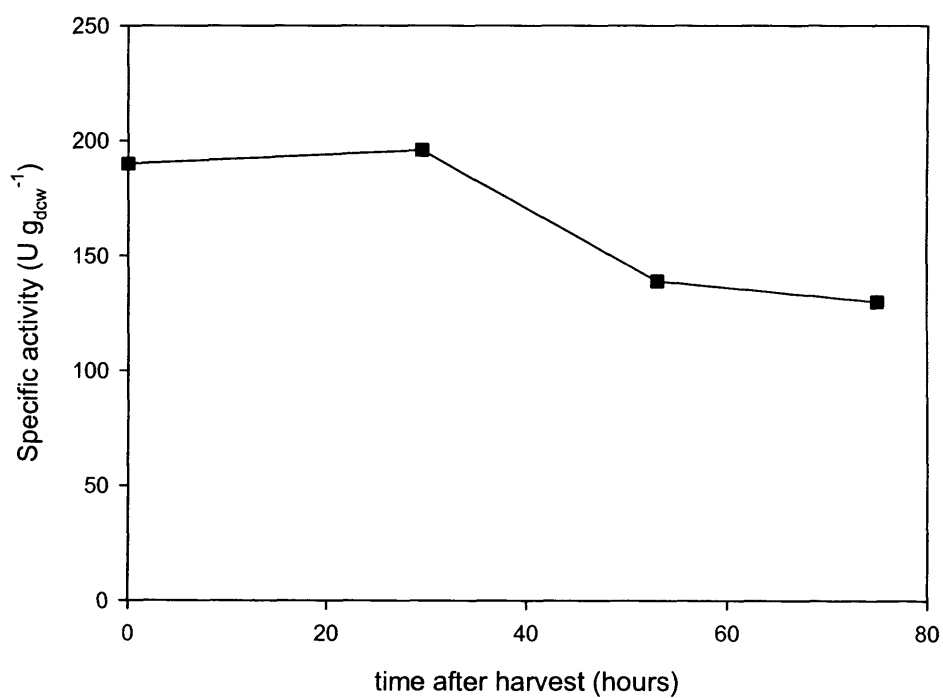


**Figure 3.6.** Stability of the whole-cell biocatalyst stored at 4 °C after harvest.

### 3.2.3.3 Substrate and product inhibition

The effect of the substrate and product concentrations on the specific activity was determined. Figure 3.7 shows the effect of the initial cyclohexanone and  $\epsilon$  – caprolactone concentration on the specific activity - the experiments are described in Section 2.5.1.1.1. The specific activity decreased linearly at initial cyclohexanone concentrations of 0.25 and 5  $\text{gl}^{-1}$ , and it was zero at 8  $\text{gl}^{-1}$ . The specific activity decreased most rapidly at initial  $\epsilon$  – caprolactone concentrations of 0.5 – 1  $\text{gl}^{-1}$ . As the concentration increased above 1  $\text{gl}^{-1}$  there was a more steady decrease up to a concentration of 10  $\text{gl}^{-1}$  when the activity was 29  $\text{U g}^{-1}$ .

Figure 3.8 shows the effect of the initial bicycloheptenone and its combined lactone concentrations on the specific activity. The experiments are described in Section 2.5.1.1.2. Bicycloheptenone inhibited the specific activity at the lowest concentrations used (0.25 – 1  $\text{gl}^{-1}$ ). At concentrations above 1  $\text{gl}^{-1}$  there was a much more rapid decrease in the specific activity – there was no activity at concentrations above 3  $\text{gl}^{-1}$ .

The oxabicyclooctenone also inhibited the specific activity when the concentration was higher than 1  $\text{gl}^{-1}$ . However, the decrease in activity was not as rapid as that observed with bicycloheptenone - the specific activity had decreased to 20  $\text{Ug}_{\text{dcw}}^{-1}$  at an oxabicyclooctenone concentration of 8  $\text{gl}^{-1}$ . These inhibition profiles are similar to those found by Doig *et al.* (2003) with a different *E.coli* strain.

The aim of these experiments was to determine which substrate and its corresponding product caused the least inhibition, so that subsequent bioconversions could be carried out with a minimum decrease in the activity. There was little difference in the amount of inhibition caused by the two different substrates at the lowest concentrations – for bicycloheptenone there was a 14 % decrease in the specific activity at concentrations of 0.25 - 1  $\text{gl}^{-1}$  compared to 12 % for cyclohexanone over the same concentration range. The oxabicyclooctenone caused no inhibition at concentrations up to 1  $\text{gl}^{-1}$ , whereas

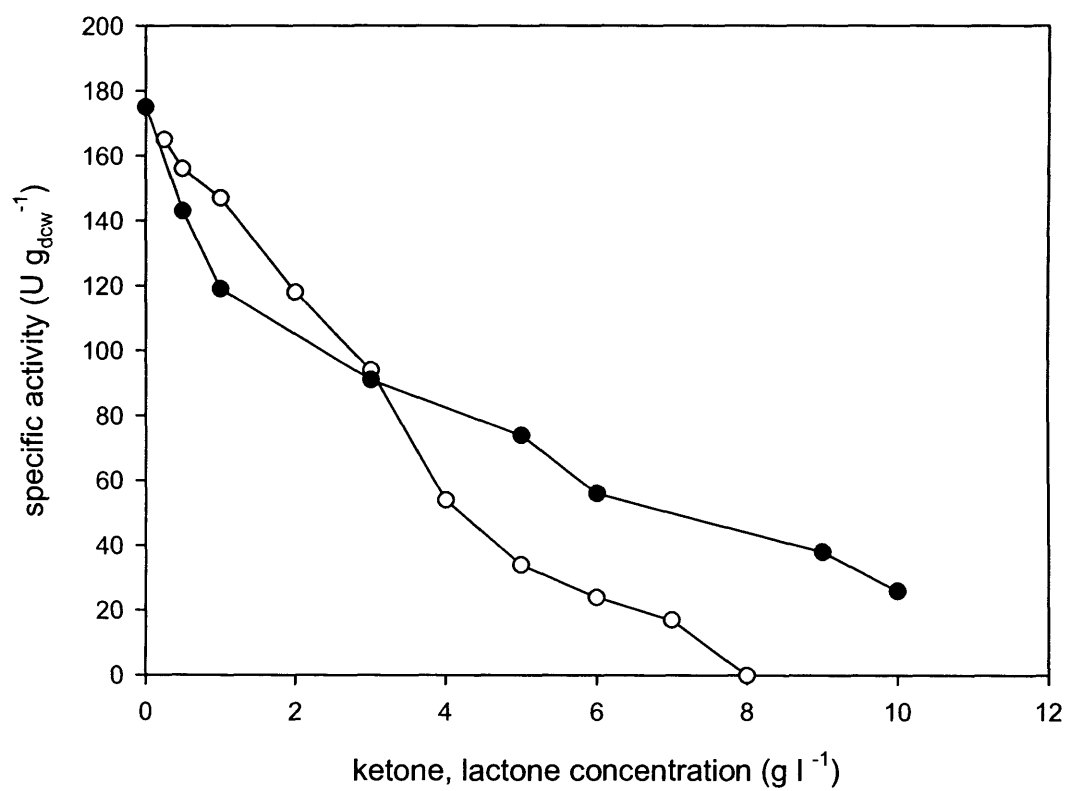


**Figure 3.7.** The effect of the initial cyclohexanone and  $\epsilon$  – caprolactone concentration on the specific activity. Cyclohexanone (○);  $\epsilon$  – caprolactone (●).

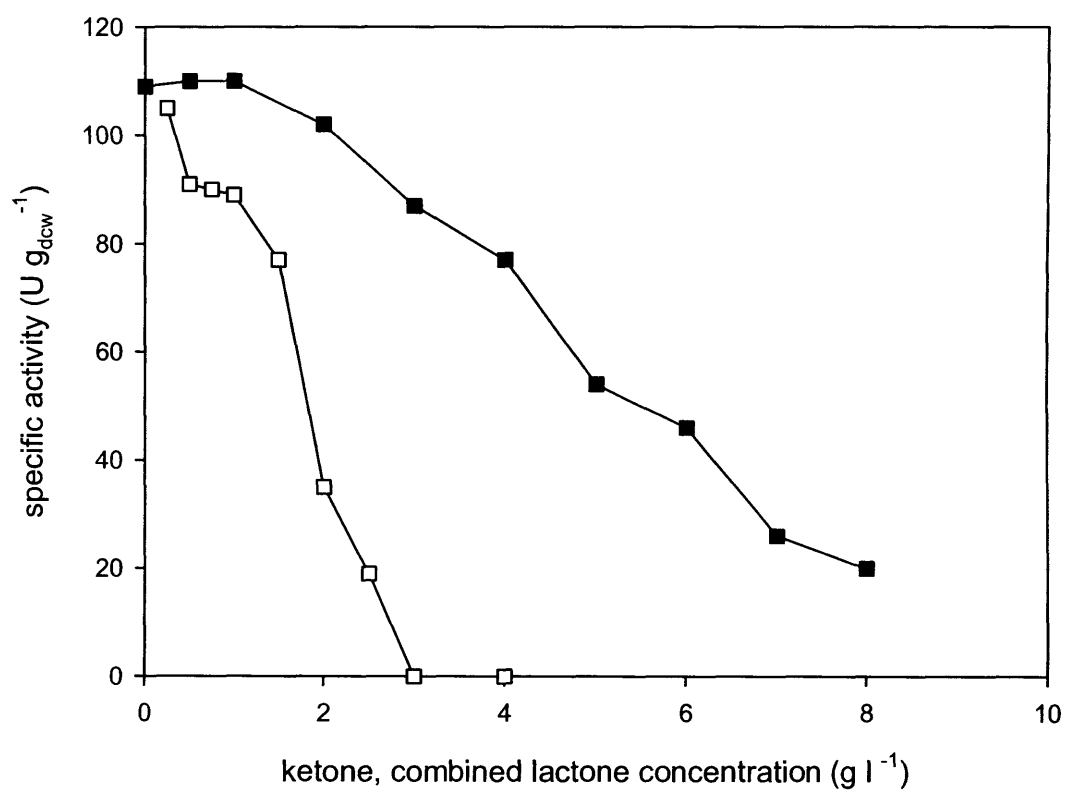


**Figure 3.8.** The effect of the initial bicycloheptenone and oxabicyclooctenone concentration on the specific activity. Bicycloheptenone (□) ; oxabicyclooctenone (■).

for  $\epsilon$  - caprolactone there was a 32 % reduction in the activity at the same initial concentration. From this point of view the bicycloheptenone was the most appropriate substrate because it caused the smallest decrease in activity.

### 3.3 Conclusions

- The *E.coli* biocatalyst can be produced up to  $9.5 \text{ g}_{\text{dcw}} \text{ l}^{-1}$  in a 7l fermenter using complex media and glycerol as a carbon source.
- The specific activity increased in proportion to the biomass concentration during the growth of the biocatalyst. The whole-cell specific activity at late exponential/early stationary phase was  $190 \text{ U g}_{\text{dcw}}^{-1}$  with cyclohexanone, and  $105 \text{ U g}_{\text{dcw}}^{-1}$  with bicycloheptenone.
- The glycerol concentration did not affect the specific activity between 5 and  $25 \text{ g l}^{-1}$ .
- There was no loss in biocatalyst activity up to 29.5 hours after harvest if the biomass was stored at  $4 \text{ }^{\circ}\text{C}$ . Therefore all experiments with the biocatalyst had to be completed within 29.5 hours after harvest.
- Cyclohexanone decreased the specific activity at concentrations of  $0.25 - 8 \text{ g l}^{-1}$ .
- $\epsilon$  - caprolactone decreased the specific activity at concentrations of  $0.5 - 10 \text{ g l}^{-1}$ .
- Bicycloheptenone decreased the specific activity at concentrations of  $0.25 - 3 \text{ g l}^{-1}$ .
- Oxabicyclooctenone had no effect on the specific activity at concentrations of  $0 - 1 \text{ g l}^{-1}$ , but at concentrations above  $1 \text{ g l}^{-1}$  the specific activity decreased.



- The conversion of bicycloheptenone to oxabicyclooctenone was chosen as the model system, because it caused less inhibition in the activity compared to the cyclohexanone reaction. Cyclohexanone and bicycloheptenone caused similar levels of inhibition at concentrations of 0.25 – 1  $\text{gl}^{-1}$ , whereas oxabicyclooctenone caused no inhibition at concentrations up to 1  $\text{gl}^{-1}$ .

## 4.0 Oxygen consumption of the biocatalyst

### 4.1 Introduction

The aim of this chapter was to characterise the oxygen consumption of the *E.coli* biocatalyst during the bioconversion of bicycloheptenone in order to obtain an understanding of the effect of oxygen limitation on the process. Increasing the biocatalyst concentration can usually increase the productivity of bioconversions. However, this might not be applicable to some whole – cell oxygenase bioconversions, because fermenters have a limited capacity to supply oxygen.

Oxygen is used as a terminal electron acceptor in the electron transport chain and as a substrate for the CHMO. Duetz *et al.* (2001) suggested that the electron transport chain and oxygenases will compete for the oxygen when it is limited, and that the electron transport chain will obtain a larger fraction because it has a lower  $k_m$  for oxygen than most oxygenases. However, when oxygen is limited the respiration rate will also decrease, which can lead to a decrease in the NAD(P)H regeneration rate.

There have been reports in the literature that the specific activity of whole-cell oxygenases decreases when oxygen is limited (Simpson *et al.*, 2001; Hilker *et al.*, 2004a; Zambianchi *et al.*, 2004; Baldwin *et al.*, 2005). However, there has been no investigation into how the oxygen is split between the electron transport chain and the oxygenase. The experiments will determine how the severity of the oxygen limitation affects the volumetric activity, the specific activity, and the relative oxygen consumption of the electron transport chain and the CHMO.

The oxygen consumption was investigated by doing bioconversions at different biomass concentrations to see when the specific activity was affected by oxygen limitation. Bioconversions were also done at two oxygen transfer rates to see how an increase in the oxygen transfer rate influenced the amount of oxygen used by the CHMO.

## 4.2 Results and Discussion

### 4.2.1 2l fermenter bioconversions

Bioconversions were done using biomass concentrations ranging from  $0.5 - 5 \text{ g}_{\text{dcw}}\text{l}^{-1}$ , and using impeller speeds of 700 and 900 rpm. The experiments are described in Section 2.6. A typical reactant profile is shown in Figure 4.1 and the corresponding exit - gas is shown in Figure 4.2. The biomass concentration was  $1 \text{ g}_{\text{dcw}}\text{l}^{-1}$  and the initial bicycloheptenone concentration was  $1 \text{ g}\text{l}^{-1}$ .

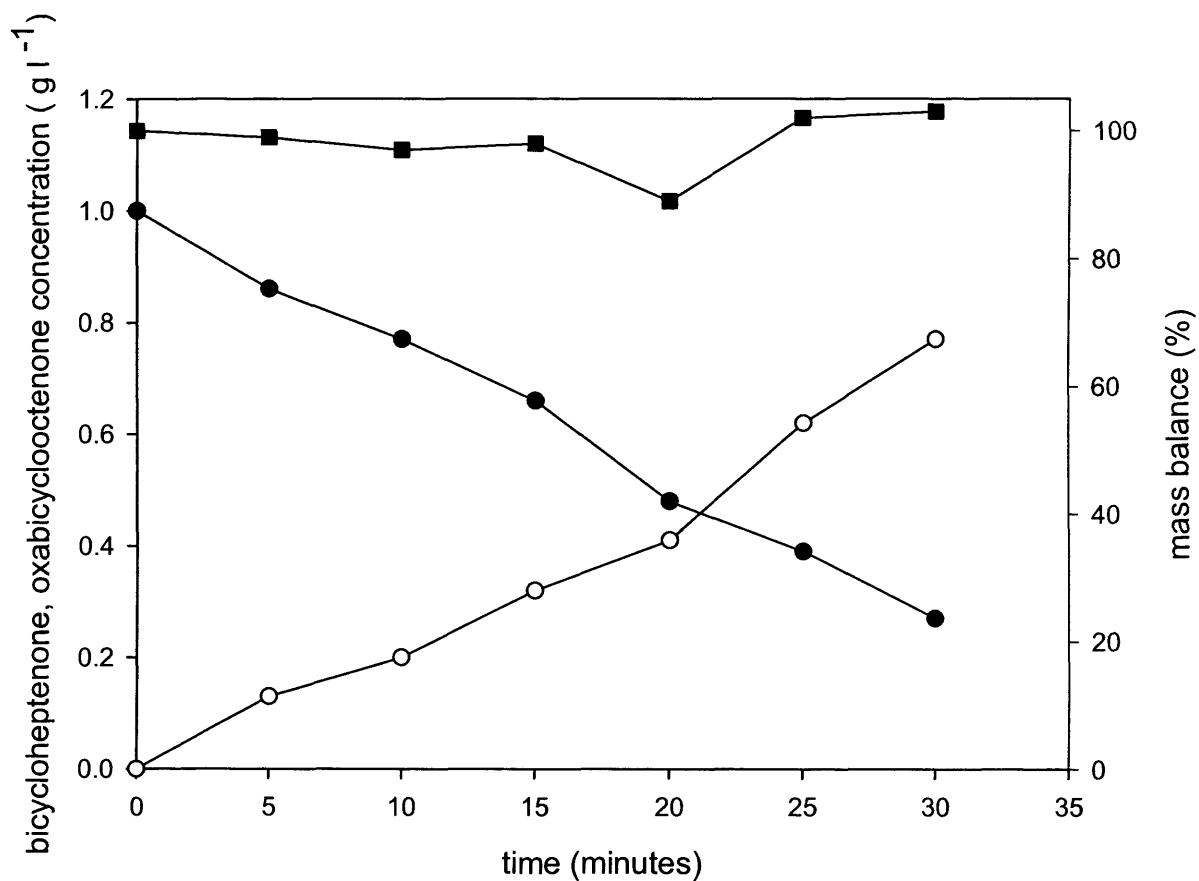
#### 4.2.1.1 Bioconversions at 700 rpm

Figure 4.3 shows that the activity increased in proportion to the biomass concentration from 0.5 to  $1.0 \text{ g}_{\text{dcw}}\text{l}^{-1}$ . The maximum volumetric activity was obtained with a biomass concentration of  $1 \text{ g}_{\text{dcw}}\text{l}^{-1}$ . Above this biomass concentration, there was no further increase in activity. At biomass concentrations from  $3 - 5 \text{ g}_{\text{dcw}}\text{l}^{-1}$  the activity remained constant at approximately  $150 \text{ U g}_{\text{dcw}}^{-1}$ .

The OUR's and the specific OUR's profiles are similar to the volumetric and specific activity profiles. The OUR increased in proportion to the biomass concentration between 0.5 and  $1 \text{ g}_{\text{dcw}}\text{l}^{-1}$ ; the DOT during these bioconversions was 60 and 45% respectively. At higher biomass concentrations, the DOT was zero and there was no further increase in the OUR. The maximum OUR was approximately  $780 \text{ U}\text{l}^{-1}$  ( $47 \text{ mmol l}^{-1}\text{h}^{-1}$ ). The oxygen limitation caused the specific activity to decrease five fold at  $5 \text{ g}_{\text{dcw}}\text{l}^{-1}$ .

#### 4.2.1.2 Bioconversions at 900 rpm

When the impeller speed was increased to 900rpm the maximum oxygen transfer rate increased 1.8 fold and the maximum volumetric activity increased approximately 2 fold. The volumetric activity and OUR profiles followed similar trends to those obtained at 700 rpm (Figure 4.4). During the bioconversions using 1 and  $2 \text{ g}_{\text{dcw}}\text{l}^{-1}$ , the DOT was 82 and 40 % respectively. The maximum specific activity was reached at  $1 \text{ g}_{\text{dcw}}\text{l}^{-1}$  – at biomass concentration above this it began to decrease. Although there was a 16 % reduction in the specific activity when the biomass concentration increased from 1 to  $2 \text{ g}_{\text{dcw}}\text{l}^{-1}$ , this was better than the 62 % reduction observed at 700 rpm.



**Figure 4.1.** Reaction profile during the bioconversion of bicycloheptenone to oxabicyclooctenone in a 2 l fermenter. Bicycloheptenone (●); oxabicyclooctenone (○); mass balance (■).

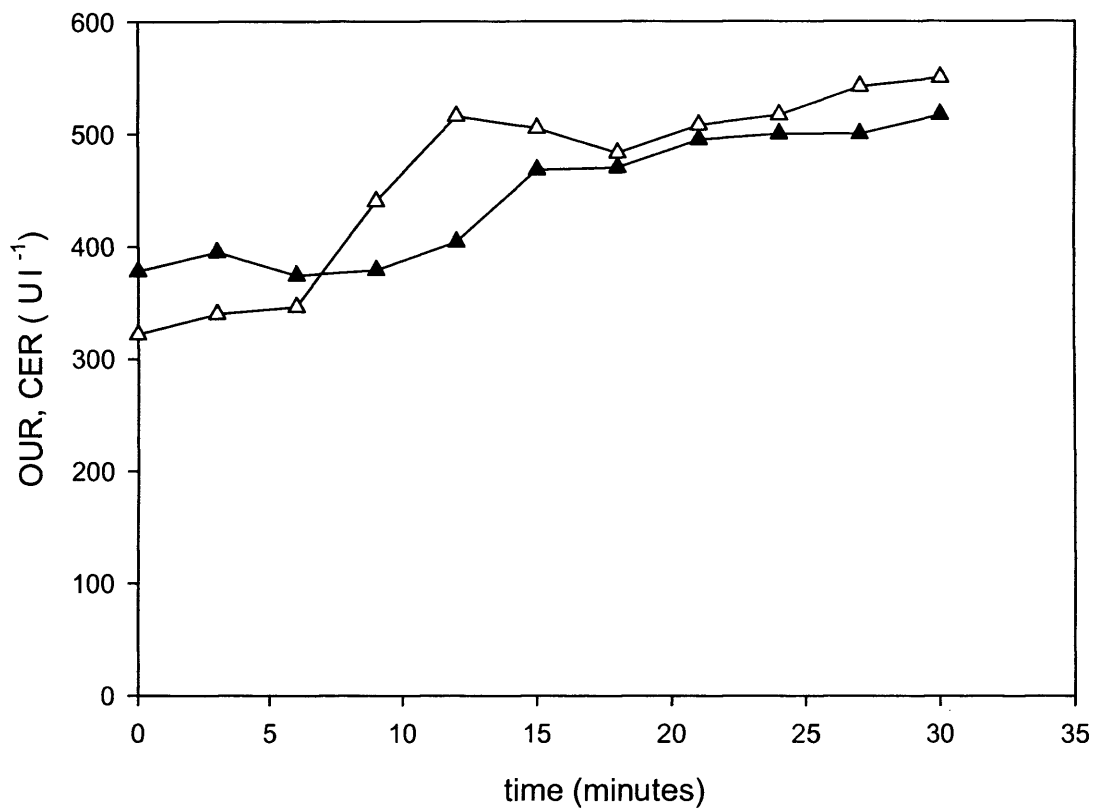


**Figure 4.2.** OUR and CER profiles corresponding to the bioconversion in Figure 4.1. OUR ( $\Delta$ ) and CER ( $\blacktriangle$ ).

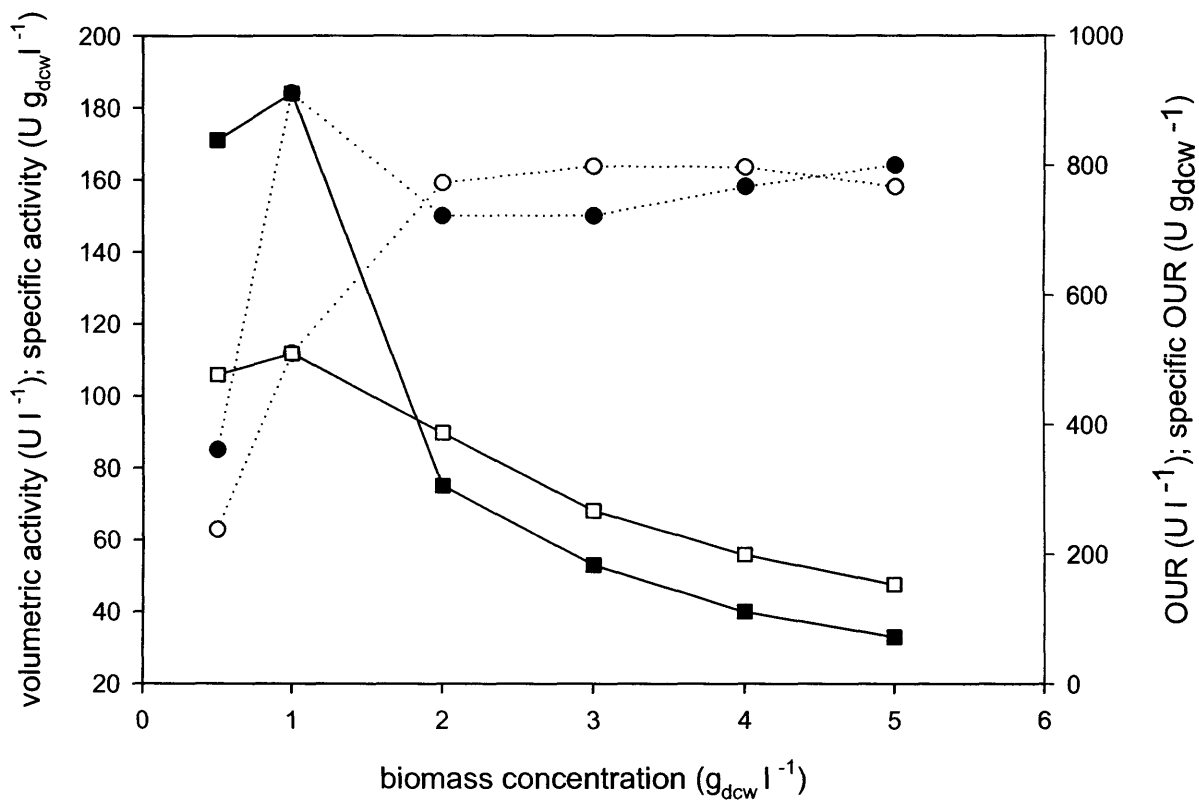


**Figure 4.3.** The effect of biomass concentration on the activity and OUR during bioconversions in 2l fermenter with an impeller speed of 700 rpm. Specific activity (■); volumetric activity (●), specific OUR (□), OUR (○).

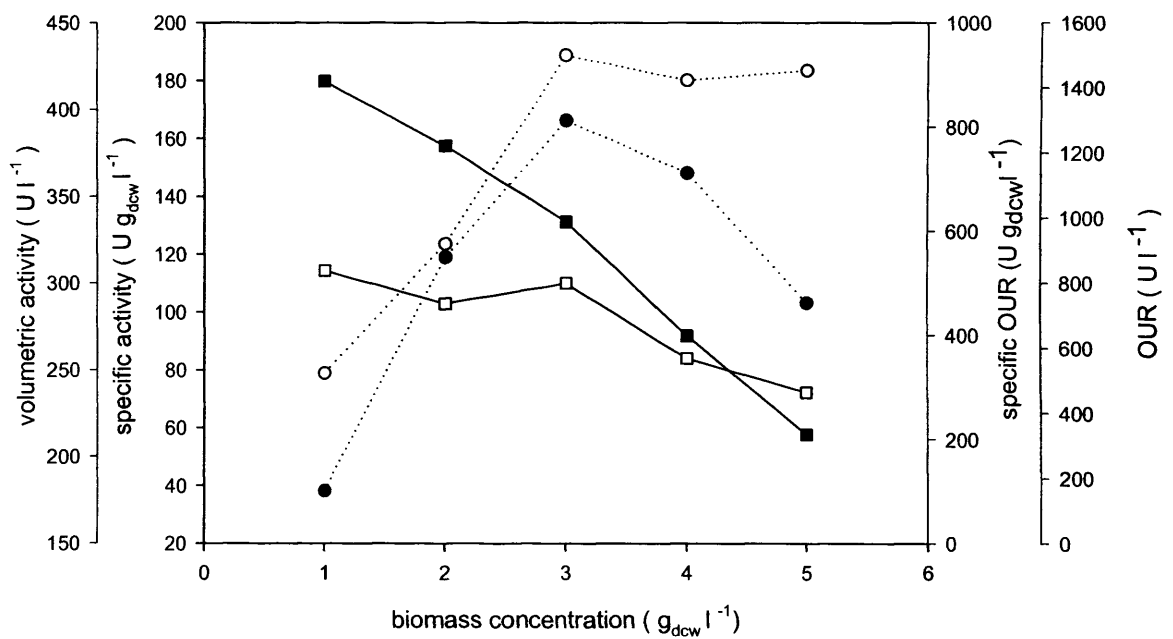


**Figure 4.4.** Effect of biomass concentration on the activity and OUR during bioconversions in 2l fermenter with an impeller speed of 900 rpm. Specific activity (■); volumetric activity (●), specific OUR (□), OUR (○).

### 4.2.2 Oxygen consumption during the bioconversions

Under aerobic conditions, the maximum specific OUR during the bioconversions was approximately  $500 \text{ U g}_{\text{dcw}}^{-1}$  ( $30 \text{ mmol g}_{\text{dcw}}^{-1} \text{ h}^{-1}$ ): the electron transport chain used two-thirds and the CHMO the other third.

Figures 4.5 and 4.6 compare the oxygen consumption rates of the CHMO (calculated from the activity) and the difference in the total OUR before and after the bioconversions began. When there was sufficient oxygen for both the electron transport chain and the CHMO, the increase in the OUR was approximately equal to the amount of oxygen used by the CHMO. However, when there wasn't, the amount of oxygen used by the CHMO was greater than the increase in the OUR.

Below a critical dissolved oxygen concentration, the specific OUR is dependent on the DOT (Longmuir, 1954). Therefore, during the bioconversions that were oxygen limited, the specific OUR of the biomass would have been sub-maximal. Figure 4.7 shows the effect of the DOT on the specific OUR of the *E.coli* – the experiments are described in Section 2.7. The maximum specific OUR was  $320 \text{ U g}_{\text{dcw}}^{-1}$  ( $19 \text{ mmol g}^{-1} \text{ h}^{-1}$ ) - calculated by taking an average of the six values measured at DOT concentrations between 7 and 69 % DOT. This is in good agreement with the specific OUR of the biocatalyst during aerobic bioconversions, and with the work of Anderson and von Meyenburg (1980) who found that the maximum OUR of *E.coli* grown on glycerol was  $20 \text{ mmol g}_{\text{dcw}}^{-1} \text{ h}^{-1}$ .

When the DOT was below 7%, the specific OUR decreased by about a third; this suggests that if the DOT was higher than approximately 7%, the *E.coli* and the CHMO would not compete for the oxygen, but if it was lower, they would. Before some of the bioconversions began, the biocatalyst was already oxygen limited. Figure 4.7 shows that the specific OURs of the biocatalyst just before these bioconversions began were sub-maximal. Therefore, the CHMO did use some of the oxygen that had been used by the electron transport chain, which suggests that oxygen rather than NADPH was limiting the activity.



Figures 4.5 and 4.6 also show the percentage of oxygen used by the CHMO during each of the bioconversions. When there was no oxygen limitation, the CHMO used approximately 37% of the total oxygen. When oxygen was limited approximately 20% of the oxygen was used by the CHMO regardless of the severity of the oxygen limitation (the specific OURs varied between 150 – 383 U g<sub>dcw</sub><sup>-1</sup>). During the oxygen limited hydroxylation of toluene by toluene dioxygenase in *Pseudomonas putida* 19% of the oxygen was also used for the reaction (Carragher *et al.*, 2001). This could be a coincidence, as there are several differences between the two systems, or it could be that despite the differences, the fraction of oxygen used by the oxygenase is determined primarily by the ability of the oxygenase to compete for the oxygen.

Duetz *et al.* (1994; 2001) proposed that the electron transport chain would out compete oxygenases for oxygen because it has a lower  $k_m$  for oxygen and would therefore have a greater affinity for oxygen at lower concentrations. Duetz *et al.*, (1994) had grown several toluene degrading *Pseudomonas* strains under oxygen limitation. Each of the strains used a different oxygenase to degrade toluene, and the strains that contained oxygenases with the greatest affinity for oxygen had the highest growth rates. Duetz *et al.* (2001) and Shaler and Klecka (1986), quoted a  $k_m$  for the electron transport chain of 1  $\mu$ M (Longmuir, 1954) compared to 10 – 60  $\mu$ M for oxygenases.

However, for *E.coli* the situation is more complicated because they can express two distinct cytochrome oxidases - cytochrome o oxidase and cytochrome d oxidase (Gunsalus, 1992). The two cytochrome oxidases have different oxygen affinities: cytochrome o oxidase has a  $k_m$  of 1.4 – 2.9  $\mu$ M, whereas cytochrome d oxidase has a higher affinity for oxygen with a  $k_m$  of 0.23 – 0.38  $\mu$ M. Cytochrome o oxidase is predominant under oxygen rich conditions, whilst cytochrome d oxidase expression increases under microaerophilic and anaerobic conditions, which suggests that the *E.coli* uses it to scavenge oxygen (Gunsalus, 1992). Ryerson *et al.* (1982) estimated the  $k_m$  for oxygen of cyclohexanone monooxygenase was between 10 – 15  $\mu$ M.

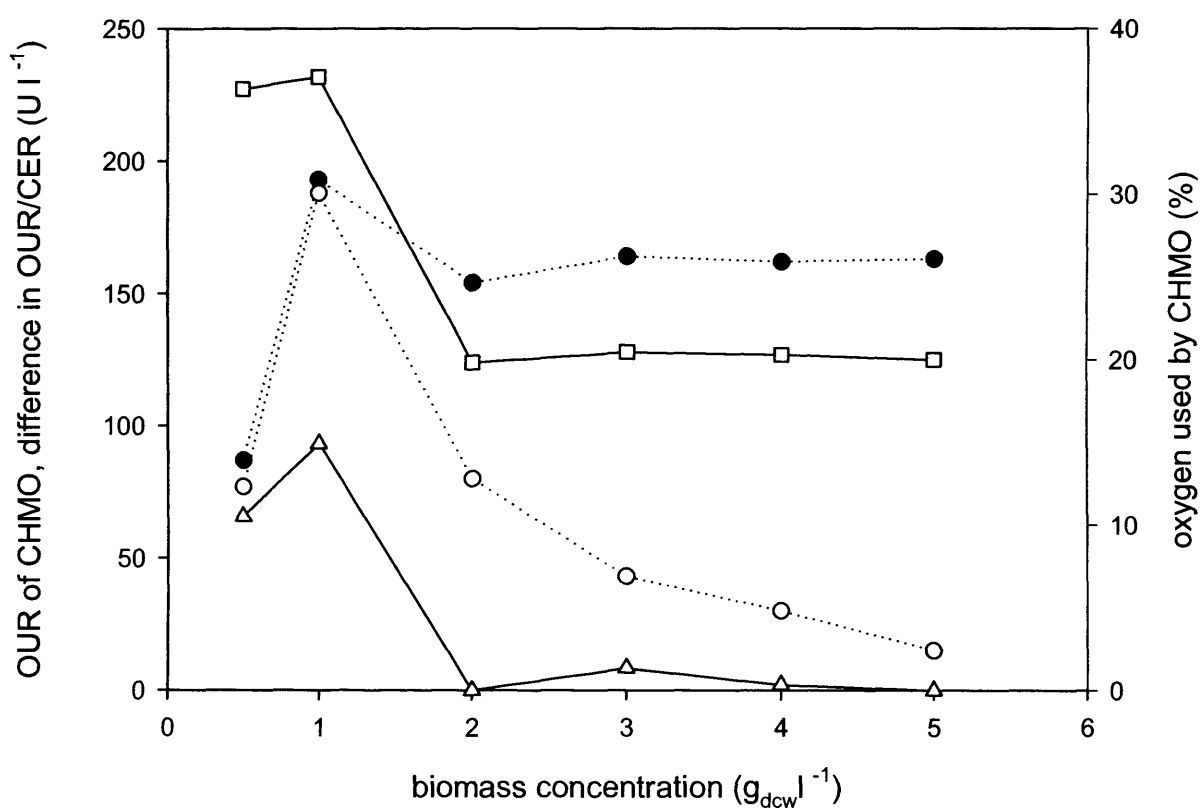


**Figure 4.5.** The effect of biomass concentration on the OUR and CER of biocatalyst during bioconversions in a 2l fermenter at 700 rpm. This data corresponds to the data in Figure 4.3. OUR of CHMO (●); change in the total OUR after bioconversion started (○); change in the total CER after bioconversion started (△), percentage of oxygen used by CHMO (□). Oxygen limitation occurred above  $1 \text{ g}_{\text{dcw}} \text{ l}^{-1}$ .

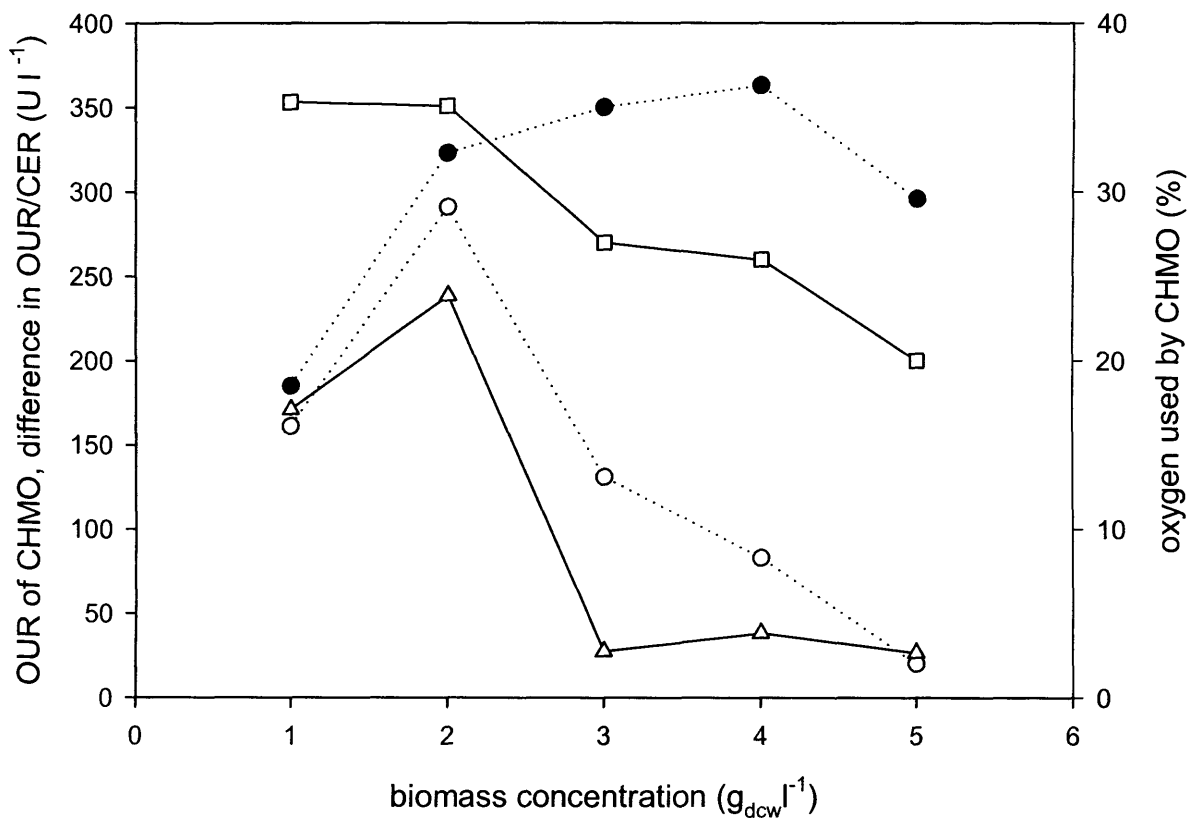


**Figure 4.6.** The effect of biomass concentration on the OUR and CER of biocatalyst during bioconversions in a 2l fermenter at 900 rpm. This data corresponds to the data in Figure 4.4. OUR of CHMO ( $\bullet$ ); change in the total OUR after bioconversion started ( $\circ$ ); change in the total CER after bioconversion started ( $\Delta$ ), percentage of oxygen used by CHMO ( $\square$ ). Oxygen limitation occurred above  $1 \text{ g}_{\text{dcw}} \text{ l}^{-1}$ .

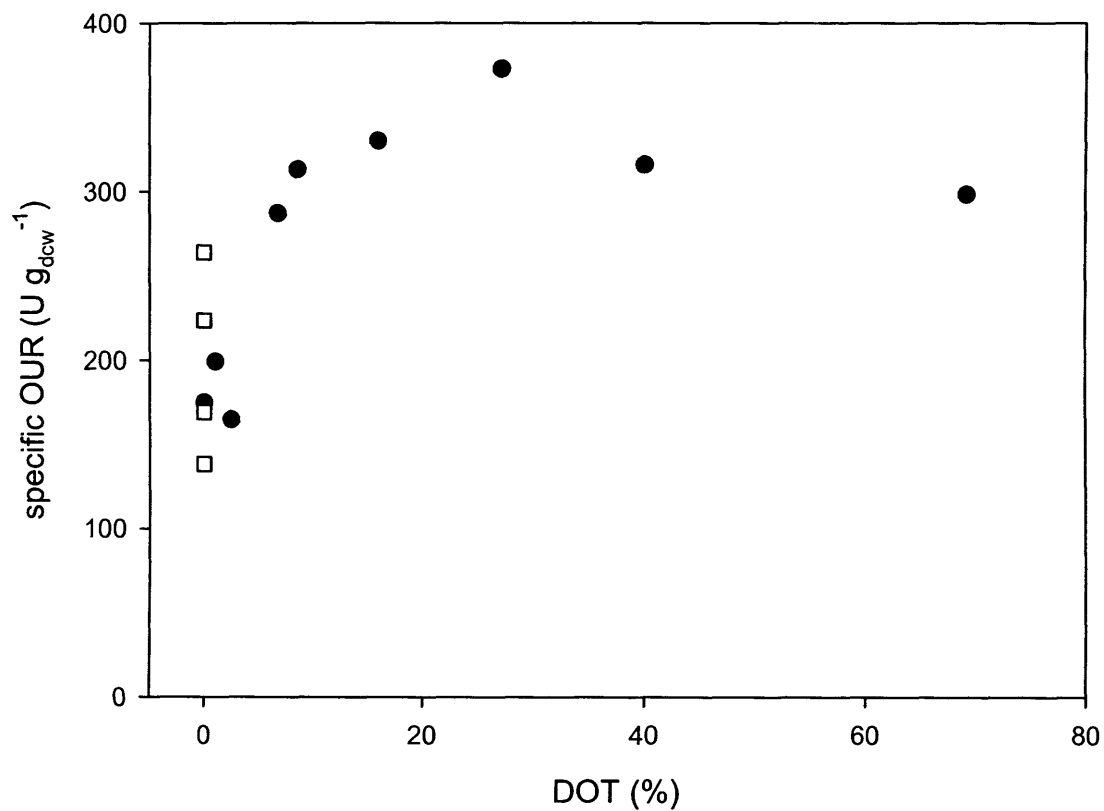


**Figure 4.7.** The effect of the DOT on the specific OUR of the biocatalyst. Specific OUR of biocatalyst with respect to DOT (●); specific OUR of the biocatalyst for experiments where the DOT was zero before the bioconversions began (□).

### 4.2.3 NADPH production

Oxygen limitation might have caused the activity of the CHMO to be limited by NADPH rather than oxygen. A decrease in the specific OUR could have led to a decrease in the NADPH regeneration rate.

The CER increased during the bioconversions that were not oxygen limited (Figures 4.5 and 4.6). The increase in the OUR was approximately equal to the amount of oxygen used by the CHMO, therefore the increase in the CER was not due to an increase in the flux through the electron transport chain. There was little or no change in the CER during the bioconversions that were oxygen limited. A similar pattern was observed during the bioconversion of indene to cis - (1S,2R) indandiol by stationary phase *Rhodococcus* (Amanullah *et al.*, 2002). Before the bioconversions began, the NADPH levels might not have been sufficient to meet the requirements of the CHMO and the *E.coli*. The addition of the substrate might have caused NADPH production to increase, and with it the production of carbon dioxide, which is often a co – product of the reactions that produce NADPH.

There are a number of routes for NADPH production in *E.coli* (Csonka and Fraenkel, 1977): glucose – 6- phosphate dehydrogenase and gluconate-6-phosphate dehydrogenase in the pentose phosphate pathway, isocitrate dehydrogenase in the TCA cycle, and various dehydrogenases. Walton and Stewart (2002) estimated that 80% of the NADPH used by a dehydrogenase over-expressed in *E.coli*, which used NADPH at a rate three fold less than the CHMO, was provided by isocitrate dehydrogenase. In this work, the specific OUR was at a maximum when the biocatalyst was not oxygen limited, and so if more NADPH was required it would have to have been supplied by another route e.g. the pentose phosphate pathway.

Leahy and Olsen (1997) found that the rate of toluene degradation by some bacteria was limited by NADPH regeneration rates at very low oxygen concentrations. There was a critical dissolved oxygen concentration below which toluene degradation was limited to a greater extent than predicted by the kinetics at higher oxygen concentrations. Below this critical concentration, the flux through the electron transport chain was limited by oxygen, and consequently the NADPH regeneration

rate was reduced. If nitrate was present when the oxygen concentration was below the critical value, the rate of toluene degradation in denitrifying strains almost doubled, because the NADPH regeneration rate increased in response to the onset of anaerobic respiration.

Figure 4.8 shows the effect of the specific OUR of the biocatalyst during the bioconversions on the specific activity - it collates the data shown in Figures 4.3 and 4.4. It does not display the trend described by Leahy and Olsen (1997), which showed a sudden steeper decrease in the specific activity below a critical oxygen concentration. However, the methods of Leahy and Olsen (1997) could be used to investigate NAD(P)H limitation in *E.coli*, because it can use nitrate as an alternative electron acceptor.

#### **4.2.4 Implications for whole-cell oxygenase processes**

If the substrates or products of a bioconversion inhibit the activity, oxygen limitation will be a secondary constraint on the process. This is because the oxygen transfer rate limits the maximum activity, whereas substrate or product inhibition limits the final concentration regardless of the activity. However, oxygen limitation should be avoided because the specific activity will decrease.

When there was no oxygen limitation approximately 63% of the oxygen was used for respiration. If the flux of reducing equivalents through the electron transport chain were decreased, the critical biomass concentration at which oxygen limitation occurs would be higher, and a higher maximum activity could be obtained. The oxygen demand could be decreased by over – expressing the oxygenase in a microorganism with a low specific OUR, or by controlling the carbon and nitrogen concentrations in the media so that the flux through the electron transport chain was reduced (Lee, 1996). However, there may be a corresponding decrease in the NAD(P)H regeneration rate.

The solvent tolerance of a microorganism is sometimes an important criterion when selecting a suitable host for biphasic bioconversions (Ramos *et al.*, 2002; de Bont 1998; Wilkinson *et al.*, 1996). For oxygenase processes, the effect of oxygen

limitation may also have to be considered. For the *E.coli* used in this chapter, the specific activity began to decrease when the DOT was close to zero. For strict aerobes the activity might decrease at higher oxygen concentrations.

The *E.coli* could be engineered so that the flux of reducing equivalents to the electron transport chain is decreased. For example, Lim *et al.* (2002) overexpressed glucose – 6-phosphate dehydrogenase and 6-phosphogluconate dehydrogenase, which are responsible for NADPH production in the pentose phosphate pathway, in *E.coli*. The NADPH level increased up to sixfold, and the flux through the TCA cycle decreased because isocitrate dehydrogenase was inhibited. These conditions would be advantageous for whole-cell oxygenase bioconversions because it would lower the specific OUR without decreasing the NADPH levels.

Protein engineering, either by rational design or by directed evolution, could be used to increase the affinity of the oxygenases for oxygen (Cirino and Arnold, 2002). But the oxygenase and the electron transport chain only compete when oxygen is limited, and so the maximum specific activity would still be sub-optimal. It would be easier to use a lower biomass concentration.

The only suitable biological method that could delay the onset of oxygen limitation is one that would reduce the oxygen consumption of the electron transport chain. Instead of using a biological method, the maximum oxygen transfer rate of the fermenter could be increased. The use of oils to do this will be discussed in the next chapter.

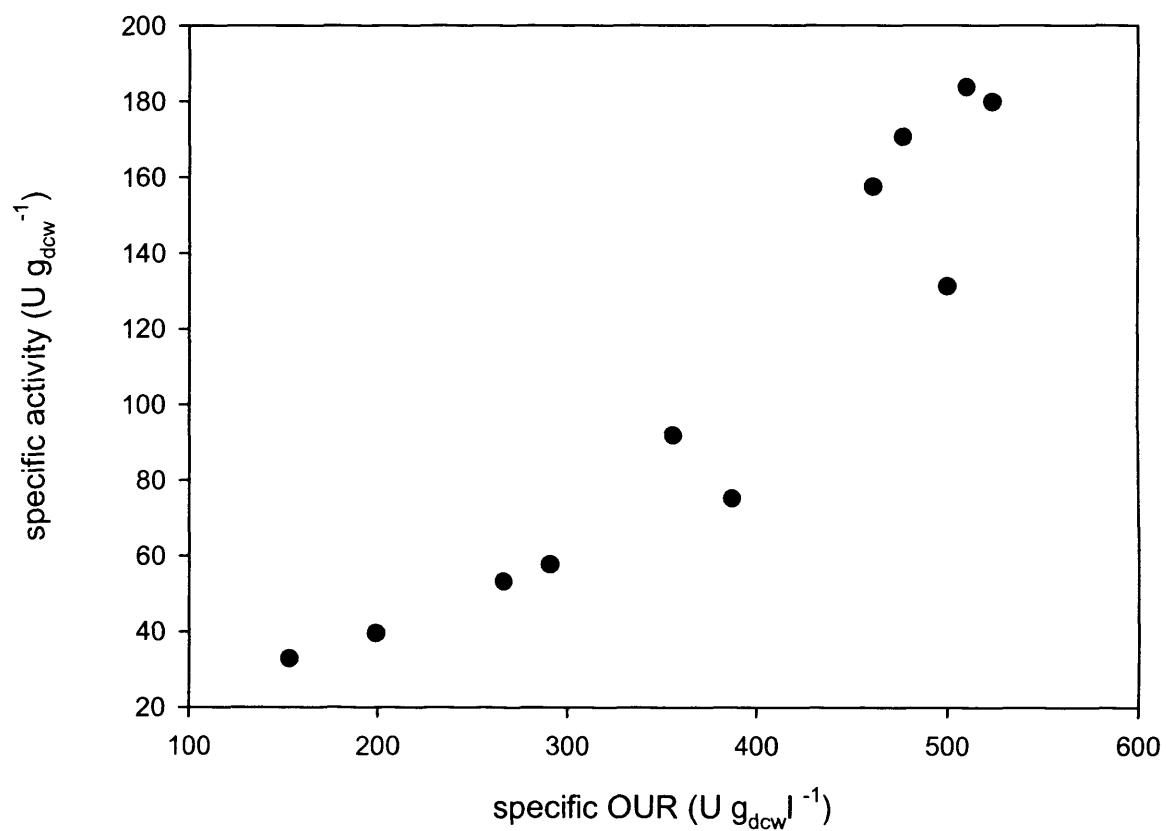


**Figure 4.8.** The effect of the specific OUR of the biocatalyst during the bioconversion on the specific activity.



### 4.3 Conclusions

The aim of this chapter was to investigate the effect of oxygen limitation on the *E.coli* biocatalyst. The main conclusions are:

- 500 U g<sub>dcw</sub><sup>-1</sup> of oxygen was required to obtain a maximum specific activity of 188 U g<sub>dcw</sub><sup>-1</sup>: the electron transport chain used approximately two thirds of the oxygen and the CHMO the rest.
- Oxygen limitation limited the maximum activity of the CHMO catalyst, and decreased its specific activity.
- When oxygen was limited the *E.coli* and the CHMO competed for the oxygen. The CHMO used approximately 20% of the available oxygen whatever the severity of the oxygen limitation.
- When the impeller speed was increased from 700 to 900 rpm the maximum OUR increased 1.8 fold; the maximum activity increased 2 fold; and oxygen limitation caused a smaller percentage decrease in the activity for all the biomass concentrations tested.
- The best way to increase the productivity of whole-cell oxygenase processes would be to decrease the amount of oxygen used by the electron transport chain or to increase the maximum oxygen transfer rate of the fermenter.

## 5.0 Enhancement of the oxygen transfer rate by oils

### 5.1 Introduction

Organic solvents are used in bioconversions to limit the toxic or inhibitory effects of substrates and products on cells, but could also be used to increase the oxygen transfer rate to the aqueous phase. The aim of this chapter was to investigate how the physiochemical properties of oils affected their ability to increase the oxygen transfer rate. The physiochemical properties that were investigated are the oxygen solubility, the viscosity, and the spreading coefficient.

Previous studies have shown that oils do increase the oxygen transfer rate (Dumont and Delmas, 2003). However, the results have been obtained using different oils and different hydrodynamic conditions, which makes comparison difficult. For design purposes, it is of interest to know if the increase in the oxygen transfer rate can be predicted from the physiochemical properties of the liquid. Also, there have been few studies that have investigated the increase in the oxygen transfer rate in the presence of biomass.

Oils can increase the oxygen transfer rate by increasing the mass transfer coefficient ( $k_L$ ), the gas-liquid interfacial area ( $a$ ), the saturation concentration ( $C^*$ ) or a combination of the three. If the oil has a higher oxygen solubility than water it can increase the overall saturation concentration. The oil viscosity can influence both the  $k_L$  and  $a$ , because it affects the degree of turbulence in the broth. It can also influence the extent to which the  $C^*$  is increased because it affects the permeability of oxygen in the oil and the oil drop size. The spreading coefficient is thought to influence the interaction between the oil droplets and the air bubbles and therefore the mechanism of oxygen transfer. As discussed in Section 1.5.2.3.1, many authors have suggested that the spreading coefficient of oils determines how they interact with the gas bubbles. Oils with

positive spreading coefficients will spread around gas bubbles, whereas oils with negative spreading coefficient do not. However, Brillman (1998) suggested that the spreading coefficients given in the literature do not reflect the conditions that occur in a fermenter, because the bubbles and the oil were forced to come into contact and the time allowed for them to do this was much greater than it would be in a fermenter

Models that predict the increase in the oxygen transfer rate are useful for process development. In this work, the  $E_{\text{shuttle}}$  model of Bruining *et al.* (1986) was assessed for its suitability to predict the increase in the oxygen transfer rate. A heterogeneous model was not used because it would require information (e.g. the boundary layer thickness, the distance of the droplets from the gas-liquid interface and the distance between the oil drops that are either difficult or impossible to obtain.

## 5.2 Results and Discussion

### 5.2.1 Selection of oils

Five oils were selected: 5cS silicone oil, 50cS silicone oil, perfluorotributylamine (FC-40), soya bean oil, and mineral oil. Organic solvents were not used because they are an explosion hazard, and also potentially toxic to the *E.coli*.

The oils were selected based on their oxygen solubility and their viscosity. Table 5.1 shows the oxygen solubility and the viscosity of the oils. The oxygen solubility values were taken from the literature and the viscosity was measured as described in Section 2.9.4.1.

The influence of the oxygen solubility on the enhancement factor were investigated by comparing FC-40 with the 5cS silicone oil, and the 50cS silicone oil with the soya bean oil. Each pair has the same viscosity but a different oxygen solubility.

The influence of the oil viscosity on the enhancement factor was investigated by comparing the 5cS silicone oil and the 50cS silicone oil. They both had the

same oxygen solubility but the 50cS silicone oil was 10 times more viscous than the 5cS silicone oil.

Oil	Oxygen solubility mmol l <sup>-1</sup>	Viscosity at 37°C mPa.s
50 cS silicone oil	7.75 *	45
5 cS Silicone oil	7.75 *	4.2
Soya oil	0.36 <sup>+</sup>	44
Mineral oil	1 #	24
FC-40	3 †	4.5
Media	0.25	1.0

**Table 5.1.** The oxygen solubility and viscosity of the oils.

\* 25°C Chibata et al 1974

+ 25°C Rols and Goma, 1991

# 30°C Yoshida et al, 1970

† 25°C Fluorinert Electronic Liquids, 3M product manual.

### 5.2.2 Experimental design

The effect of the oils on the oxygen uptake rate was quantified by measuring the OUR before and after the oils were added to a suspension of the biocatalyst. The biomass had to be oxygen limited to ensure that the OUR increased after the oils were added. The DOT could not increase above zero because the driving force would not be the same as it was before the addition of the oil. If it did, any increase in the oxygen transfer rate would be underestimated. It was shown in Section 2.8 that a biomass concentration  $7\text{g}_{\text{dcw}}\text{l}^{-1}$  would be sufficient.

The OUR of  $7\text{g}_{\text{dcw}}\text{l}^{-1}$  of the biocatalyst at an agitation speed of 700 rpm and an aeration rate of 1 vvm was measured for one hour. This was done as a reference to check that there was no background change in the OUR during the experiments. Figure 5.1 shows that there was no change in the OUR, and for

subsequent experiments any change in the OUR was assumed to be due to the addition of the oils.

Figure 5.1 shows a typical OUR profile before and after the addition of oil. In this case it is 5cS silicone oil at a volume fraction of  $\Phi = 0.01$ . There was an increase in the OUR about ten minutes after the addition of the oil. When the impeller speed was increased from 700 to 900 rpm the OUR of the biocatalyst increased (Figure 5.1). There was an approximately 10 minute delay from the time the impeller speed was increased to the time an increase in the OUR could be seen on the data logger. This was not because it took ten minutes for the  $k_{La}$  to increase in response to the increase in impeller speed, but because of the time it took for the exit - gas to reach and to be analysed by the mass spectrometer.

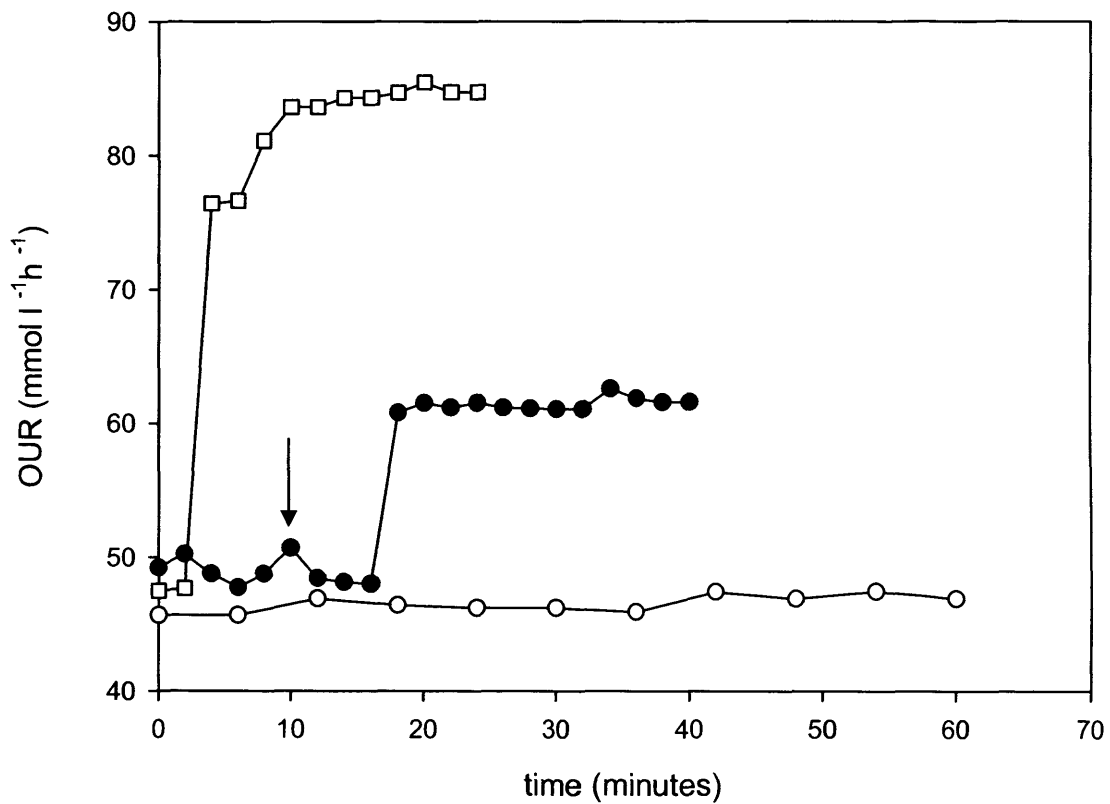
The change in the OUR was quantified using an enhancement factor ( $E_{OUR}$ ), which is the ratio of the OUR with oil to the OUR without – assuming the same hydrodynamic conditions and the same driving force for mass transfer:

$$E_{OUR} = \frac{OUR_{oil}}{OUR_{no\ oil}} \quad (5.1)$$

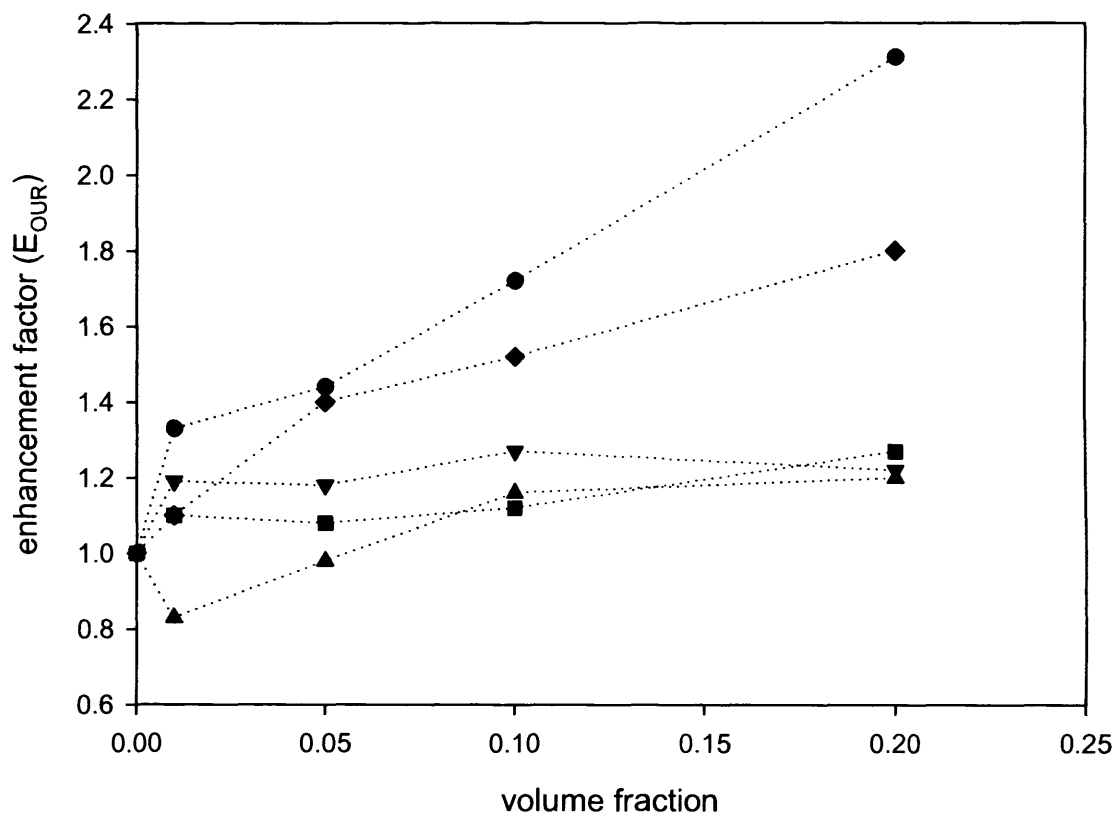
### 5.2.3 Effect of the oils on the oxygen uptake rate

Figure 5.2 shows the OUR enhancement factors obtained with each of the oils on a total volume basis. The experiments were carried out as described in Section 2.8. The experiments were carried out in triplicate, but the error bars are omitted for clarity.

The maximum OUR enhancement factors for 5cS silicone oil, FC-40, 50cS silicone oil, soya bean oil, and mineral oil were 2.3, 1.8, 1.2, 1.27, and 1.22 respectively. The OUR enhancement factors obtained with 5cS silicone oil and FC-40 increased by 73 and 64 % between 0.01 and 0.2. There was not a significant increase in the OUR enhancement factors obtained with soya bean oil and 50cS silicone above  $\Phi = 0.01$  – 14 and 7 % respectively between  $\Phi =$



**Figure 5.1.** The effect of an oil on the OUR of the biocatalyst. OUR profile for the addition of 14ml of the 5cS silicone oil to  $7g_{dcw}l^{-1}$  of the *E.coli* biocatalyst - the arrow indicates when the oil was added (●); OUR of  $7g_{dcw}l^{-1}$  of the *E.coli* biocatalyst (reference) (○); OUR profile of  $7g_{dcw}l^{-1}$  of the *E.coli* biocatalyst after the impeller speed was increased from 700 to 900 rpm (□).



**Figure 5.2.** The effect of the oil volume fraction on the OUR enhancement factors on a total volume basis. 5cS silicone oil (●); 50cS silicone oil (▼); FC-40 (◆); soya bean oil (■); mineral oil (▲).

0.01 and 0.2. The enhancement factors obtained with mineral oil increased by 45% between 0.01 and 0.2; but, because the enhancement factor was less than one at  $\Phi = 0.01$ , the enhancement factors obtained at higher volume fractions were similar to those of 50cS silicone oil and soya bean oil.

The oils could have affected the oxygen transfer rate by influencing the mass transfer coefficient ( $k_L$ ), the gas-liquid interfacial area ( $a$ ), the driving force ( $C^*$ ), or a combination of the three. In the following sections the effects of the oils on these parameters will be discussed.

### 5.2.3.1 Effect of the oils on the $k_L a$

In gas – liquid systems the dynamic gassing – out method is commonly used to determine the  $k_L a$ . The method involves de - oxygenating the media with nitrogen until the DOT is zero. Air is then reintroduced and the change in the DOT from zero to steady state is recorded. The rate of change of the DOT during this period is equal to the rate of oxygen transfer from gas to liquid.

This method was used to determine the effect of the oils on the  $k_L a$ . The experiments are described in Section 2.12. The  $k_L a$  for each of the oils at volume fractions  $\Phi = 0.01 - 0.2$  was determined. The enhancement factor for the  $k_L a$  ( $E_{k_L a}$ ) was then calculated using the following equation:

$$E_{k_L a} = \frac{k_L a_{oil}}{k_L a_{no\ oil}} \quad (5.2)$$

Figure 5.3 shows the enhancement factor ( $E_{k_L a}$ ) for the volumetric mass transfer coefficient ( $k_L a$ ) for the oils at each volume fraction. Except for soya bean oil at a volume fraction of  $\Phi = 0.01$ , all of the enhancement factors were less than one. As the volume fraction increased the enhancement factors for the  $k_L a$  decreased for all of the oils.



Although the graphs in Figure 5.3 indicate that the oils cause the  $k_L a$  to decrease (i.e. increase the mass transfer resistance ( $k_L$ ) or the bubble diameter ( $a$ )) – that conclusion would be incorrect because the presence of the oil makes the system more complex than a simple gas-liquid system.

As stated above, the dynamic gassing out method measures the  $k_L a$  by measuring the rate of change in the dissolved oxygen concentration after the reintroduction of air. It is assumed that the rate of change of the DOT is equal to the rate of oxygen transfer from the gas to air. The technique is suitable, and is often used, for investigating the effect of factors such as power input because they affect the  $k_L a$  only (i.e. the resistance to mass transfer ( $k_L$ ) or the bubble diameter ( $a$ )). For example, if the  $k_L a$  is measured at different power inputs the amount of gas that needs to be transferred from the gas to the liquid to reach saturation is the same – but the rate of mass transfer will be higher at higher impeller speeds.

However, when oils that had a higher oxygen solubility than water were present, the bulk average oxygen concentration of the dispersion was increased, and so more oxygen had to be added before the system was saturated. The  $k_L a$  was measured by recording the rate of change of the DOT in the aqueous phase. Although the oil did not increase the saturation concentration of oxygen in the aqueous phase, the aqueous phase would not become saturated with oxygen (i.e. DOT = 100 %) until the oil phase was saturated.

The results for the OUR enhancement factor shown in Figure 5.2 show that the oils do increase the oxygen transfer rate to the aqueous phase – so the large decrease in the  $k_L a$  enhancement factors shown in Figure 5.3 may not be due to their effects on the  $k_L a$  (i.e. the resistance to mass transfer of the bubble diameter), otherwise the increases in the OUR obtained with 5cS silicone and FC-40 would not have been achieved.

Table 5.2 shows the average oxygen concentration of the dispersions at each volume fraction. The oxygen solubility of the media was  $0.25 \text{ mmol l}^{-1}$ . Even at

a volume fraction of  $\Phi = 0.01$  the silicone oils and the FC – 40 required 1.3 and 1.1 times as much oxygen as the media on its own before the system was saturated and the DOT in the aqueous phase reached 100 %.

Oil	Average oxygen solubility of dispersions mmol l <sup>-1</sup>			
	0.01	0.05	0.10	0.20
50 cS Silicone oil	0.325	0.625	1	1.75
5 cS Silicone oil	0.325	0.625	1	1.75
Soya oil	0.252	0.26	0.27	0.29
Mineral oil	0.258	0.289	0.325	0.4
FC-40	0.278	0.388	0.525	0.8

**Table 5.2.** Average oxygen solubility of the dispersions.

At a volume fraction of  $\Phi = 0.2$ , the silicone oils required seven times more oxygen than media to be added before they were saturated. If the  $k_{La}$  enhancement factors obtained were due entirely to the extra time it takes to saturate the system then those for the silicone oils at  $\Phi = 0.02$  would be approximately 0.14. Figure 5.3 shows that the  $k_{La}$  enhancement factors at a volume fraction of  $\Phi = 0.2$  were in fact 0.27 and 0.42 for 50 cS and 5cS respectively.

This suggests that although those systems needed seven times more oxygen to be supplied before they were saturated compared to an aqueous system, it does not mean that it took seven times longer to supply that extra oxygen. It would take seven times longer to saturate an aqueous system that had a sevenfold increase in its saturation concentration, but because the oils increase the rate of oxygen transfer from the gas phase via the shuttle mechanism the additional oxygen could be supplied quicker. The  $k_{La}$  enhancement factor for 5cS silicone oil was greater than that of 50cS silicone oil at a volume fraction of

$\Phi = 0.2$ , which might be because the 5 cS silicone oil increased the oxygen transfer rate much more than the 50cS silicone oil.

There was good agreement between the OUR and  $k_{La}$  enhancement factors obtained for the soya bean oil ( $E_{OUR} = 1.1 \pm 0.06$  and  $E_{k_{La}} = 1.05 \pm 0.04$ ) and the mineral oil ( $E_{OUR} = 0.83 \pm 0.04$  and  $E_{k_{La}} = 0.74 \pm 0.03$ .) at a volume fraction of  $\Phi = 0.01$ . These results suggest that the changes in the oxygen transfer rate – an increase in the case of soyabean oil, and a decrease in the case of mineral oil, were due to the affects of the oils on the  $k_{La}$  (the resistance to mass transfer or the gas bubble diameter). The soya bean oil and the mineral oil increased the average oxygen concentrations of the dispersions by only 1.01 and 1.03 respectively, and so the extra time required to saturate the system might have been insignificant.

The dynamic gassing-out method has been used by many authors to investigate the effect of antifoams and surfactants on the  $k_{La}$  (Morao *et al.*, 1999; Liu *et al.*, 1994; Kawase and Moo – Young, 1990). But those experiments were carried out using very low concentrations i.e. less than a volume fraction of  $\Phi = 0.01$ . The results in Figure 5.3 show that if the addition of the oil causes a significant increase in the average oxygen concentration of the dispersion, the method is not an appropriate technique to determine the effect of the oils on the  $k_{La}$ .

If the oils do cause a significant increase in the average oxygen concentration, the rate of change of the DOT is not only a result of the effect of the oils on the  $k_{La}$  (i.e. on the bubble diameter or resistance to mass transfer), but also on the following factors:

- the time it takes to add the extra oxygen required by the dispersion
- the increased rate of oxygen transfer because the overall driving force has increased.

The results suggest that the  $k_{La}$  enhancement factors obtained at a volume fraction of  $\Phi = 0.01$  for the soya bean oil and the mineral were largely a result of the effect of the oils on the  $k_{La}$ . This is because they did not cause a significant increase in the average oxygen solubility of the dispersion. The mineral oil caused a decrease in both the  $k_{La}$  ( $E_{kLa}$ ) and the OUR ( $E_{OUR}$ ) enhancement factors at this volume fraction.

The oils could have changed the  $k_{La}$  in three ways: the mass transfer coefficient ( $k_L$ ) by changing the surface mobility or causing interfacial blockage; the gas-liquid interfacial area ( $a$ ) by changing the rate of coalescence; and increasing the gas-liquid interfacial area ( $a$ ) by decreasing the surface tension. The  $k_{La}$  value obtained when oil is added is a result of the relative effect of each of these factors.

The  $k_{La}$  often decreases after the addition of very low concentrations of surfactants and oils, but then increases as the oil fraction increases (Yoshida *et al.*, 1970; Linek and Benes, 1976; Morão *et al.*, 1999; Liu *et al.*, 1994). Marão *et al.* (1999) found that soya bean oil and silicone oil decreased the  $k_{La}$  between concentrations of 50 –100 ppm, but increased it at concentrations above 1000ppm.

Many authors have also found that the  $k_L$  initially decreases at very low concentrations and then increases at higher concentrations (Eckenfelder and Barnhart, 1961; Yoshida *et al.*, 1970; Linek and Benes, 1976; Liu *et al.*, 1994; Morão *et al.*, 1999). Therefore, the decrease in the  $k_{La}$  and the OUR at a mineral oil volume fraction of  $\Phi = 0.01$  may have been due to its effects on the  $k_L$ .

At a volume fraction of  $\Phi = 0.01$  the mineral oil decreased the enhancement factor for both the  $k_{La}$  and the OUR. However, at the higher volume fractions used the OUR enhancement factor did increase, but unfortunately it was not possible to see if the mineral oil caused the  $k_{La}$  to increase at higher volume fractions because of the reasons described above.

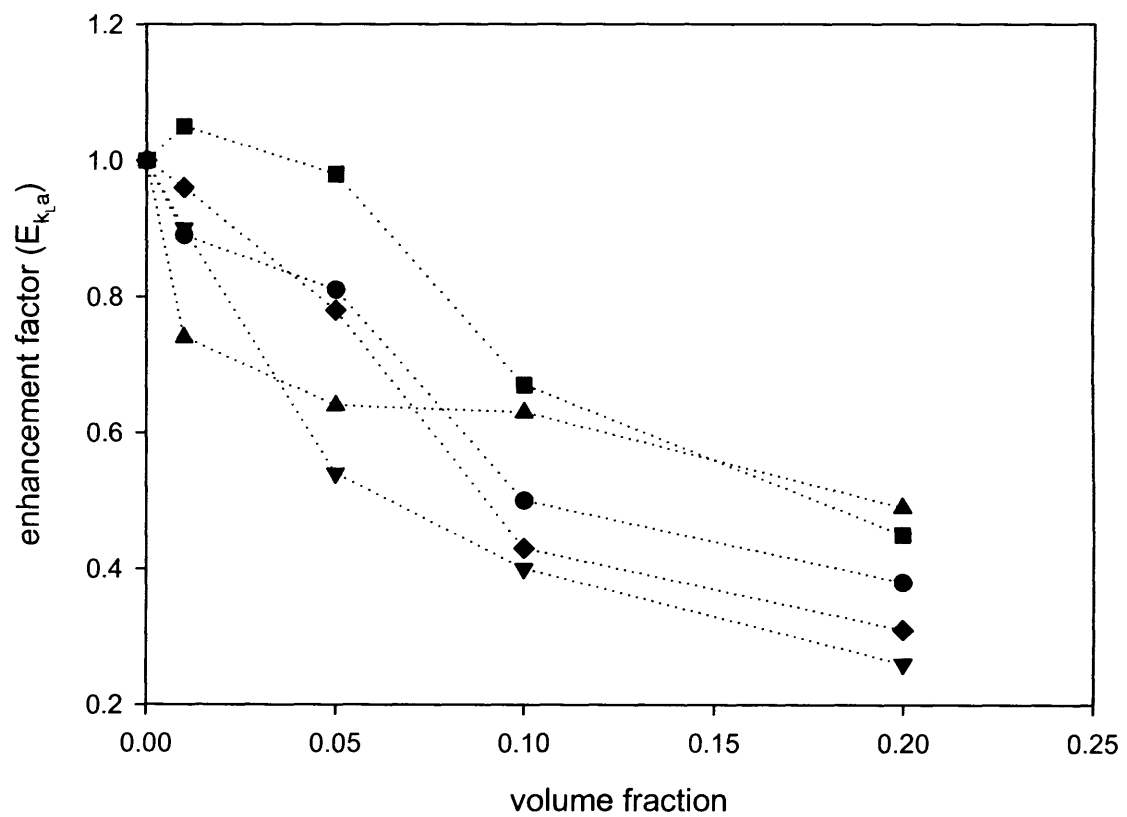


**Figure 5.3.** The effect of the oil volume fraction on the  $k_{La}$  enhancement factor ( $E_{k_{La}}$ ). 5cS silicone oil (●); 50cS silicone oil (▼); FC-40 (◆); soya bean oil (■); mineral oil (▲).

The mineral oil might also have changed the gas – liquid interfacial area ( $a$ ) by decreasing the surface tension and therefore decreasing the bubble size or by increasing or decreasing the rate of bubble coalescence. However, the effects of the mineral oil on the interfacial area would be easier to determine than its effect on the  $k_L$  because photographic techniques could be used to determine the mean bubble size.

### 5.2.3.1.1 Effect of the viscosity on the $k_L a$

The 5cS silicone oil and the FC-40 had larger OUR enhancement factors than the other oils at volume fractions between  $\Phi = 0.05$  and 0.2, and both had viscosities five to 10 fold less than the other oils. Rols *et al.* (1990), Rols and Gomer (1991) and MacMillan and Wang (1987), found that after an initial linear increase, the enhancement factor began to decline above a critical oil volume fraction. Both authors suggested that this was due to an increase in the overall viscosity of the broth, which would cause a reduction in the volumetric mass transfer coefficient ( $k_L a$ ).

Oil	Average viscosity (37°C)			
	m.Pas			
	0.01	0.05	0.10	0.20
50 cS Silicone oil	1.01	1.12	1.26	1.60
5 cS Silicone oil	1.01	1.11	1.23	1.54
Soya oil	1.01	1.12	1.26	1.60
Mineral oil	1.01	1.12	1.26	1.59
FC-40	1.01	1.11	1.24	1.54

**Table 5.3.** Average viscosity of the dispersions at each volume fraction.

Table 5.3 shows that the average viscosities of the oil dispersions - calculated as described in Section 2.9.4.2 - were similar at each volume fraction. The OUR enhancement factors of 5cS and FC-40 increased linearly between volume fractions 0.05 and 0.2, and did not seem to be affected by the increase in viscosity. Therefore, the low OUR enhancement factors obtained with 50cS

silicone oil, mineral oil and soya bean oil, were probably not due to an increase in the bulk viscosity.

### 5.2.3.2 Effect of the oils on the saturation concentration ( $C^*$ )

#### 5.2.3.2.1 Spreading coefficient

There was no correlation between the enhancement factors obtained for each of the oils and their spreading coefficients. The spreading coefficients of the oils with complex media and complex media with  $7 \text{ gl}^{-1}$  *E.coli* JM107 are shown in Table 5.4 – the experiments are described in Section 2.9.3. To reflect the conditions of the fermenter, the oils and aqueous phases had been pre-saturated with one another before the interfacial tension measurements were made. All of the oils, except FC-40, had negative spreading coefficients with both aqueous phases. Brillman (1998) demonstrated that the spreading coefficient of the oil is not a good indicator of the ability of oil to spread under the hydrodynamic conditions that occur in stirred tank reactors. However, without photographic evidence it is not possible to conclude whether or not the oils did spread. The results suggest that the  $C^*$  is not increased via the bubble-covering mechanism.

<b>Oil</b>	<b>Complex media (<math>\text{mNm}^{-1}</math>)</b>	<b>Complex media with <math>7 \text{ gl}^{-1}</math> <i>E.coli</i> JM107 (<math>\text{mNm}^{-1}</math>)</b>
<b>50 cS silicone oil</b>	-8	-11.2
<b>5 cS Silicone oil</b>	-3.2	-7.6
<b>Soya oil</b>	-7.6	-17.5
<b>Mineral oil</b>	-12.5	-25.5
<b>FC-40</b>	14.9	14.1

**Table 5.4.** Spreading coefficients of the oils with different aqueous phases.

#### 5.2.3.2.2 Oxygen solubility

The 5cS silicone and the FC-40 had the highest oxygen solubility's and they also caused the highest OUR enhancement factors. The 50cS silicone oil and the 5cS silicone oil have the same oxygen solubility; therefore, the lower OUR enhancement factors obtained with the 50cS silicone must be due to the effect of another physical property. Similarly, the lower OUR enhancement factors obtained with soya bean oil and mineral oil might not only be due to their lower oxygen solubility, but also to another physical property.

#### 5.2.3.2.3 Viscosity

The viscosity of the oils can affect the diffusivity of oxygen in the oil and the oil drop size – both these properties will influence the ability of the oil to increase the saturation concentration.

#### 5.2.3.2.4 Diffusivity and permeability

MacMillan and Wang (1987) and Junker *et al.* (1990b), suggested that the OUR enhancement factor could be better estimated from the permeability of oxygen in the oil rather than from the oxygen solubility. The effect of high oxygen solubility on the enhancement factor might be cancelled out if the diffusivity of oxygen in the oil is very low.

Table 5.5 shows the solubility, diffusivity, and permeability of oxygen in each of the oils. The diffusivities were calculated as described in Section 2.9.5.2. The diffusivity of oxygen in 50cS silicone oil, mineral oil and soya bean oil was less than in water. However, the permeability of oxygen in 50cS silicone oil is approximately the same as FC-40, and approximately 30 fold greater than in soya bean oil and mineral oil. Therefore, the lower enhancement factors obtained with 50cS silicone oil could not have been entirely due to low oxygen permeability; therefore, the lower enhancement factors obtained with soya bean oil and mineral oil might not have been due to their low oxygen diffusivity and permeability. Leung *et al.* (1997) found that microencapsulated silicone oil with a viscosity of 10000 mPa caused a 1.7 fold increase in the  $k_L a$ . The oxygen diffusivity would have been lower than the oils used in this study, which



indicates that the low diffusivity does not necessarily prevent an increase in the oxygen transfer rate.

Oil	Oxygen solubility mmol m <sup>-3</sup>	Oxygen diffusivity m <sup>2</sup> s <sup>-1</sup>	Oxygen permeability mol m <sup>-1</sup> s <sup>-1</sup>
50 cS silicone oil	7.75	9.2 x 10 <sup>-9</sup>	7 x 10 <sup>-8</sup>
5 cS Silicone oil	7.75	2.2 x 10 <sup>-9</sup>	1.7 x 10 <sup>-8</sup>
Soya oil	0.36	8.0 x 10 <sup>-10</sup>	2.9 x 10 <sup>-10</sup>
Mineral oil	1	5.0 x 10 <sup>-10</sup>	5 x 10 <sup>-10</sup>
FC-40	3	5.4 x 10 <sup>-9</sup>	1.6 x 10 <sup>-8</sup>

**Table 5.5.** The oxygen solubility, diffusivity and permeability of the oils.

#### 5.2.3.2.5 Drop size

The shuttle mechanism assumes that oils can only increase the saturation concentration if they are small enough to enter the boundary layer. Bruining *et al.* (1986) found that drops with a diameter of 10 µm increased the oxygen transfer rate in a system with an estimated film thickness 23 µm, but 50 µm drops did not. van der Meer *et al.* (1992) found that neat n- octane did not increase the oxygen transfer rate, whereas emulsified n-octane, which had smaller diameters, did. Nagy and Hadik (2003) found that the enhancement factor increased with decreasing particle size, but once the oil droplets reached a small enough size there was no further increase in the enhancement factor. Solid particles that have a diameter smaller than the boundary layer thickness can also increase the oxygen transfer rate to the aqueous phase (Beenackers and Swaaij, 1993).

The diameters of the oil drops were estimated using correlations that relate the Sauter mean diameter to the oil volume fraction and to the tank Weber number

( $We_T$ ). The Weber number represents the ratio between the disruptive forces that cause a drop to break up and the cohesive forces that hold a drop together (Zhou and Kresta, 1998; Hinze, 1955). The disruptive forces are due to the turbulence in the system, whereas the cohesive forces are due to the interfacial tension and to the internal viscous forces. The majority of the correlations in the literature assume the viscous forces are negligible. However, in high viscosity oils the viscous forces are not negligible, and consequently the drop size increases.

There are only a few correlations that account for the viscosity of the oil. The drop sizes were estimated using the correlation of Nishikawa *et al.* (1987), which takes into account the effect of viscous forces, and of Godfrey and Grilc (1977), which does not – the correlations are shown in Section 2.11.

Figure 5.4 shows that the Sauter mean diameters of 50cS silicone oil, soya bean oil, and mineral oil, as predicted by the Nishikawa correlation, were approximately two and ten fold greater than the 5cS silicone oil and the FC-40 respectively. The 5cS silicone oil and the FC – 40 drops might have been sufficiently small to enter the boundary layer, whereas the other oil droplets may have been too large. The Sauter mean diameters of the high viscosity oils, as predicted by the Godfrey correlation, were similar to that of 5cS silicone oil. The Nishikawa and the Godfrey correlations predicted similar drop sizes for the 5cS silicone oil and the FC-40.

The predicted size of the boundary layer in a stirred tank reactor has been estimated to be approximately 10  $\mu\text{m}$  (van't Riet, 1991). Only the FC-40 oil droplets had predicted Sauter mean diameters of 10  $\mu\text{m}$ . However, the Sauter mean diameter represents a mean – the smallest droplets may have been responsible for the increase in the oxygen transfer rate. Nishikawa *et al.* (1994) found that aeration changes the drop size distribution so that there are smaller and larger particles and less in the normal range.

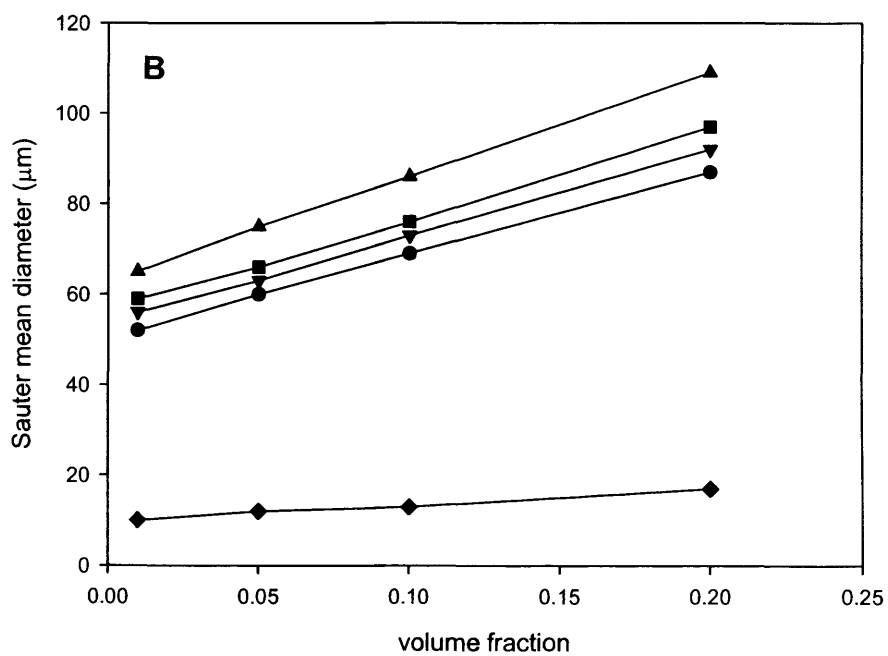
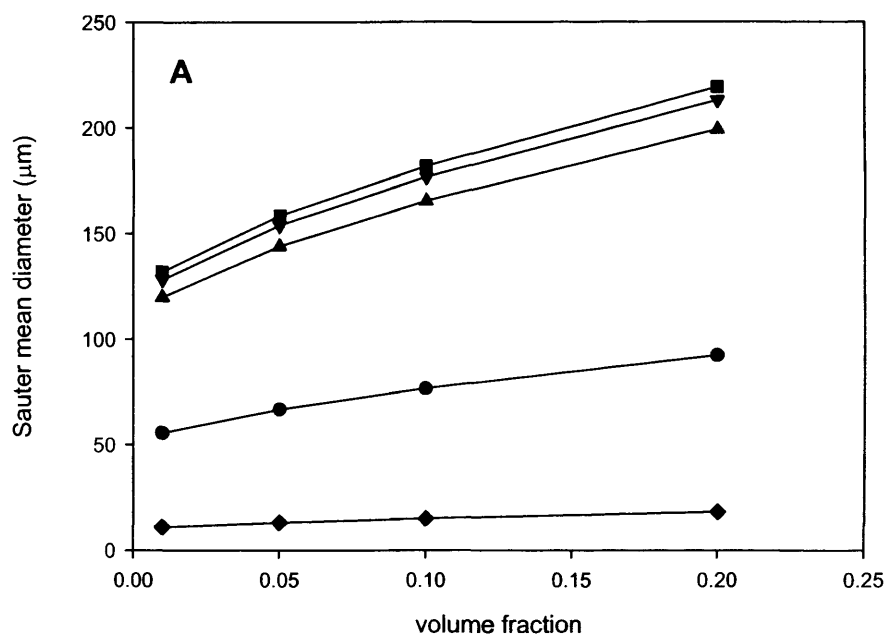


**Figure 5.4.** Predicted Sauter mean diameters of the oils at 700 rpm and 1vvm. A. Nishikawa correlation B. Godfrey correlation. 5cS silicone oil (●), 50cS silicone oil (▼), FC-40 (◆), soya bean oil (■), mineral oil (▲).

### 5.2.3.2.6 Impeller speed

If the impeller speed is changed the oil droplet size should also change. Experiments were carried out to determine if the OUR enhancement factors obtained with 5cS silicone oil decreased when the impeller speed was 500 rpm, and if those obtained with 50cS silicone oil increased when the impeller speed was 900 rpm. The experiments were carried out as described in Section 2.8. Figure 5.5 shows that there was no change in the enhancement factors of 5cS silicone oil or 50cS silicone oil when the impeller speed was changed.

The drop sizes of the oils might not have increased or decreased enough. The Godfrey correlation predicted that the Sauter mean diameter of the 5cS silicone oil would increase from 50 – 90  $\mu\text{m}$  to 80 – 130  $\mu\text{m}$  at volume fractions of 0.01 – 0.2, but there still might have been enough smaller drops present to increase the enhancement factor. The Nishikawa correlation predicted that the Sauter mean diameter of the 50cS silicone oil would decrease from 130 – 210  $\mu\text{m}$  to, 90 – 145  $\mu\text{m}$ , but this might not have been enough to produce drops that were small enough.

The change in the oil drop size might have been counteracted by a change in the boundary layer thickness. According to film theory, the boundary layer thickness is inversely proportional to the mass transfer coefficient ( $k_L$ ). The mass transfer coefficient will increase and the boundary layer size will decrease if the impeller speed is increased – the opposite will happen if the impeller speed is decreased.

Kollmer *et al.* (1999) found that biosurfactants, which are excreted by cells, stabilise the oil drops and thus droplet coalescence and break – up stops. The effect of biosurfactants on the oil drop size might have outweighed the effect of the change in the impeller speed.

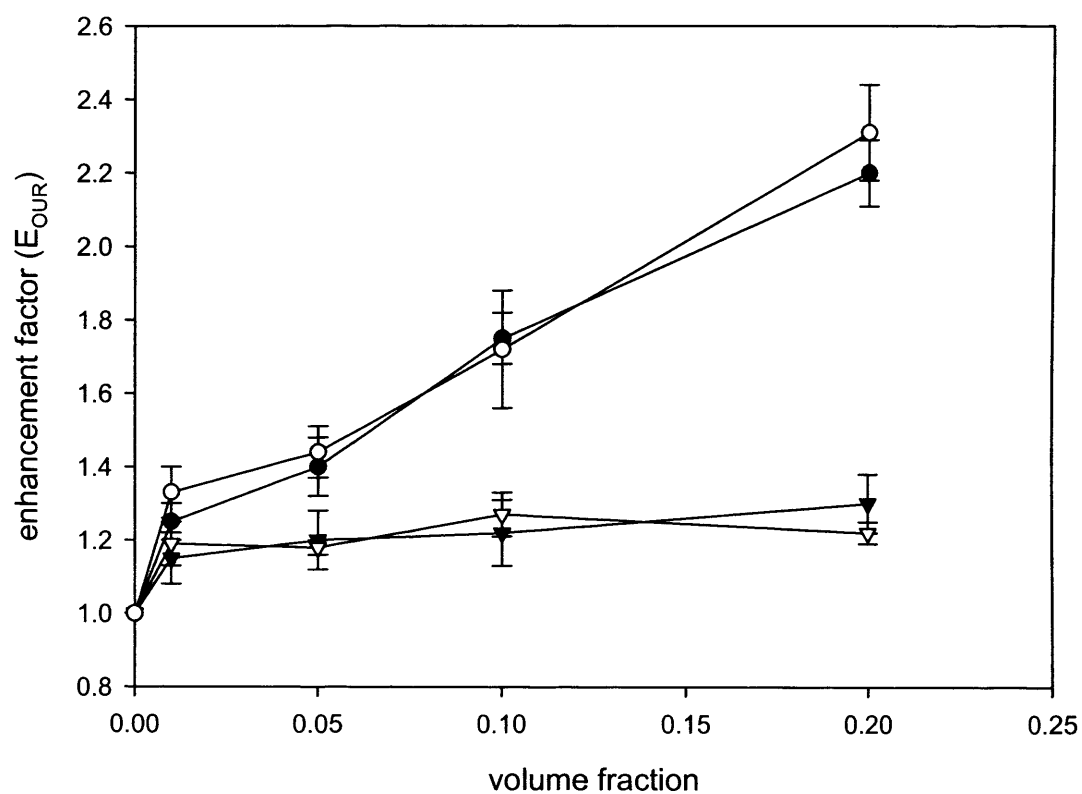


**Figure 5.5.** The effect of the 5cS and 50cS silicone oil volume fraction on the OUR enhancement factors ( $E_{OUR}$ ) on a total volume basis. 5cS silicone oil at 500 rpm (●); 50cS silicone oil at 900 rpm (▼); 5cS silicone oil at 700 rpm (○); 50cS silicone oil at 700rpm (▽). The experiments were carried out in triplicate and the error bars represent

### 5.2.4 Assessment of $E_{shuttle}$ model

The  $E_{shuttle}$  model was developed by Bruining *et al.* (1986) and is based on the shuttle mechanism that was described in Section 1.5.2.3.2. The model uses the penetration theory as the mass transfer model and makes the following assumptions:

- solubility ratio between the oil and the aqueous phase is greater than 10
- no contact between the gas and the oil phase
- oil droplets are smaller than the boundary layer
- oil is homogeneously distributed throughout the aqueous phase
- mass transfer resistances within the oil can be neglected

The  $E_{shuttle}$  model is defined as:

$$E_{shuttle} = \sqrt{(1 + \Phi(m - 1))} \quad (5.3)$$

The difference between the experimental and predicted data was calculated as follows:

$$\% \text{ difference} = 100 \left( \frac{E_{experimental} - E_{shuttle}}{E_{shuttle}} \right) \quad (5.4)$$

If the difference is negative, the model has overestimated the OUR enhancement factor, and if it is positive, it has underestimated the enhancement factors. If the experimental and predicted enhancement factors are the same the difference will be zero. Figures 5.6 and 5.7 show the percentage differences at each volume fraction. The values were calculated using the experimental data shown in Figure 5.2. These experiments were done in triplicate - the error bars represent the standard deviation of the mean.

Figure 5.6 shows that the experimental and predicted data for FC-40 were in good agreement – the difference between the two was 10% or less. For the 5cS silicone oil, the enhancement factor ( $E_{OUR}$ ) was underestimated at a volume

fraction of  $\Phi = 0.01$  – possibly because it does not take into account the affect on  $k_{L,a}$ . At higher volume fractions, the model overestimated the enhancement factor by up to 15 %. For the 50cS silicone oil the enhancement factor ( $E_{OUR}$ ) was overestimated by up to 53%. This is probably because the oil drop size was too large and so the assumption that they are small enough to enter the boundary layer was not met.

Figure 5.7 shows that the model appears to be in reasonable agreement with the experimental data for the soya bean oil and the mineral oil. However, this would be a false conclusion, because any changes in the enhancement factors ( $E_{OUR}$ ) for these oils were probably due to their effect on the  $k_{L,a}$ . As with the 50cS silicone oil, the drop sizes of these oils were probably too large. Also, the solubility ratios for these oils were less than ten.

Dumont and Delmas (2003) calculated the percentage difference between the experimental and predicted enhancement factors for data from the literature, and found that the  $E_{shuttle}$  underestimated the enhancement factor up to 15 – 20% depending on the oil and the volume fraction. This might be because the model does not account for the effect of the oils on the  $k_{L,a}$ . Most of the data used by Dumont and Delmas was from chemical systems. In this work the  $E_{shuttle}$  model tended to overestimate the enhancement factor ( $E_{OUR}$ ) for 5cS silicone oil.

The results from this work show that the  $E_{shuttle}$  model is in reasonable agreement with the experimental data as long as the drop size is small enough. However, Nagy and Hadik (2003) demonstrated that the  $E_{shuttle}$  model only predicted the maximum enhancement factor – there was drop range where the oxygen transfer rate increased, but not by the potential maximum.

Mass transfer is more complicated in biological systems compared to chemical ones because of the presence of biosurfactants and whole cells, which can accumulate at the gas-water and oil-water interfaces.

Microorganisms produce biosurfactants such as proteins, phospholipids, and lipopolysaccharides that adsorb at interfaces. Their effects vary by extent and nature and they can increase or decrease the mass transfer rate, but at present these effects cannot be predicted. This is of particular significance for systems containing organic solvents, because they can cause the disintegration of the cell membrane resulting in the release of biosurfactants.

The presence of biosurfactants could reduce the ability of the oil droplets to enhance the oxygen transfer rate by decreasing the rate of oxygen from the aqueous phase to the oil in the boundary layer and from the oil phase to the bulk aqueous phase. Therefore, the OUR enhancement factors ( $E_{OUR}$ ) might not be as great as those obtained with a chemical system with the same hydrodynamic conditions.

Biosurfactants concentrate at the interface between phases; the existence of a biosurfactant monolayer can cause interfacial blockage, which reduces the permeability of a solute through the interface. Also, the biosurfactant monolayer can add mechanical stability to the droplets, which decreases the transmission of shear stress and thus turbulence across the interface (Lye and Stuckey, 2001).

Schmid *et al.* (1998b) investigated the maximum volumetric growth rates obtained in two-liquid phase *Pseudomonas oleovorans* cultures grown on n-decane as the sole carbon source. Biosurfactants, which had been harvested from previous fermentations, were added to the growth media before the experiments were begun. They found that although the biosurfactants decreased the mean droplet diameter, the volumetric mass transfer coefficient was decreased, which they proposed was due to increased resistance to mass transfer across the liquid – liquid interface.

The work of Schmid *et al.* (1998b) was carried out in a fermenter, and so the effects of the biosurfactants on the interfacial area and the mass transfer coefficient could not be separated. However, a piece of equipment called a



Lewis cell can be used to measure the mass transfer coefficient ( $k_L$ ). It provides a flat interface between two liquids, and because the area available for mass transfer between the two liquids is known the  $k_L$  can be calculated (Lewis, 1954).

Purcell *et al.* (2004) used a Lewis cell to investigate the effect of filtered fermentation broth on the mass transfer coefficient for the extraction of chloramphenicol into octanol. The biosurfactant concentration was varied by using different dilutions of fermentation broth. The overall mass transfer coefficient decreased by up to 70 % as the filtered broth concentration increased. They also used the Lewis cell to investigate the effect of three different proteins on the mass transfer rate of chloramphenicol from water to octanol, and found that as their concentration was increased the mass transfer coefficient decreased.

The experimental methods of Schmid *et al.* (1998b) and Purcell *et al.* (2004) could be adapted to investigate the effects of biosurfactants on the OUR enhancement factors obtained with the oils. The oxidation of sodium sulphite to sulphate could be used as a model system so that the effects of the biosurfactants on the oxygen transfer rate in a clean system could be investigated.

The  $E_{\text{shuttle}}$  model tends to underestimate the enhancement factors obtained in chemical systems, but the results from this chapter indicate that the model tends to overestimate the enhancement factor for biological systems. Sodium sulphite oxidation could be carried out in a fermenter using the same hydrodynamic conditions that were used for the experiments in this chapter. This could be used to investigate how the biosurfactant concentration affects the enhancement factors obtained with each of the oils. Comparison with a reference that contained no biosurfactant might indicate to what extent biosurfactants cause the  $E_{\text{shuttle}}$  model to overestimate the OUR enhancement ( $E_{\text{OUR}}$ ) factor for biological systems.

Organic solvents can cause the disintegration of the cell membrane resulting in the release of biosurfactants into the media. This means that during the course of a bioconversion the biosurfactant concentration in the media will increase. Carrying out experiments using the sodium sulphite oxidation with increasing biosurfactant concentrations might also indicate whether the OUR enhancement factors are likely to decrease during the course of a bioconversion.

The results of these experiments would not separate the effects of the biosurfactant on the interfacial area and the resistance to mass transfer. Further experiments could also be carried out in a Lewis cell to quantify the effect of the biosurfactants on the  $k_L$ . The aqueous phase could be deoxygenated so that a driving force for mass transfer was created and the rate of oxygen transfer from either the gas or the oil could be recorded using a DOT probe. It could be used to compare the effect of the biosurfactants on the rate of mass transfer from the gas to the aqueous phase and from the oil to the aqueous phase. It could be also be used to see if particular biosurfactants had a greater effect and whether this depended on which oil was used.

Whole - cells can cause interfacial blockage at gas – water interfaces, and thus decrease the  $k_{La}$  (Ju and Sundararajan, 1994; Bungay and Masak, 1981). However, when cells adsorb at an interface a hydrodynamic drag is created which moves the interface and is believed to increase the collision frequency between cells and the bubbles and so lead to the attachment of more cells at the bubble surface – a phenomenon known as the snowball effect (Andrews *et al.*, 1980a;1980b). This mechanism is thought to increase the oxygen transfer rate, but it is possible that it might prevent oil droplets from getting sufficiently close to the interface to enhance the oxygen transfer rate.

Whole – cells can also adsorb at the oil – aqueous interface, and therefore cause interfacial blockage (Mimura *et al.*, 1973; Yoshida *et al.*, 1977; Purcell *et al.*, 2004). The degree to which cell adsorption occurs depends on the type of microorganism and the carbon source (microorganisms growing on hydrocarbo-

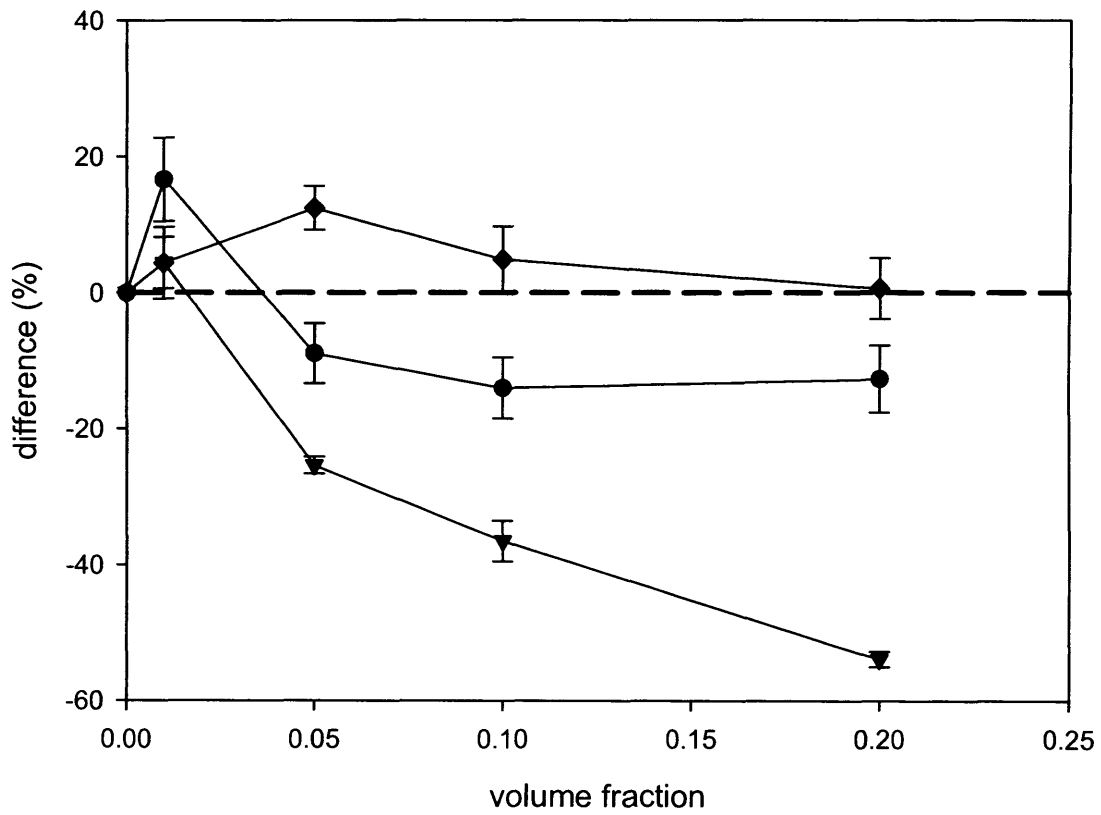


**Figure 5.6.** Percentage difference between experimental and  $E_{shuttle}$  model predicted OUR enhancement factors ( $E_{OUR}$ ) at different volume fractions. 5cS silicone oil (●); FC-40 (◆); 50 cS silicone oil (▼).

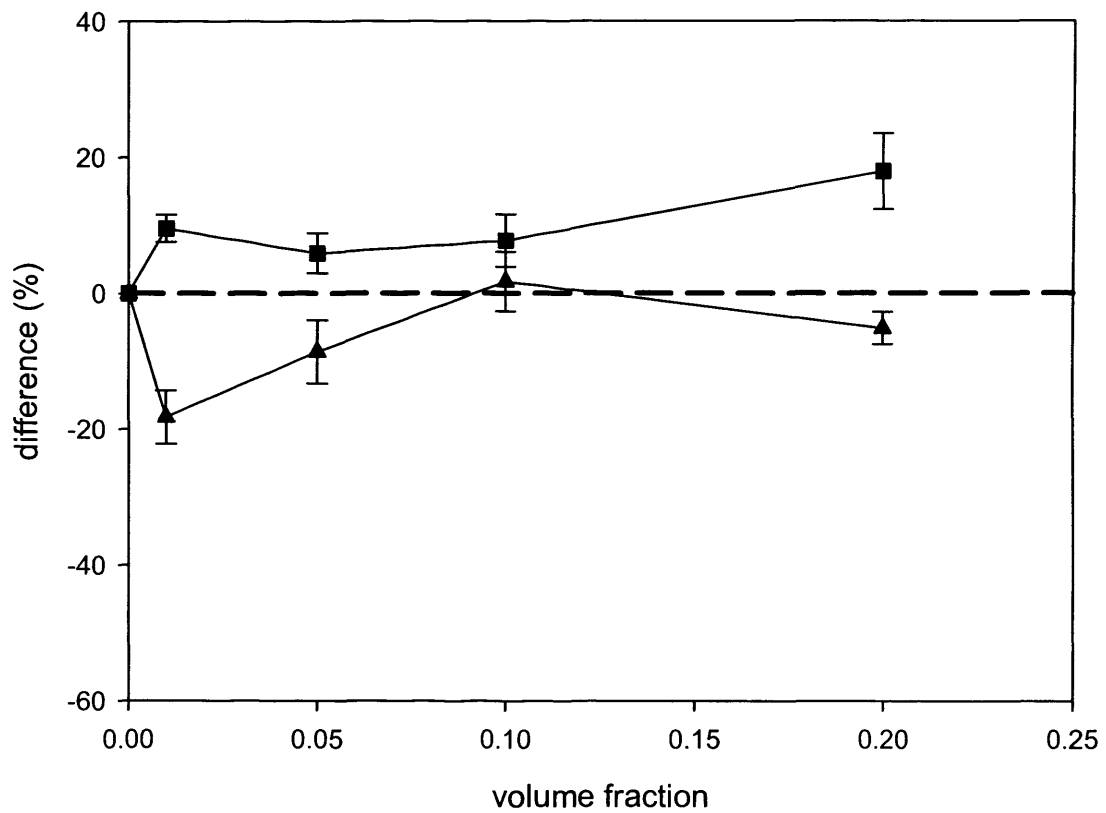


**Figure 5.7.** Percentage difference between experimental and  $E_{shuttle}$  model predicted OUR enhancement factors ( $E_{OUR}$ ) at different volume fractions. Soya bean oil (■); mineral oil (▲).

-ns have a higher affinity for oils than those growing on carbohydrate) (Rols and Goma, 1999).

### 5.2.5 Implications for whole-cell oxygenase processes

Figure 5.8 shows the enhancement factors obtained with each of the oils on an aqueous phase basis. This represents the increase in the oxygen transfer rate to the aqueous phase, and is defined as:

$$E_{OUR} = \frac{1}{1-\phi} \cdot \frac{OUR_{oil}}{OUR_{no\ oil}} \quad (5.5)$$

Organic solvents should increase the oxygen transfer rate to the aqueous phase as long as the drop diameters are small enough, and if they do not have an adverse affect on the  $k_L a$ .

Cull *et al.* (2002) found that scale-up based on constant power input per unit volume was the best way to ensure identical drop size distributions at different scales. The power input of the experiments carried out at impeller speed of 700 rpm and 1vvm was determined to be  $1.3 \pm 0.1 \text{ kWm}^{-3}$ . The experiment is described in Section 2.10.

Industrial fermenters have power inputs between  $1 - 4 \text{ kWm}^{-3}$  (Woodley, 1990; Doran 1999), therefore it might be possible to increase the oxygen transfer rate in industrial scale fermenters. However, this would only be the case for the 5cS silicone oil and the FC-40. The more viscous oils had drop sizes that were too large to increase the oxygen transfer rate. Most organic solvents have a viscosity less than water: at the power input used in these experiments, the drop sizes of most organic solvents should be small enough to increase the oxygen transfer rate.

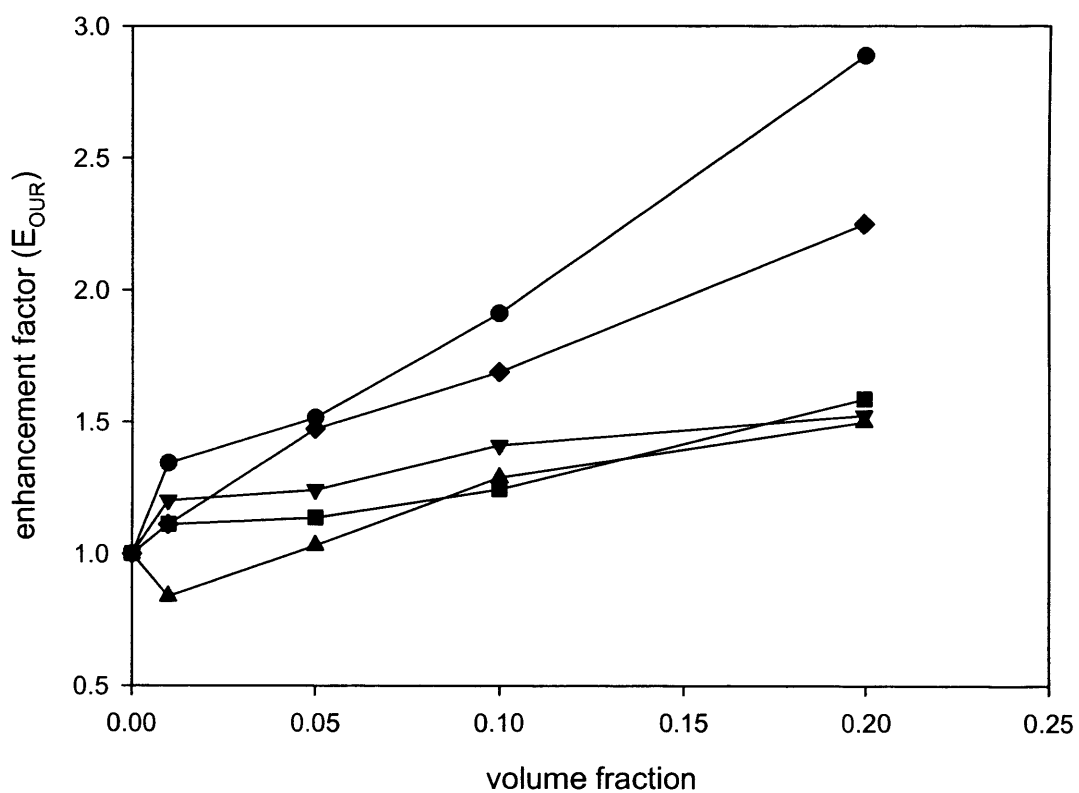


**Figure 5.8.** The effect of the oil volume fraction on OUR enhancement factors ( $E_{OUR}$ ) on an aqueous phase basis. 5cS silicone oil (●); 50cS silicone oil (▼); FC-40 (◆); soya bean oil (■); mineral oil (▲).

### 5.3 Conclusions

The aim of this chapter was to investigate how the physiochemical properties of oils affect their potential to increase the oxygen transfer rate. The conclusions are:

- The oxygen transfer rate increased up to 2.5 fold depending on the physical properties of the oil and the volume fraction used.
- The oils affected the volumetric transfer coefficient ( $k_La$ ) and the saturation concentration ( $C^*$ ).
- By comparing 5cS and 50cS silicone oil, which have the same oxygen solubility, it was shown that the viscosity of the oil influenced the enhancement factor ( $E_{OUR}$ ). This was not due to an increase in the diffusivity or permeability of oxygen in the oils, but due to the effect of viscosity on droplet size.
- There was no correlation between the spreading coefficient and the enhancement factors. This suggests that the saturation concentration was not increased via the bubble-covering mechanism.
- The  $E_{shuttle}$  model predicted the OUR enhancement factors well as long as the assumptions of the model were met.

## 6.0 Enhancement of the oxygen transfer rate during whole-cell bioconversions

### 6.1 Introduction

Organic solvents can be used in whole-cell oxygenase bioconversions to alleviate the effects of low water solubility and toxicity of the substrates and products. The aim of this chapter was to show that they can also increase the oxygen transfer rate to the aqueous phase during a bioconversion.

In Chapter 4 it was shown that when oxygen was limited the specific activity of the biocatalyst decreased. At an impeller speed of 700 rpm, the process became oxygen limited at biomass concentrations above  $1\text{g}_{\text{dcw}}\text{l}^{-1}$ . If the biomass concentration was increased above a critical point, there was no further increase in the activity. The CHMO and the electron transport chain competed for the oxygen, and the CHMO used 20 % regardless of the severity of the oxygen limitation. When the oxygen transfer rate was increased the specific activity increased by the same proportion. In Chapter 5 it was shown that 5cS silicone oil and FC-40 could increase the oxygen transfer rate to the aqueous phase up to 2.5 fold.

In this chapter the results of Chapters 4 and 5 were linked. Bioconversions were carried out under the same conditions as the experiments in the previous chapters i.e. in a 2 l fermenter at 700 rpm and 1vvm, so that the results could be compared. However, in this chapter, the bioconversions were carried out at a biomass concentration high enough to ensure the reactions were oxygen limited so that the effect of the oil on the specific activity and the OUR could be determined.



## 6.2 Results and Discussion

### 6.2.1 Outline of experiments

The purpose of the experiments in this chapter was to determine how the specific activity of the *E.coli* biocatalyst was affected by the addition of oil. Bioconversions were carried out in a 1.4 l working volume fermenter using an impeller speed of 700rpm and an aeration rate of 1vvm so that the results could be compared with the experiments in the previous chapters.

FC-40 was used in these experiments because it does not dissolve organics - the solubility of bicycloheptenone and oxabicyclooctenone in FC-40 was determined as described in Section 2.14 and was found to be negligible. It was desirable that the substrate and product were not soluble in FC-40 because the specific activity might have been affected by the mass transfer rate between the two phases. It would then have been difficult to relate the specific activity to the increase in the oxygen transfer rate.

In Chapter 4 it was shown that at a biomass concentration of  $4\text{g}_{\text{dcw}}\text{l}^{-1}$  the specific activity was over four fold less than when there was no oxygen limitation. The calculations in Section 2.13.1 show that if the biomass concentration in the aqueous phase was  $4\text{g}_{\text{dcw}}\text{l}^{-1}$  the biocatalyst would be sufficiently oxygen limited to ensure that the DOT did not increase above zero.

### 6.2.2 Bioconversions with FC-40

Bioconversions of bicycloheptenone to oxabicyclooctenone using  $4\text{g}_{\text{dcw}}\text{l}^{-1}$  *E.coli* were carried out using FC - 40 in volume fractions from 0 to 0.2. The experiments are described in Section 2.13.2. Figure 6.1 shows the reaction profile for the bioconversion using  $\Phi = 0.05$  FC-40. Figure 6.2 shows that the specific activity and the specific OUR increased as the FC-40 volume fraction increased from  $\Phi = 0$  to 0.2. At a volume fraction of 0.2 the specific activity was 2.25 fold higher than for the bioconversion with no FC-40. The activity also increased with volume fraction even though the total biomass decreased.

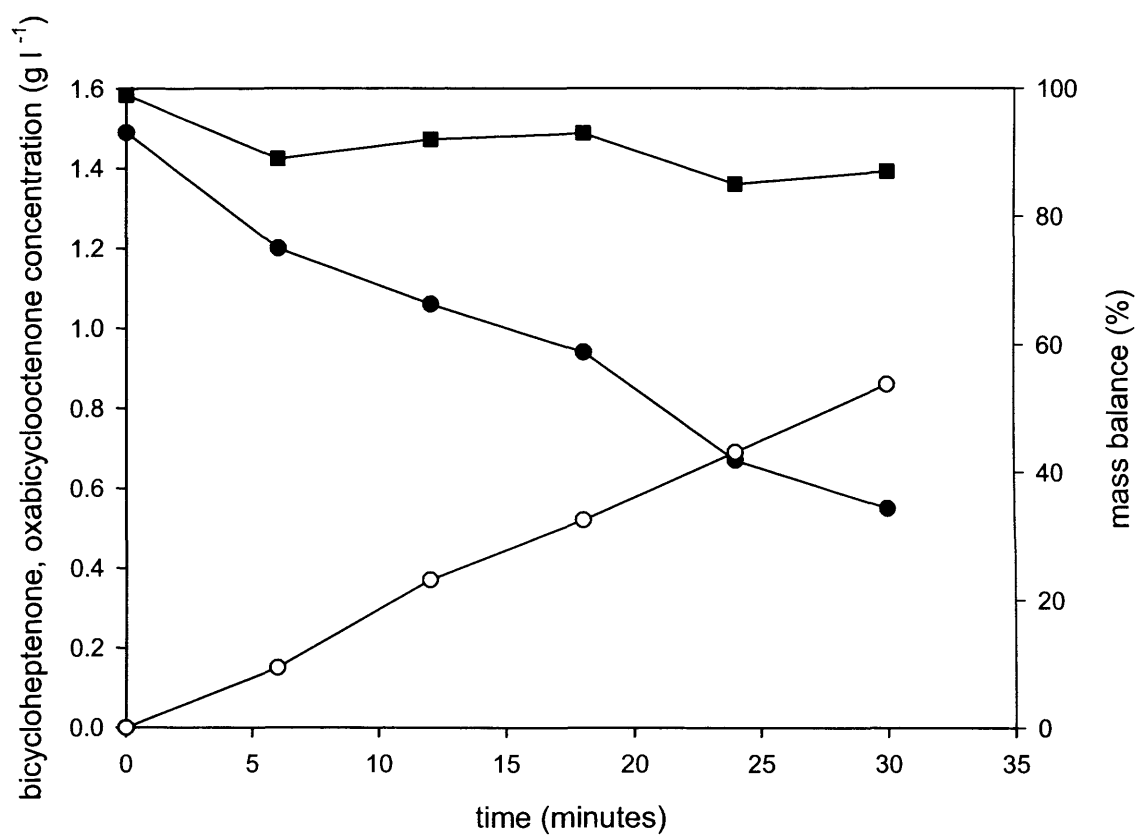


**Figure 6.1.** Reaction profile for a bioconversion using FC-40 at a volume fraction of 0.05 in a 2 l fermenter. Bicycloheptenone (●); oxabicyclooctenone (○) mass balance (■).

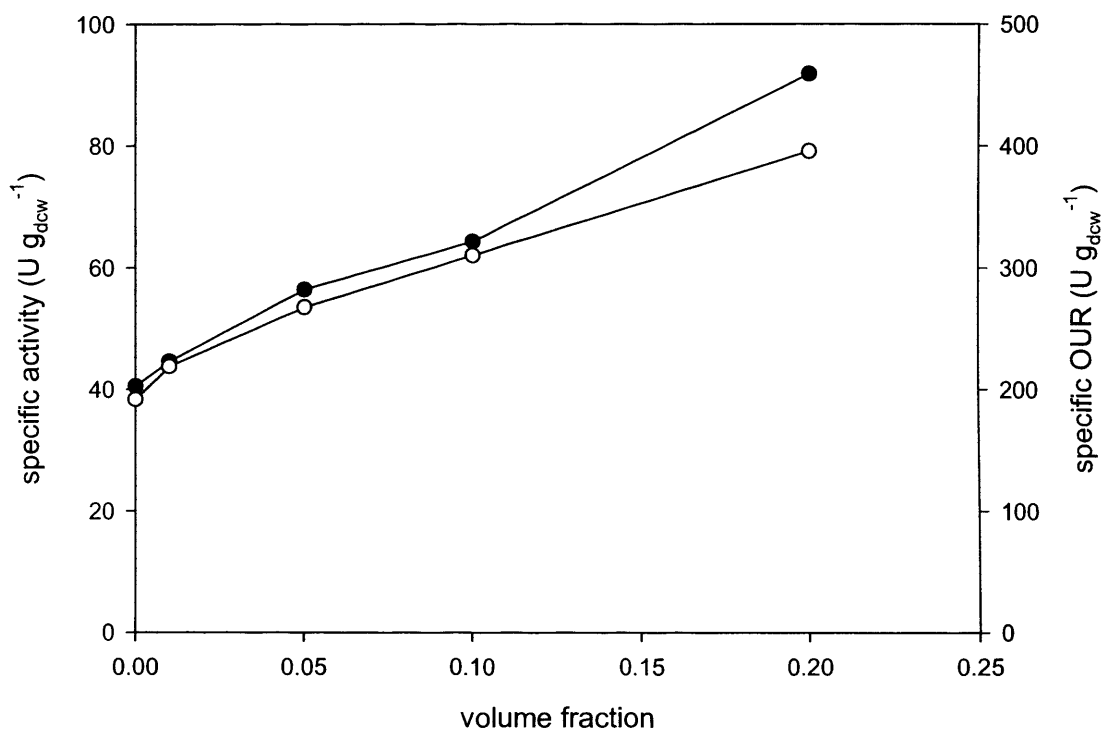


**Figure 6.2.** The effect of FC-40 volume fraction on the specific activity and OUR during bioconversions carried out in a 2l fermenter. The biomass concentration in the aqueous phase was  $4\text{g}_{\text{dcwl}}^{-1}$ . Specific activity (●); specific OUR (○).

The results are consistent with those in Chapter 4, which showed that the specific activity increased by the same amount as the oxygen transfer rate. It was also shown in Chapter 4 that the CHMO consumed approximately 20% of the oxygen when it was limited. For the experiments in this chapter, between 21 and 22 % of the oxygen was used by the CHMO during the experiments using FC-40 volume fractions between  $\Phi = 0$  and 0.1. At a volume fraction of  $\Phi = 0.2$ , 24% of the oxygen was consumed by the CHMO.

### 6.2.3 Comparison of experimental and predicted results

Figure 6.3 shows the OUR enhancement factors ( $E_{OUR}$ ) on an aqueous phase basis for: the OUR during the bioconversions, the specific activity, and as predicted by the  $E_{shuttle}$  model. The OUR enhancement factors ( $E_{OUR}$ ) were calculated using equation 5.5. As discussed in Chapter 5, the  $E_{shuttle}$  model predicted the enhancement factors obtained with FC-40 well. The experimental enhancement factors ( $E_{OUR}$ ) from this chapter are also in good agreement with the  $E_{shuttle}$  model.

The  $E_{shuttle}$  model assumes that the oxygen transfer rate increases because the average saturation concentration  $C^*$  increases. However, the oils can also affect the  $k_L a$ . Although a good fit was obtained with the FC-40, this might not be the case with other oils. Mineral oil caused the overall enhancement factor ( $E_{OUR}$ ) to decrease at volume fractions up to  $\Phi = 0.05$ , and other oils might have a similar effect. As discussed in Section 5.2.3.1, the gassing out method is not a suitable technique to determine the effect of the oils on the  $k_L a$ . Other techniques, such as the Lewis cell, which can be used to measure the  $k_L$ , could be used determine if the oils have a significant effects on the  $k_L a$ .

The  $E_{shuttle}$  model tends to underestimate the enhancement factors obtained in chemical systems, but the results from Chapter 5 indicated that the model tends to overestimate the enhancement factor for biological systems. This might be due to the effects of biosurfactants on the rate of mass transfer, and a better understanding of these effects might allow a better prediction of the enhancement factors.

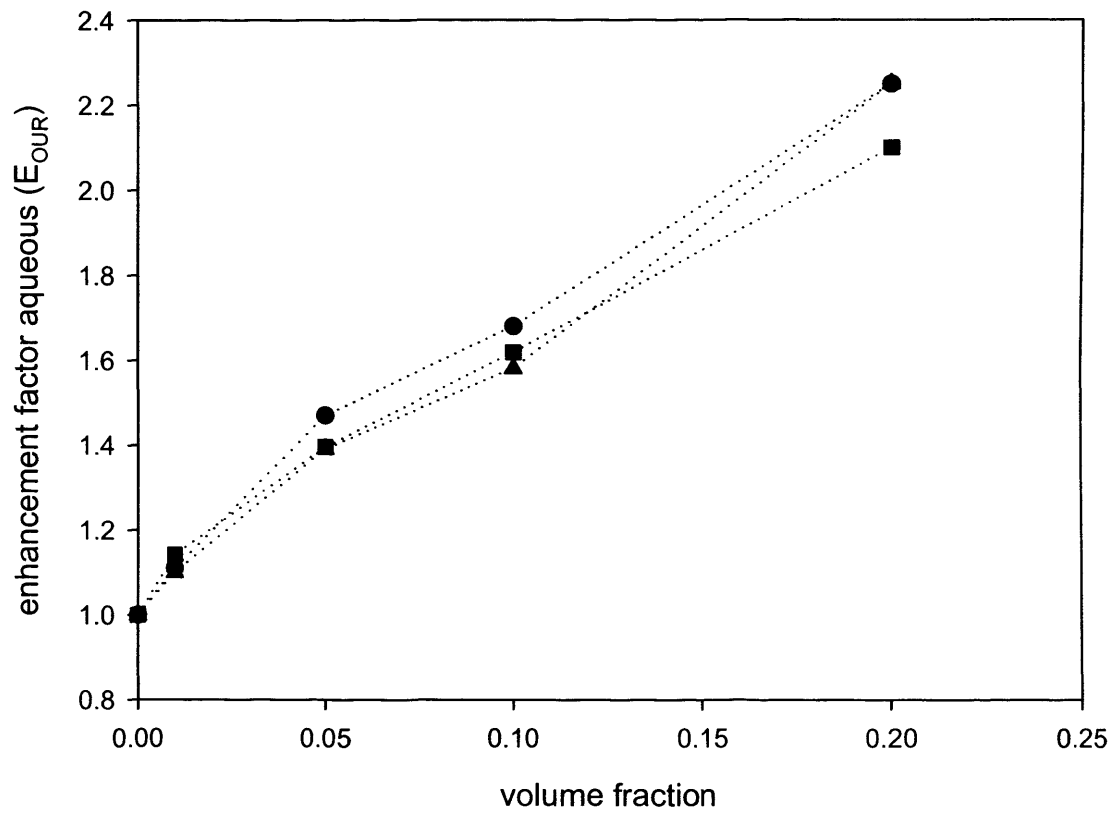


**Figure 6.3.** Comparison of experimental and predicted OUR enhancement factors ( $E_{OUR}$ ) for 2l bioconversions on an aqueous phase basis.  $E_{shuttle}$  model (●); OUR during bioconversions (■); specific activity (▲).

#### 6.2.4 Application to whole – cell bioconversions

The results show that the addition of FC-40 to the whole-cell CHMO bioconversion increased the oxygen transfer rate and consequently the specific activity.

Many whole – cell oxygenase bioconversions use organic solvents to act as a reservoir for the substrates or products. If this is the case, the selection of the organic solvent will be based on the interaction of the organic solvent with the substrate and product rather than its capacity to enhance the oxygen transfer rate. Not every organic solvent is suitable for a given set of substrates and products. Three key factors that influence solvent selection are the distribution coefficients of the substrate and product, the volume fraction, and the biocompatibility. The distribution coefficient and the volume fraction of the organic solvent influence the rate of mass transfer of the substrate and product between the two phases.

If the organic solvent acts as a reservoir for the substrate, either the oxygen or the substrate transfer rate could limit the activity. The design of a two – liquid phase bioconversions tries to optimise the productivity by taking into consideration the biocatalyst activity, the substrate mass transfer rate, and the initial concentration of the substrate in the organic phase (Woodley and Lilly, 1992; Cull *et al.*, 2001).

The  $E_{\text{shuttle}}$  model could assist process design because it enables the oxygen transfer rate to the aqueous phase to be predicted. Figure 6.4 shows the maximum oxygen uptake rate to the aqueous phase at each volume fraction of FC-40 (oxygen solubility ratio = 12). The oxygen uptake rate varied between 46 – 95  $\text{mmol l}^{-1} \text{h}^{-1}$ . Figure 6.4 also shows the predicted oxygen transfer rates for toluene and n-dodecane, which have oxygen solubility ratios of 18 and 8 respectively (Dumont and Delmas, 2003). Oxygen transfer rates of 46 – 120  $\text{mmol l}^{-1} \text{h}^{-1}$  could be obtained depending on the volume fraction and oxygen solubility.

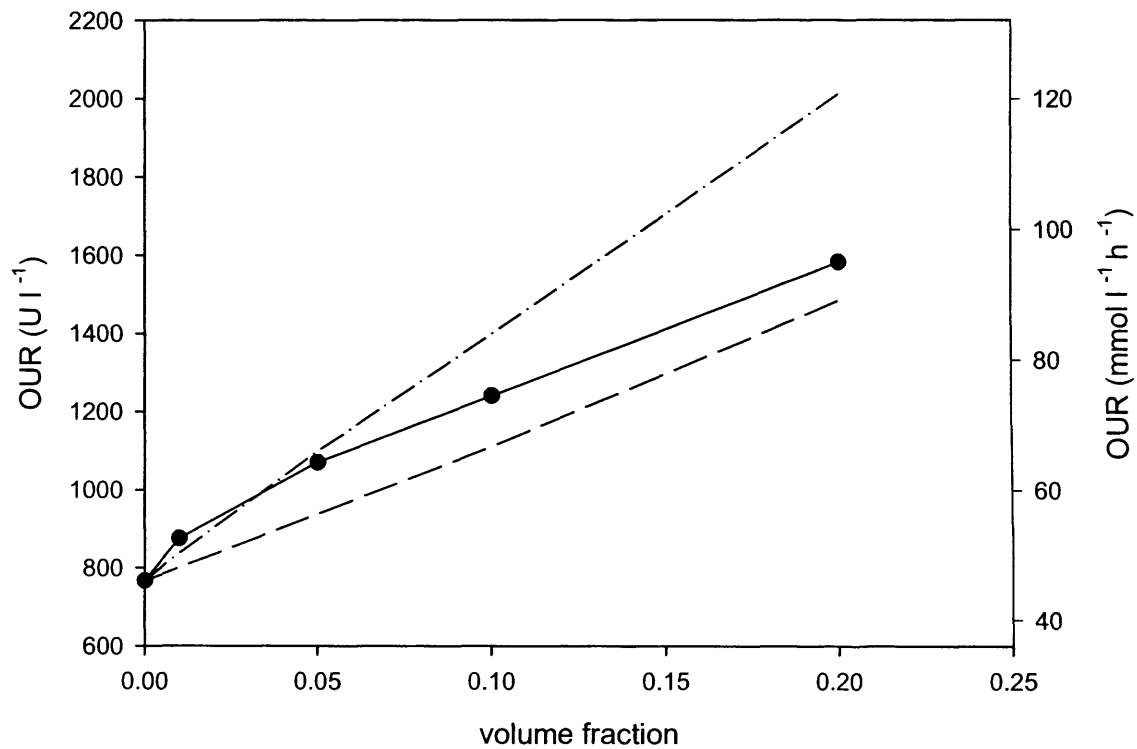


**Figure 6.4.** The effect of the oil volume fraction on the OUR (aqueous phases basis) – predicted and experimental. Experimental data for FC-40 during bioconversions (●); predicted by  $E_{shuttle}$  model - toluene (- · - · -); predicted by  $E_{shuttle}$  model - n-dodecane (- - - - -)

### 6.3 Conclusions

- FC-40 increased the oxygen transfer rate to the aqueous phase and the specific activity of the *E.coli* biocatalyst during the bioconversions.
- The specific activity of the *E.coli* biocatalyst increased by the same factor as the oxygen uptake rate. At the highest volume fraction used ( $\Phi = 0.2$ ), the specific activity increased 2.25 fold.
- The OUR enhancement factor predicted by the  $E_{\text{shuttle}}$  model was in good agreement with the experimental enhancement factors ( $E_{\text{OUR}}$ ). As long as the assumptions of the model are met, the model could be used in the design process to estimate the maximum oxygen transfer rate of the fermenter.



## 7.0 Discussion and Conclusions

### 7.1 Discussion

The results in this thesis have shown how oxygen limitation affects the activity of a whole-cell CHMO biocatalyst, and how oils can be used to increase the oxygen transfer rate to the aqueous phase.

If the concentration or the specific activity of a biocatalyst is increased the volumetric activity should also increase; however, this is not the case for whole-cell oxygenase processes because fermenters have a limited capacity to supply oxygen. The electron transport chain and the CHMO competed for oxygen when it was limited: the CHMO used 20 % of the oxygen whatever the severity of the limitation. Therefore, methods that increase the affinity of the oxygenase for oxygen are unnecessary, because the specific activity would be sub-maximal even if the fraction of oxygen used increased. Instead, methods that delay the onset of oxygen limitation are required.

Biological techniques can be used to reduce the amount of oxygen used by the electron transport chain. The simplest method would be to use nutrient feeding strategies to control the flux through the electron transport chain, but the NAD(P)H recycle rate might then limit the activity. Metabolic engineering methods could be used to decrease the flux through the electron transport chain without decreasing the cofactor recycle rate. However, it would require time and money that may not be available, and the increase in productivity might not be significant. If the specific OUR of the electron transport chain for the biocatalyst used in this work had been halved, the biocatalyst concentration would only have increased 1.5 fold. This is because the overall oxygen demand of the biocatalyst would have decreased by a third rather than a half.

Processing techniques increase the oxygen transfer rate of the fermenter, and are generally easier to implement than biological techniques. Most methods that increase the oxygen transfer rate - e.g. power input, aeration rate, pressure - will already be maximised; the use of an organic solvent provides a method of

further increasing the oxygen transfer rate. If the oxygen transfer rate is increased the biocatalyst concentration will increase by the same factor.

The  $E_{\text{shuttle}}$  model can be used to predict the increase in the oxygen transfer rate if the oxygen solubility of the organic solvent is known. This is useful for process design because it can help select an appropriate biocatalyst concentration.

There will be an upper limit to how much the oxygen transfer rate of the fermenter can be increased or the respiration rate decreased. Once this upper limit is reached the maximum activity – if it is limited by oxygen – will be set. The rate of substrate transfer, through the cell wall or from the organic solvent, or the NAD(P)H recycle rate may then become rate limiting. In the long – term, the best way to improve the productivity may be to make isolated oxygenases economically feasible by improving their stability and developing viable NAD(P)H recycle systems.

The results also raise some questions related to process design. First, some microorganisms are more tolerant to organic solvents than others. The selection of a host for whole-cell bioconversions where the substrate, product or organic solvent are toxic could therefore depend on the tolerance of the microorganism. For whole-cell oxygenases, the effect of oxygen concentration on the host should also be considered. For the system used in this work, the electron transport chain and the CHMO did not compete for oxygen until the DOT was almost zero. For strict aerobes such as the *Pseudomonas* species, the competition may begin at much higher DOTs, in which case higher oxygen transfer rates might be needed.

Secondly, sometimes processes developed in the pilot – plant do not give the same results when scaled – up to industrial scale (Sweere *et al.*, 1987). For example, the maximum cell density dropped 20 % for an *E.coli* based recombinant protein process when it was scaled – up from 3 l to 9 m<sup>3</sup> (Bylund *et al.*, 1998).

Industrial scale fermenters can have long mixing and circulation times. If the time for liquid mixing is higher than the time constant for oxygen consumption, oxygen concentrations will be created: the DOT will be highest in the impeller regions and then gradually decrease in the outer regions. Regions of oxygen limitation have been shown to exist in fermenters with volumes of 12 – 30 m<sup>3</sup>; *E.coli* was in the oxygen limited regions long enough for mixed – acid fermentation to occur (Oosterhuis and Kossen, 1983; O’Beirne and Hamer, 2000; Enfors *et al.*, 2001). Oxygen limitation can also exist in the feed zone of the fermenter; if mixing is poor, high concentrations of the carbon source can accumulate and increase the oxygen consumption rate (Bylund *et al.*, 1998).

If there were regions of the fermenter where the DOT is zero, the average oxygen transfer rate would be lower than expected. The implications for whole-cell oxygenase bioconversions are that the biocatalyst production and the volumetric activity could decrease. If the substrate for the bioconversion was fed to the aqueous phase, it could begin to accumulate to toxic concentrations if the activity was lower than predicted. If a second-liquid phase was present, the predicted increase in the oxygen transfer could decrease, as could the rate of substrate mass transfer to the aqueous phase.

## 7.2 Conclusions

The aim of this thesis was to investigate the effect of oxygen limitation on a whole-cell CHMO bioconversion, and to investigate how the physiochemical properties of the oils affect the oxygen transfer rate. The main conclusions are:

- The maximum activity of the whole-cell CHMO bioconversion was determined by the maximum oxygen transfer rate - above a critical biomass concentration the specific activity decreased.
- When oxygen was limited the CHMO used 20% of the oxygen - whatever the severity of the limitation. Therefore, if the oxygen transfer rate increased the specific activity of the biocatalyst would increase by the same factor.

- To prevent oxygen limitation either the oxygen transfer rate has to be increased or the amount of oxygen used by the electron transport chain decreased.
- Oils increased the oxygen transfer rate to the aqueous phase up to 2.5 fold depending on the oxygen solubility of the oil and the volume fraction, and as long as the oil drop diameters were small enough.
- The  $E_{\text{shuttle}}$  model can be used to predict an increase in the oxygen transfer rate that is caused by an increase in the saturation concentration, as long as the drop size is small enough. However, the effect of the oils on the  $k_L a$  should also be considered.

### 7.3 Future Work

- Further work could be carried out to determine whether oxygen or NADPH initially limited the specific activity of the CHMO. Also, one method to delay the onset of oxygen limitation is to decrease the flux through the electron transport chain, but this will decrease the NAD(P)H regeneration rate. Therefore, further work could determine when NAD(P)H is limited by the respiration rate, and what biocatalyst activities can be supported at different respiration rates.
- Investigate whether the onset of oxygen limitation differs between microorganisms. Repeat the oxygen consumption experiments with different oxygenases overexpressed in *E.coli* to see if the percentage of oxygen consumed by the oxygenases when it is limited varies.
- Confirm that it was the drop diameter that prevented the 50cS silicone oil from causing the same enhancement factors as the 5cS silicone oil. A high-speed camera could be used to size the oil droplets, and the pictures might show how the bubbles and oil drops interact. The effect of the drop

diameter on the enhancement factor could be further investigated by micro-encapsulating the oils. At a fixed power-input, the range of drop diameters that cause enhancement could then be determined.

- Organic solvents have been used at volume fractions of up to 0.5 v/v for bioconversions. In this work the highest volume fraction used was 0.2. More experiments, at higher volume fractions, could be done to check that the enhancement factor continues to increase, and that the data is in good agreement with the  $E_{\text{shuttle}}$  model.
- Scale-up the bioconversions to check that the same enhancement factors that were obtained at small scale.

## 8.0 References

Abril, O. (1989). Enzymatic Baeyer-Villiger type oxidations of ketones catalysed by cyclohexanone oxygenase. *Bioorganic Chemistry*. 17: 41 - 52.

Alphand, V., Archelas, A., Furstoss, R. (1990). Microbiological transformations 13: a direct synthesis of both S and R enantiomers of 5-hexadecanone via an enantioselective microbiological Baeyer-villiger reaction. *Journal of Organic Chemistry*. 55: 347 - 350.

Alphand, V., Carrea, G., Wohlgemuth, R., Furstoss, R., Woodley, J.M. (2003). Towards large-scale synthetic applications of Baeyer-Villiger monooxygenases. *Trends in Biotechnology*. 21(7): 318 - 323.

Amanullah, A., Hewitt, C.J., Nienow, A.W., Lee, C., Chartrain, M., Buckland, B.C., Drew, S.W., Woodley, J.M. (2002). Fed-batch bioconversion of indene to cis-indandiol. *Enzyme and Microbial Technology*. 31: 954 - 967.

Anderson, K. B., von Meyenburg, K. (1980). Are growth rates of *Escherichia coli* in batch cultures limited by respiration. *Journal of Bacteriology*. 144: 114 - 123.

Andrews, G.F., Fonta, J.P., Marrotta, E., Stroeve, P. (1980a). The effect of cells on oxygen transfer coefficients 1: cell accumulation around bubbles. *Chemical Engineering Journal*. 29: B39 – B46

Andrews, G.F., Fonta, J.P., Marrotta, E., Stroeve, P. (1980a). The effect of cells on oxygen transfer coefficients 2: analysis of enhancement mechanisms. *Chemical Engineering Journal*. 29: B47 – B55.

Aono, R. (1998). Improvement of organic solvent tolerance level of *Escherichia coli* by overexpression of stress-responsive genes. *Extremophiles*. 2: 239 - 248.

Ates, S., Dingil, N., Bayraktar, E., Mehmetoglu (2002). Enhancement of citric acid production by immobilized and freely suspended *Aspergillus niger* using silicone oil. *Process Biochemistry* . 38: 433 - 436.

Baeyer, A., Villiger, V. (1899). Einwirkung des caroschen reagens auf ketone. *Berline Deutsche Chem ges.* 32: 3625 - 3633.

Baldwin, C., Woodley, J.M. (2005). Oxygen limitation in whole cell biocatalytic Baeyer-Villiger oxidation processes. *Biotechnology and Bioengineering*. In press.

Beenackers, A. A. C. M., Swaaij, W.P.M. (1993). Mass transfer in gas-liquid slurry reactors. *Chemical Engineering Science*. 48(18): 3109 - 3139.

Berry, A., Dodge, T.C., Pepsin, M., Weyler, W. (2002). Application of metabolic engineering to improve both the production and use of biotech indigo. *Journal of Industrial Microbiology*. 28: 127 - 133.

Bird, P. A., Sharp, D.C., Woodley, J.M. (2002). Near-IR spectroscopic monitoring of analytes during microbially catalysed Baeyer-Villiger bioconversions. *Organic Process Research and Development*. 6: 569 - 576.

Bolm, C., Luong, T.K.K., Schlingloff, G. (1997). Enantioselective metal-catalysed Baeyer - Villiger oxidation of cyclobutanones. *Synlett*: 1151.

Brilman, D. W. F. Mass transfer and chemical reactions in gas-liquid-liquid systems, Thesis University of Twente, The Netherlands, 1998.

Brilman, D. W. F., Goldschmidt, M.J.V., Versteeg, G.F., van Swaaij, W.P.M. (2000). Heterogenous mass transfer models for gas absorption in multiphase systems. *Chemical Engineering Science*. 55: 2793 - 2812.

Bruining, W. J., Joosten, G.E.H., Beenackers, A.A.C.M, Hofman, H. (1986). Enhancement of gas-liquid mass transfer by a dispersed second liquid phase. *Chemical Engineering Science*. 41(7): 1873 - 1877.

Buhler, B., Hauer, B., Witholt, B., Schmid, A. (2002). Characterization and application of xylene monooxygenase for multistep biocatalysis. *Applied and Environmental Microbiology*. 68(2): 560 - 568.

Buhler, B., Bollhalder, I., Hauer, B., Witholt, B., Schmid, A. (2003a). Use of two-liquid phase concept to exploit kinetically controlled multistep biocatalysis. *Biotechnology and Bioengineering* 81(6): 683 - 694.

Buhler, B., Bollhalder, I., Hauer, B., Witholt, B., Schmid, A. (2003b). Chemical biotechnology for the specific oxyfunctionalization of hydrocarbons on a technical scale. *Biotechnology and Bioengineering*. 82(7): 833 - 842.

Buhler, B., Schmid, A. (2004). Process implementation aspects for biocatalytic hydrocarbon oxyfunctionalization. *Journal of Biotechnology*. 113: 183 - 210.

Bungay, H.R., Masak, R.D. (1981). Estimation of thickness of bacterial films at an air-water interface. *Biotechnology and Bioengineering*. 23: 1155 – 1157.

Burton, S. G., Cowan, D.A., Woodley, J.M. (2002). The search for the ideal biocatalyst. *Nature Biotechnology*. 20: 37 - 45.

Bylund, F., Collet, E., Enfors, S.-O., Larsson, G. (1998). Substrate gradient formation in the large-scale bioreactor lowers cell yield and increases by-product formation. *Bioprocess Engineering*. 18: 171 - 180.

Carragher, J. M., McClean, W.S., Woodley, J.M., Hack, C.J. (2001). The use of oxygen uptake rate measurements to control the supply of toxic substrate: toluene hydroxylation by *Pseudomonas putida* UV4. *Enzyme and Microbial Technology*. 28: 183 - 188.



Castan, A., Nasman, A., Enfors, S. (2002). Oxygen enriched air supply in *Escherichia coli* processes: production of biomass and recombinant human growth hormone. *Enzyme and Microbial Technology*. 30: 847 - 854.

Cents, A. H. G., Brillman, D.W.F., Versteeg, G.F. (2001). Gas absorption in an agitated gas-liquid-liquid system. *Chemical Engineering Science*. 56: 1075 - 1083.

Chen, G., Kayser, M.M., Mihovilovic, M., Mrstik, M.E., Martinez, C.A., Stewart, J.D. (1999). Asymmetric oxidations at sulfur catalysed by engineered strains that over-express cyclohexanone monooxygenase. *New J Chemistry*. 8: 827 - 832.

Chen, Y. C. J. (1988). Acinetobacter cyclohexanone monooxygenase: gene cloning and sequence determination. *Journal of Bacteriology*. 170: 781 - 789.

Cheng, A. T. Y. (1999). Stationary vortex system for direct injection of supplemental reactor oxygen. United States Patent US5939313.

Cheng, A. T. Y. (1998). How to make oxygen economical for fermentation. 1998 Pharmaceutical Ingredients Worldwide (CPhI) Conference at Amsterdam, Netherlands.

Chibata, S., Shigeki Yamada, T., Mitsuru Wada, N., Nobuhiko Izuo, Y., Totaro Yamaguchi, Y. (1974). Cultivation of aerobic microorganisms. US 3850753.

Cirino, P. C., Arnold, F.H. (2002). Protein engineering of oxygenases for biocatalysis. *Current Opinion in Chemical Biology*. 6: 130 - 135.

Coulson, J.M., Richardson, J.F. (1990). Chemical Engineering, Volume 1. Fluid flow, heat transfer and mass transfer. 4th Edition. Oxford Pergamon.

Csonka, L. N., Fraenkel, D.G. (1977). Pathways of NADPH formation in *Escherichia coli*. *Journal of Biological Chemistry*. 252(10): 3382 - 3391.

Cull, S. G., Lovick, J.W., Lye, G.J., Angeli, P. (2002). Scale-down studies on the hydrodynamics of two-liquid phase biocatalytic reactors. *Bioprocess and Biosystems Engineering*. 25: 143 - 153.

Cull, S. G., Woodley, J.M., Lye, G.J. (2001). Process selection and characterisation for the biocatalytic hydration of poorly-water soluble aromatic dinitriles. *Biocatalysis and Biotransformations*. 19: 131 - 154.

Damiano, D., Wang, S. (1985). Novel use of a perfluorocarbon for supplying oxygen to aerobic submerged cultures. *Biotechnology Letters* 7(2): 81 - 86.

Das, T. R., Bandopadhyay, A., Parthasarathy, R., Kumar, R. (1985). Gas-liquid interfacial area in stirred vessels: the effect of an immiscible liquid phase. *Chemical Engineering Science*. 40(2): 209 - 214.

de Bont, J. A. M. (1998). Solvent - tolerant bacteria in biocatalysis. *Trends in Biotechnology*. 16: 493 - 499.

Dingler, C., Ladner, W., Krei, G.A., Cooper, B., Hauer, B. (1996). Preparation of (R)-2-(4-hydroxyphenoxy)propionic acid by biotransformation. *Pesticide Science*. 46: 33 - 35.

Doig, S. D., Avenell, P.J., Bird, P.A., Gallati, P., Lander, K.S., Lye, G.J., Wohlgemuth, R., Woodley, J.M. (2002a). Reactor operation and scale-up of whole-cell Baeyer - Villiger catalyzed lactone synthesis. *Biotechnology Progress*. 18: 1039 - 1045.

Doig, S. D., Simpson, H., Alphand, V., Furstoss, R., Woodley, J.M. (2003). Characterization of a recombinant *Escherichia coli* TOP10 [pQR239] whole-cell

biocatalyst for stereoselective Baeyer-Villiger oxidations. *Enzyme and Microbial Technology* 32: 347 - 355.

Doig, S. D., O'Sullivan, L.M., Patel, S., Ward, J.M., Woodley, J.M. (2001). Large scale production of cyclohexanone monooxygenase from *Escherichia coli* TOP10 pQR239. *Enzyme and Microbial Technology*. 28: 265 - 274.

Doig, S. D., Pickering, S.C.R., Lye, G.J., Woodley, J.M. (2002b). The use of microscale processing technologies for quantification of biocatalytic Baeyer-Villiger oxidation kinetics. *Biotechnology and Bioengineering*. 80(1): 42 - 49.

Donoghue, N. A., Trudgill, P.W. (1975). The metabolism of cyclohexanol by *A. calcoaceticus* NCIB 9871. *European Journal of Biochemistry*. 60: 1 - 7.

Donoghue, N. A., Norris, D.B., Trudgill, P.W. (1976). The purification and properties of cyclohexanone oxygenase from *Nocardia globerula* and *A.calcoaceticus* NCIMB 9871. *European Journal of Biochemistry*. 63: 175 - 192.

Doran, A. (1999). *Bioprocess Engineering Principles*. Academic press.

Duetz, W. A., van Beilen, J.B., Witholt, B. (2001). Using proteins in their natural environment: potential and limitations of microbial whole-cell hydroxylations in applied biocatalysis. *Current Opinion in Biotechnology*. 12: 419 - 425.

Duetz, W. A., de Jong, C., Williams, P.A., van Andel, J.G. (1994). Competition in chemostat culture between *Pseudomonas* strains that use different pathways for the degradation of toluene. *Applied and Environmental Microbiology*. 60(8): 2858 - 2863.

Dumont, E., Delmas, H. (2003). Mass transfer enhancement of gas absorption in oil - in - water systems: a review. *Chemical Engineering and Processing*. 42: 419-438.

Dunn, J. J., Einsele, A. (1975). Oxygen transfer coefficients by the dynamic method. *Journal of Chemistry and Biotechnology*. 25: 707 - 720.

Eckenfelder, W. W., Barnhart, E.L. (1961). The effect of organic substances on the transfer of oxygen from air bubbles in water. *A.I.Ch.E. Journal* 7(4): 631 - 634.

Elibol, M., Mavituna, F. (1996). Use of perfluorocarbon for oxygen supply to immobilised *Streptomyces coelicolor* A3(2). *Process Biochemistry*. 31(5): 507 - 512.

Elibol, M. (2001). Improvement of antibiotic production by increased oxygen solubility through the addition of perfluorodecalin. *Journal of Chemical Technology and Biotechnology*. 76: 418 - 422.

Elibol, M., Ozer, D. (2000). Influence of oxygen transfer on lipase production by *Rhizopus arrhizus*. *Process Biochemistry*. 36: 325 - 329.

Enfors, S.-O., Jahic, M., Rozkov, A., Xu, B., Hecker, M., Jurgen, B., Kruger, E., Schweder, T., Hamer, G., O'Beirne, D., Noisommit-Rizzi, N., Reuss, M., Boone, L., Hewitt, C., McFarlane, C., Nienow, A., Kovacs, T., Tragardh, C., Fuchs, L., Revstedt, J., Friberg, P.C., Hjertager, B., Blomsten, G., Skogman, H., Hjort, S., Hoeks, F., Lin, H.Y., Neubauer, P., van der Lans, R., Luyben, K., Vrabel, P., Manelius, A. (2001). Physiological responses to mixing in large scale bioreactors. *Journal of Biotechnology*. 85: 175 - 185.

Fetzner, S. (2002). Oxygenases without requirement for cofactors or metal ions. *Applied Microbiology and Biotechnology*. 60: 243 - 257.

Galindo, E., Pacek, A.W., Nienow, A.W. (2000). A study of drop and bubble sizes in a simulated mycelial fermentation broth up to four phases. *Biotechnology and Bioengineering*. 69: 491 - 494.

Gbewonyo, K., Buckland, B.C., Lilly, M.D. (1991). Development of a large-scale continuous substrate feed process for the biotransformation of simvastatin. *Biotechnology and Bioengineering*. 37: 1101 - 1107.

Godfrey, J. C., Grilc, V. (1977). Drop size and drop size distribution for liquid - liquid dispersions in agitated tanks of square cross-section. In Proc. 2nd European Conference on Mixing, Cambridge, England, BHRA Fluid Engineering, Cranfield, UK.

Graham-Lorence, S., Truan, G., Peterson, J.A., Falck, J.R., Wei, S., Helvig, C., Capdevilla, J.C. (1997). An active site substitution, F87V, converts cytochrome P450 BM-3 into a regio- and stereoselective (14S,15R)-arachidonic acid epoxygenase. *Journal of Biological Chemistry*. 272: 1127 - 1135.

Grattoni, C., Moosai, R., Dawe, R.A. (2003). Photographic observations showing spreading and non-spreading of oil on gas bubbles of relevance to gas flotation for oily wastewater cleanup. *Colloids and Surfaces A: Physicochemical and Engineering Aspects*. 214(151 - 155).

Green, D. W. (1997). Perry's chemical engineers handbook. 7th Edition. Mc Graw Hill.

Guillinger, T. R., Grislingas, A.K., Erga, O. (1988). Phase inversion behaviour of water-kerosene dispersions. *Industrial and Engineering Chemistry Research*. 27: 978 - 982.

Gunsalus, R. P. (1992). Control of electron flow in *Escherichia coli*: coordinated transcription of respiratory pathway genes. *Journal of Bacteriology*. 174(22): 7069 - 7074.

Hack, C. J., Woodley, J.M., Lilly, M.D., Liddell, J.M. (1994). The production of *Pseudomonas putida* for the hydroxylation of toluene to its cis-glycol. *Applied Microbiology and Biotechnology*. 41: 495 - 499.

- Hack, C. J., Woodley, J.M., Lilly, M.D., Liddell, J.M. (2000). Design of a control system for biotransformation of toxic substrates: toluene hydroxylation by *Pseudomonas putida* UV4. *Enzyme and Microbial Technology*. 26: 530 - 536.
- Held, M., Schmid, A., Kohler, H.E., Suske, W., Witholt, B., Wubbolts, M.G. (1999). An integrated process for the production of toxic catechols from toxic phenols based on a designer biocatalyst. *Biotechnology and Bioengineering*. 62(6): 641 - 648.
- Hilker, I., Gutierrez, M.C., Alphand, V., Wohlgemuth, R., Furstoss, R. (2004a). Facile and efficient resin-based in situ SFPR preparative -scale synthesis of an enantiopure unexpected lactone regioisomer via a Baeyer - Villiger oxidation process. *Organic Letters*. 6(12): 1955 - 1958.
- Hilker, I., Alphand, V., Wohlgemuth, R., Furstoss, R. (2004b). Preparative scale asymmetric Baeyer - Villiger oxidation using a highly productive two-in-one resin based in situ SFPR concept. *Advanced Synthetic Catalysis*. 346: 203 -214.
- Hinze, J. O. (1955). Fundamentals of the hydrodynamic mechanism of splitting in dispersion processes. *AIChE Journal*. 1(3): 289 - 295.
- Hogan, M. C., Woodley, J.M. (2000). Modelling of two enzyme reactions in a linked cofactor recycle system for chiral lactone synthesis. *Chemical Engineering Science*. 55: 2001 - 2008.
- Husken, L., Dalm, M., Tramper, J., Wery, J., de Bont, J.A.M., Beeftink, R. (2001). Integrated bioproduction and extraction of 3 - methylcatechol. *Journal of Biotechnology*. 88: 11 - 19.
- Jia, S., Chen, G., Kahar, P., Choi, D., Okabe, M. (1999). Effect of soybean oil on oxygen transfer rate in the production of tetracycline with an airlift bioreactor. *Journal of Bioscience and Bioengineering*. 87(6): 825 - 827.

Ju, L.K., Sundararajan, A. (1994). The effects of cells on oxygen transfer in bioreactors: physical presence of cells as solid particles. *Chemical Engineering Journal*. 56: B15 – B21

Junker, B. H., Hatton, T.A., Wang, D.I.C. (1990a). Oxygen transfer enhancement in aqueous/perfluorocarbon fermentation systems: 1. experimental observations. *Biotechnology and Bioengineering*. 35: 578 - 585.

Junker, B. H., Hatton, T.A., Wang, D.I.C. (1990b). Oxygen transfer enhancement in aqueous/perfluorocarbon fermentation systems:II. theoretical analysis. *Biotechnology and Bioengineering*. 35: 586 - 597.

Kawase, Y., Moo-Young, M. (1990). The effect of antifoam agents on mass transfer in bioreactors. *Bioprocess Engineering*. 5: 169 - 173.

Kayser, M. M., Chen, G., Stewart, J.D. (1998). Enantio- and regioselective Baeyer-Villiger oxidations of 2- and 3- substituted cyclopentanones using engineered bakers yeast. *Journal of Organic Chemistry*. 63: 7103 - 7106.

Kiener, A. (1995). Biosynthesis of functionalized aromatic N-heterocycles. *Chemtech* 25: 31 - 35.

Kollmer, A., Schmid, A., Rudolf von Rohr, Ph., Sonnleitner, B. (1999). On liquid-liquid mass transfer in two-liquid-phase fermentations. *Bioprocess Engineering*. 20: 441-448.

Laane, C., Boeren, S., Hilhorst, R., Veeger, C. (1987). Optimisation of biocatalysis in organic media. In. *Biocatalysis in Organic Media*, p 65-84, eds Laane, C., Tramper, J., Lilly, M.D., Elsevier Science Publishers, Amsterdam.

Lamping, S. R., Zhang, H. Allen, B., Ayazi Shamlou, P. (2003). Design of prototype miniature bioreactor for highthroughput automated bioprocessing. *Chemical Engineering Science*. 58: 747 - 758.

Lander, K. (2001). In-situ product recovery from a Baeyer-Villiger monooxygenase catalysed bioconversion. P.h.D thesis. University of London.

Larralde-Corona, C. P., Cordova, M.S., Galindo, E. (2002). Distribution of the free and oil-trapped air bubbles in simulated broths containing fungal biomass. *Canadian Journal of Chemical Engineering*. 80: 491 - 494.

Leahy, J. G., Olsen, R.H. (1997). Kinetics of toluene degradation by toluene-oxidizing bacteria as a function of oxygen concentration, and the effect of nitrate. *FEMS Microbiology Ecology*. 23: 23 - 30.

Lee, S. Y. (1996). High cell-density culture of *Escherichia coli*. *Trends in Biotechnology*. 14: 98 - 105.

Lekhal, A., Chaudhari, R.V., Wilhelm, A.M., Delmas, H. (1997). Gas-liquid mass transfer in gas-liquid-liquid dispersions. *Chemical Engineering Science*. 52(21-22): 4069 - 4077.

Leonhardt, A., Szwajcer, E., Mosbach, K. (1985). The potential use of silicon compounds as oxygen carriers for free and immobilized cells containing L-amino acid oxidase. *Applied Microbiology and Biotechnology*. 21: 162 - 166.

Leung, R., Poncelet, D., Neufeld, R.J. (1997). Enhancement of oxygen transfer rate using microencapsulated silicone oils as oxygen carriers. *Journal of Chemical Technology and Biotechnology*. 68: 37 - 46.

Li, Z., van Beilen, J.B., Duetz, W.A., Schmid, A, de Raadt, A., Griengl, H., Witholt, B. (2002). Oxidative biotransformations using oxygenases. *Current Opinion in Chemical Biology*.6: 136 - 144.



- Liese, A., Filho, M.V. (1999). Production of fine chemicals using biocatalysis. *Current Opinion in Biotechnology*. 10: 595 - 603.
- Lilly, M. D., Woodley, J.M. (1996). A structured approach to design and operation of biotransformation processes. *Journal of Industrial Microbiology*. 17: 24 - 29.
- Lim, S. J., Jung, Y.M., Shin, H.D., Lee, Y.H. (2002). Amplification of the NADPH - related genes *zwf* and *gnd* for the oddball biosynthesis of PHB in an *E.coli* transformant harboring a cloned *phbCAB* operon. *Journal of Bioscience and Bioengineering*. 93(6): 543 - 549.
- Linek, V., Benes, P. (1976). A study of the mechanism of gas absorption into oil-water emulsions. *Chemical Engineering Science*. 31: 1037 - 1046.
- Littel, R. J., Versteeg, G.F., van Swaij. (1994). Physical absorption of CO<sub>2</sub> and propene into toluene/water emulsions. *AIChE Journal*.40(10): 1629 - 1638.
- Liu, H. S., Chiung, W.C., Wang, Y.C. (1994). Effect of lard oil, olive oil, and castor oil on oxygen transfer in an agitated fermenter. *Biotechnology Techniques*. 8(1): 17 - 20.
- Longmuir, I. S. (1954). Respiration rate as a function of oxygen concentration. *Biochemistry Journal*.57: 81 - 87.
- Lucatero, S., Larralde-Corona, C.P., Corkidi, G., Galindo, E. (2003). Oil and air dispersion in a simulated fermentation broth as a function of mycelial morphology. *Biotechnology Progress*. 19: 285 - 292.
- Lye, G.J., Stuckey, D.C. (2001). Extraction of erythromycin – A using colloidal liquid aphrons: Part 2. Mass transfer kinetics. *Chemical Engineering Science*. 56: 97 – 108.

Lye, G. J., Woodley, J.M. (1999). Application of in situ product-removal techniques to biocatalytic processes. *Trends in Biotechnology*. 17: 395 - 402.

Lye, G. J., Dalby, P.A., Woodley, J.M. (2002). Better biocatalytic processes faster: new tools for the implementation of biocatalysis in organic synthesis. *Organic Process Research and Development*. 6: 434 - 400.

MacMillan, J. D., Wang, D.I.C. (1987). Enhanced oxygen transfer using oil-in-water dispersions. *Annals of the New York Academy of Sciences*. 506: 569.

MacMillan, J. D., Wang, D.I.C. (1990). Mechanisms of oxygen transfer enhancement during submerged cultivation in perfluorochemical - in water dispersions. *Annals of the New York Academy of Sciences*. 589: 283 -300.

Mareclis, C. L. M., van Leeuwen, M., Polderman, H.G., Janssen, A.J.H., Lettinga, G. (2003). Model description of dibenzothiophene mass transfer in oil/water dispersions with respect to biodesulfurization. *Biochemical Engineering Journal*. 16: 253 - 264.

Mathys, R. G., Schmid, A., Witholt, B. (1999). Integrated two-liquid phase bioconversion and product recovery processes for the oxidation of alkanes: process design and economic evaluation. *Biotechnology and Bioengineering*. 64: 459 - 477.

Matsui, T., Yokota, H., Sato., S., Mukataka, S., Takahashi., J. (1989). Pressurised culture of *Escherichia coli* B in fed-batch culture. *Biotechnology Letters* 9(2): 89 - 94.

May, S. W. (1999). Applications of oxidoreductases. *Current Opinion in Biotechnology*. 10: 370 - 375.

- Menge, M., Mukherjee, J., Scheper, T. (2001). Application of oxygen vectors to *Claviceps purpurea* cultivation. *Applied Microbiology and Biotechnology*. 55: 411 - 416.
- Meyer, A., Wursten, M., Schmid, A., Kohler, H.E., Witholt, B. (2002). Hydroxylation of indole by laboratory -evolved 2-hydroxybiphenyl 3 monooxygenase. *Journal of Biological Chemistry*. 277(37): 34161 - 34167.
- Mihovilovic, M. D., Muller, B., Stanetty, P. (2002). Monooxygenase - mediated Baeyer-Villiger oxidations. *European Journal of Organic Chemistry*. 3711 - 3730.
- Mimura, A., Takeda, I., Wakasa, R. (1973). Some characteristic phenomena of oxygen transfer in hydrocarbon fermentation. *Biotechnology and Bioengineering Symposia*. No 4: 467 – 484.
- Moosai, R., Dawe, R. (2003). Gas attachment of oil droplets for gas flotation for oily wastewater cleanup. *Separation and Purification Technology*. 33: 303 - 314.
- Morao, A., Maia, C.I., Fonseca, M.M.R., Vasconcelos, J.M.T., Alves, S.S. (1999). Effect of antifoam addition on gas - liquid mass transfer in stirred fermenters. *Bioprocess Engineering*. 20: 165 - 172.
- Nagy, E., Hadik, P. (2003). Three-phase mass transfer: effect of the size distribution. *Industrial Engineering Chemical Research*. 42: 5363 - 5372.
- Nagy, E., Moser, A. (1995). Three-phase mass transfer: improved pseudo-homogeneous model. *A.I.Ch.E. Journal*. 41: 23 - 34.
- Nickerson, D. P., Hartford-Cross, C.F., Fulcher, S.R., Wong, L.L. (1997). The catalytic activity of cytochrome P450cam towards styrene oxidation is increased by site-specific mutagenesis. *FEBS Letters*. 405: 153.

Nienow, A. W. (1998). Hydrodynamics of stirred bioreactors. *Applied Mechanical Reviews*. 51(1): 3 - 33.

Nishikawa, M., Mori, F., Fujieda, S. (1987). Average drop size in a liquid-liquid phase mixing vessel. *Journal of Chemical Engineering Japan*. 20: 82-88.

Nishikawa, M., Kayama, T., Nishioka, S., Nishikawa, S. (1994). Drop size distribution in mixing vessel with aeration. *Chemical Engineering Science*. 49(14): 2379 - 2384.

Noorman, H. J. (2004). Industrial aspects of antibiotics process development and implementation. *European Symposium on Biochemical Engineering Science 5*. Stuttgart September 2004.

O'Beirne., H., G., Hamer, G. (2000). Oxygen availability and the growth of *Escherichia coli* W3110: a problem exacerbated by scale-up. *Bioprocess Engineering*. 23: 487 - 494.

Oosterhuis, N. M. G., Kossen, N.W.F. (1983). Oxygen transfer in a production scale bioreactor. *Chemical Engineering Research and Design*. 61: 308 - 312.

Panke, S., Held, M., Wubbolts, M., Witholt, B., Schmid, A. (2002). Pilot-scale production of (S)- styrene oxide from styrene by recombinant *Escherichia coli* synthesizing styrene monooxygenase. *Biotechnology and Bioengineering*. 80(1): 33 - 41.

Prins, A., van't Riet, K. (1987). Proteins and surface effects in fermentation: foam, antifoam and mass transfer. *Trends in Biotechnology*. 5: 296 - 301.

Pulido - Mayoral, N., Galindo, E. (2004). Phase dispersion and oxygen transfer in a simulated fermentation broth containing castor oil and proteins. *Biotechnology Progress*. 20: 1608 - 1613.

Pursell, M. R., Mendes - Tatsis, M.A., Stuckey, D.C. (2004). Effect of fermentation broth and biosurfactants on mass transfer during liquid-liquid extraction. *Biotechnology and Bioengineering*. 85(2): 155 - 165.

Ramos, J. L., Duque, E., Gallegos, M.T., Godoy, P., Ramos-Gonzalez, M.I., Rojas, A., Teran, W., Segura, A. (2002). Mechanisms of solvent tolerance in gram-negative bacteria. *Annual Reviews of Microbiology*. 56: 743 - 768.

Reddy, J., Lee, C., Neeper, M., Greasham, R., Zhang, J. (1999). Development of a bioconversion process for production of cis-1S,2R-indandiol from indene by recombinant *Escherichia coli* constructs. *Applied Microbiology and Biotechnology*. 51: 614 - 620.

Renz, M., Meunier, B. (1999). 100 Years of Baeyer-Villiger Oxidations. *European Journal of Organic Chemistry*. 4: 737 - 750.

Rissom, S. (1997). Synthesis of chiral  $\epsilon$ -lactones in a two-enzyme system of cyclohexanone monooxygenase and formate dehydrogenase with integrated bubble-free aeration. *Tetrahedron Asymmetry*. 8: 2523 - 2526.

Rols, J. L., Goma, G. (1989). Enhancement of oxygen transfer rates in fermentation using oxygen-vectors. *Biotechnology Advances*. 7: 1 - 14.

Rols, J. L., Condoret, C., Fonade, C., Goma, G. (1990). Mechanism of enhanced oxygen transfer in fermentation using emulsified oxygen - vectors. *Biotechnology and Bioengineering*. 35: 427 - 435.

Rols, J. L., Goma, G. (1991). Enhanced oxygen transfer rates in fermentation using soybean oil-in-water dispersions. *Biotechnology Letters*. 13(1): 7 -12.

Ryerson, C. C., Ballou, D.P., Walsh, C. (1982). Mechanistic studies on cyclohexanone oxygenase. *Biochemistry*. 21: 2644 - 2655.

Schmid, A., Kollmer, A., Sonnleitner, B., Witholt, B. (1999). Development of equipment and procedures for the safe operation of aerobic bacterial bioprocesses in the presence of bulk amounts of flammable organic solvents. *Bioprocess Engineering*. 20: 91 - 100.

Schmid, A., Kollmer, A., Mathys, R.G., Witholt, B. (1998a). Developments toward large-scale bacterial bioprocesses in the presence of bulk amounts of organic solvents. *Extremophiles*. 2: 249 - 256.

Schmid, A., Kollmer, A., Witholt, B. (1998b). Effects of biosurfactant and emulsification on two-liquid phase *Pseudomonas oleovorans* cultures and cell-free emulsions containing n-decane. *Enzyme and Microbial Technology* 22: 487 - 493.

Schneider, S., Wubbolts, M.G., Sanglard, D., Witholt, B. (1998). Biocatalyst engineering by assembly of fatty acid transport and oxidation activities for in vivo application of cytochrome P450 monooxygenase. *Applied and Environmental Microbiology* 64: 3784 - 3790.

Shaler, T. A., Klecka, G.M. (1986). Effects of dissolved oxygen concentration on biodegradation of 2,4 - dichlorophenoxyacetic acid. *Applied and Environmental Microbiology*. 51(5): 950 - 955.

Shibasaki, T., Hashimoto, S., Mori, H., Ozaki, A. (2000a). Construction of a novel hydroxyproline -producing recombinant *Escherichia coli* by introducing a proline 4-hydroxylase gene. *Journal of Bioscience and Bioengineering*. 90: 522 - 525.

Shibasaki, T., S., Mori, H., Ozaki, A. (2000b). Enzymatic production of trans-4-hydroxy-L-proline by regio- and stereospecific hydroxylation of L-proline. *Bioscience, Biotechnology, and Biochemistry*. 64: 746-750.

- Simpson, H. D., Alphand, V., Furstoss, R. (2001). Asymmetric biocatalysed Baeyer-Villiger oxidation: improvement using a recombinant *Escherichia coli* whole cell biocatalyst in the presence of an adsorbent resin. *Journal of Molecular Catalysis B: Enzymatic*. 16: 101 - 108.
- Stark, D., von Stockar, U. (2003). In situ product removal (ISPR) in whole cell biotechnology during the last twenty years. *Advances in Biochemical Engineering/Biotechnology*. 80: 149 - 175.
- Stewart, J. D., Reed, K.W., Kayser, M.M. (1996). Designer yeast: A new reagent for enantioselective Baeyer-Villiger oxidation. *Journal of the Chemistry Society., Perkin. Trans.1*. 8: 755 - 757.
- Stewart, J. D. (1998). Cyclohexanone monooxygenase: a useful reagent for assymmetric Baeyer-Villiger reactions. *Current Organic Chemistry*. 2: 195 - 216.
- Straathof, A. J. J., Panke, S., Schmid, A. (2002). The production of fine chemicals by biotransformations. *Current Opinion in Biotechnology*. 13: 548 - 556.
- Sweere, A. P. J., Luyben, K.A.M., Kossen, N.W.F. (1987). Regime analysis and scale-down: tools to investigate the performance of bioreactors. *Enzyme and Microbial Technology*. 9: 386 - 398.
- Uden, G. (1994). Oxygen regulated gene expression in facultatively anaerobic bacteria. *Antonie van Leeuwenhoek*. 66: 3 - 23.
- van Beilen, J. B., Duetz, W.A., Schmid, A., Witholt, B. (2003). Practical issues in the application of oxygenases. *Trends in Biotechnology*. 21: 170 - 177.
- van der Meer, A. B., Beenackers, A.A.C.M., Burghard, R., Mulder, N.H., Fok, J.J. (1992). Gas/liquid mass transfer in a four-phase stirred fermenter: effects of

organic phase hold-up and surfactant concentration. *Chemical Engineering Science*. 47(9-11): 2369 - 2374.

van Ede, C. J., Van Houten, R., Beenackers, A.A.C.M. (1995). Enhancement of gas to water mass transfer rates by a dispersed organic phase. *Chemical Engineering Science*. 50(18): 2911 - 2922.

van't Riet, K. (1991). Basic Bioreactor Design. Eds. van't Riet, Tramper, J. M.Dekker press.

Walton, A. Z., Stewart, J.D. (2004). Understanding and improving NADPH-dependent reactions by nongrowing *Escherichia coli* cells. *Biotechnology Progress*. 20: 403 - 411.

Walton, A. Z., Stewart, J.D. (2002). An efficient enzymatic Baeyer-Villiger oxidation by engineered *Escherichia coli* cells under non-growing conditions. *Biotechnology Progress*. 18(262 - 268).

Wilkinson, D., Ward, J.M., Woodley, J.M. (1996). Choice of microbial host for the naphthalene dioxygenase bioconversion. *Journal of Industrial Microbiology*. 16: 274 - 279.

Willetts, A. (1997). Structural studies and synthetic applications of Baeyer - Villiger monooxygenases. *Trends in Biotechnology*. 15: 55 - 61.

Wong, J. W., Watson, H.A., Bouressa, J.F., Burns, M.P., Cawley, J.J., Doro, A.E., Guzek, D.B., Hintz, M.A., McCormick, E.L., Scully, D.A., Siderewicz, J.M., Taylor, W.J., Trusedell, S.J., Wax, R.G. (2002). Biocatalytic oxidation of 2-methylquinoxaline to 2-quinoxalinecarboxylic acid. *Organic Process Research and Development*. 6: 477 - 481.



Woodley, J. M., Lilly, M.D. (1994). Biotransformation reactor selection and operation. In: Applied Biocatalysis (Cabral, J.M.S., Best, D., Boross, L., Tramper, J., eds): 371 - 393, Harwood Academic, Chur, Switzerland.

Woodley, J. M. (1990). Stirred tank power input data for the scale-up of two-liquid phase biotransformations. In: L.G. Copping, R.E. Martin, J.E. Pickett, C. Bucke, and A.W. Bunch (eds.), Opportunities in biotransformations. Elsevier, London.: 63 - 66.

Woodley, J. M., Lilly, M.D. (1990). Extractive biocatalysis: the use of two-liquid phase biocatalytic reactors to assist product recovery. *Chemical Engineering Science*. 45(8): 2391 - 2396.

Woodley, J. M., Lilly, M.D. (1992). Process engineering of two liquid phase biocatalysis. In: Biocatalysis in non-conventional media p 147 -154, Eds., Tramper, J., Vermue, M.H., Beeftink, H.H., and von Stockar, U., Elsevier Science Publishers, Amsterdam.

Wubbolts, M. G., Favre - Bull, O., Witholt, B. (1996). Biosynthesis of synthons in two-liquid phase media. *Biotechnology and Bioengineering*. 52(2): 301 - 308.

Yoshida, F., Yamane, T., Miyamoto, Y. (1970). Oxygen absorption into oil-in-water emulsions. *Industrial Engineering Chemical Process Design and Development*. 9(4): 570 - 577.

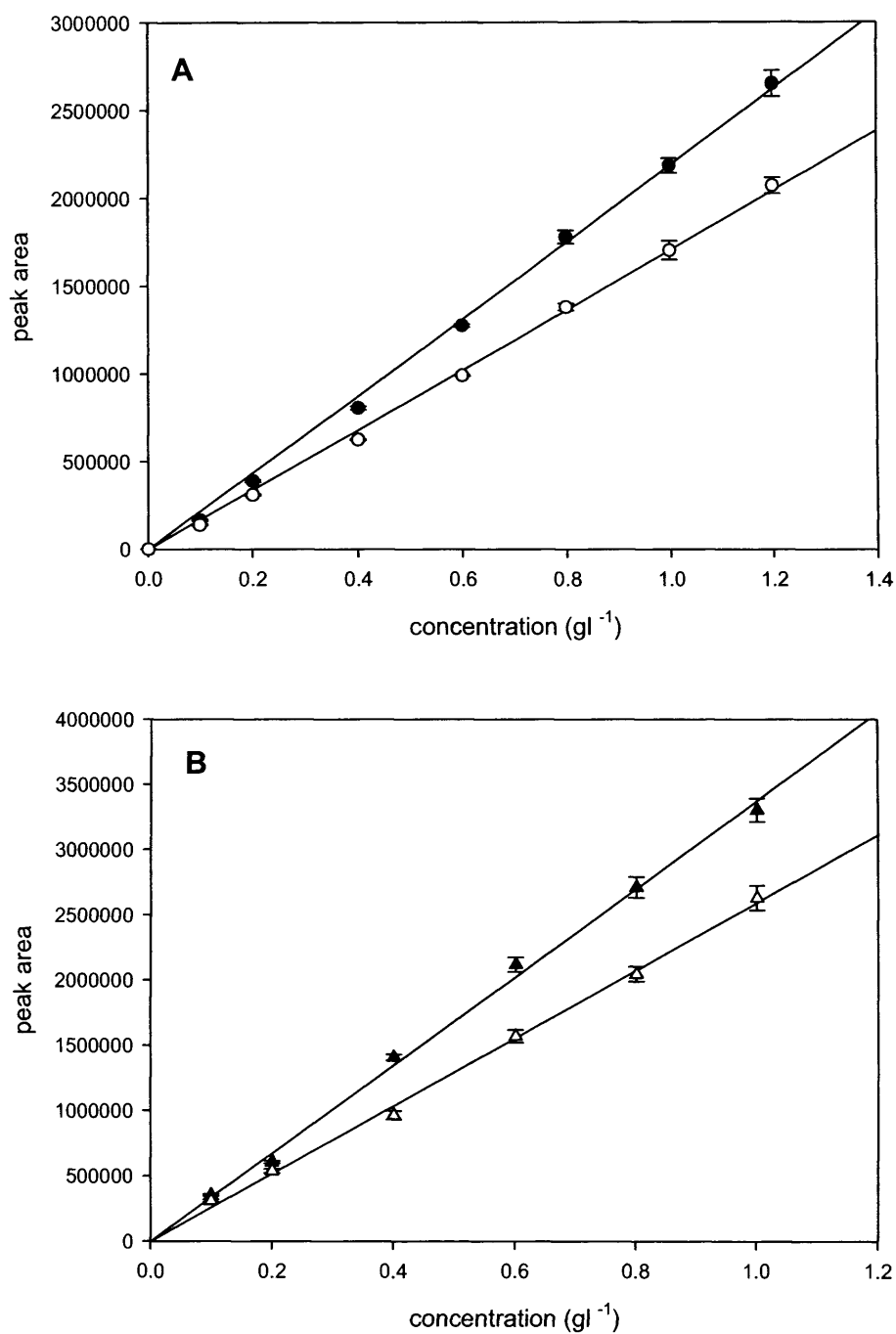
Yoshida, T., Yokoyama, K., Chen, K.C., Sunouchi, T., Taguchi, H. (1977). Oxygen transfer in hydrocarbon fermentation by *Candida rugosa*. *Journal of Fermentation Technology*. 55(1): 76 - 83.

Zambianchi, F., Raimondi, S., Pasta, P., Carrea, G., Gaggero, N., Woodley, J.M. (2004). Comparison of cyclohexanone monooxygenase as an isolated enzyme and whole cell biocatalyst for the enantioselective oxidation of 1,3 - dithiane. *Journal of Molecular Catalysis B: Enzymatic*. 31(165 - 171).

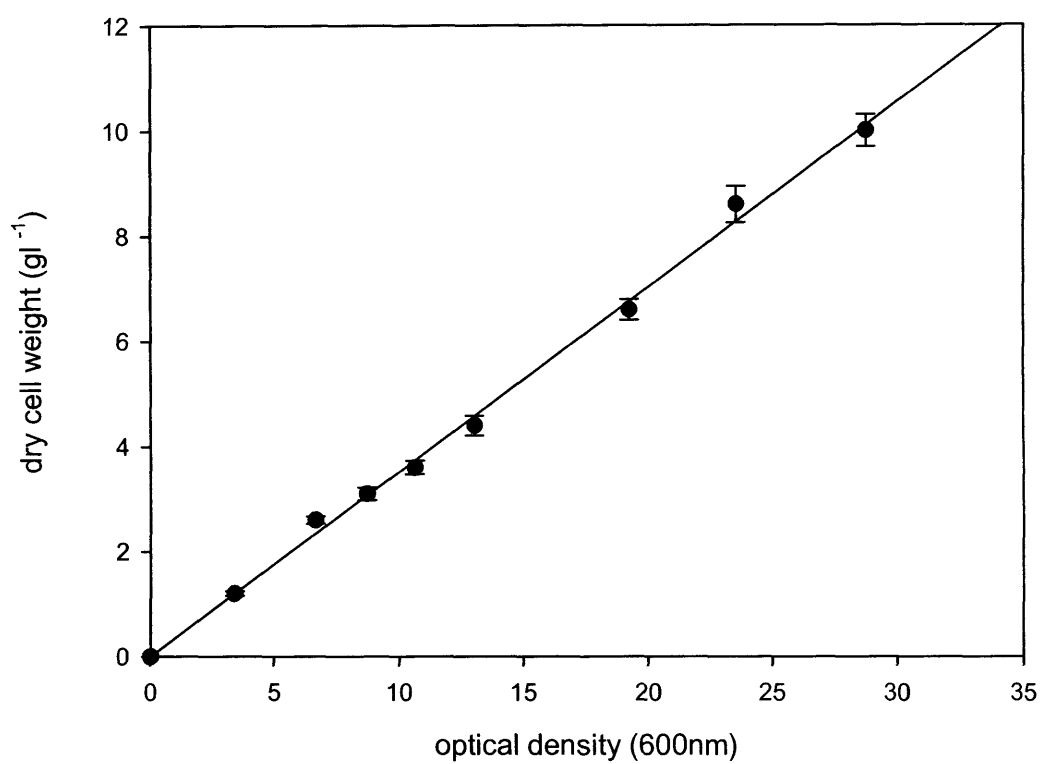
Zambianchi, F., Colonna, S., Pasta, P., Carrea, G., Gaggero, N., Woodley, J.M. (2002). Use of isolated cyclohexanone monooxygenase from recombinant *Escherichia coli* as a biocatalyst for Baeyer - Villiger and sulfide oxidations. *Biotechnology and Bioengineering*. 78(5): 489 - 496.

Zhou, G., Kresta, S. (1998). Correlation of mean drop size and minimum drop size with the turbulence energy dissipation and the flow in an agitated tank. *Chemical Engineering Science*. 53(11): 2063 - 2079.

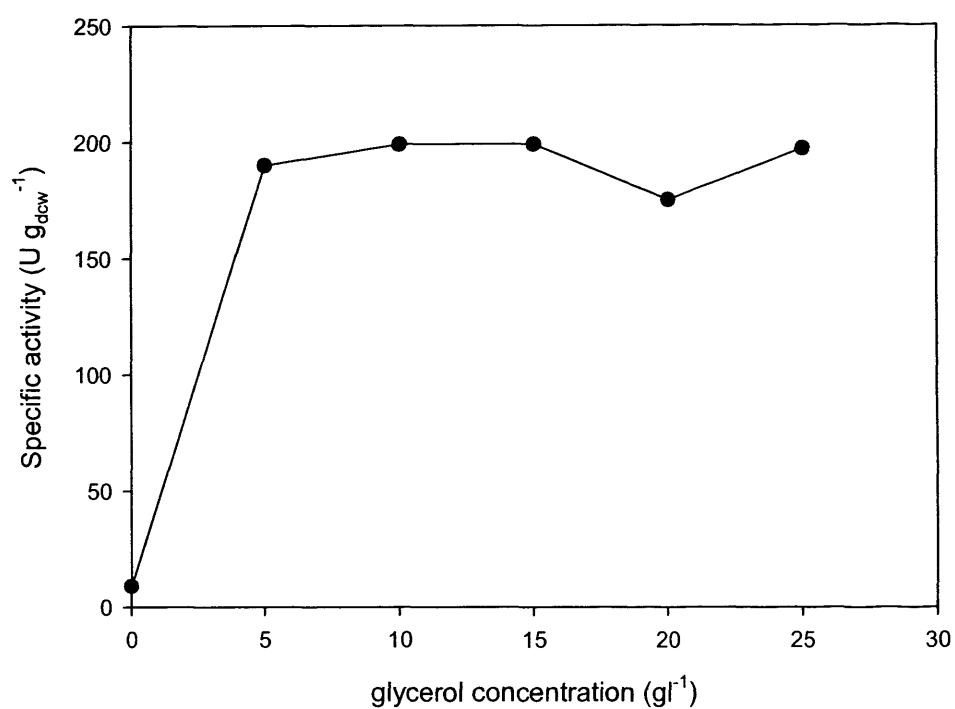
## Appendix 1: Calibration curves



**Figure A.1.** Calibration curves for substrates and products. A – cyclohexanone (●); caprolactone (○); B. Bicycloheptenone (▲); oxabicyclooctenone (△).



**Figure A.2.** Calibration curve correlating the optical density with the dry cell weight.

**Appendix 2: Glycerol concentration**

**Figure A.3.** The effect of glycerol concentration on the specific activity of 1g<sub>dcw</sub> l<sup>-1</sup> of the biocatalyst in a 1 l shake flask.

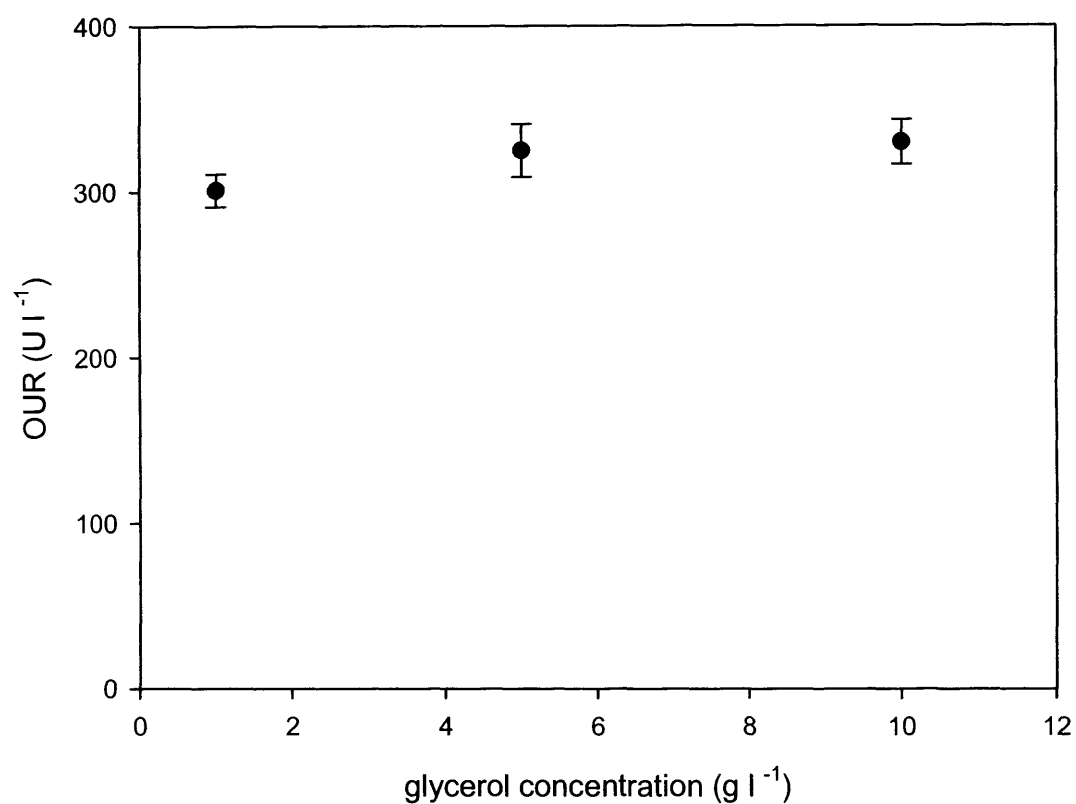


**Figure A.4.** The effect of the glycerol concentration on the OUR of  $1g_{dcw} l^{-1}$  of the biocatalyst in a 2l fermenter. Experiments were carried out in triplicate – error bars represent the standard deviation of the mean.

### Appendix 3. Eng.D. requirements: business

The purpose of process design is to minimise any constraints that limit the productivity and hence the cost of a process. Mathys *et al.* (1999) did an economic evaluation of a fed-batch two-liquid phase fermentation process for the oxidation n-octane to 1-octanol by *Pseudomonas*. The key factors that influenced the cost of the product were the activity of the biocatalyst and the final product concentration.

The activity of the biocatalyst influenced the variable production costs: 52 % of the total production costs were for raw materials such as nutrients, process water, and packaging. These costs, per kilogram of product, and in particular the media costs, decreased if the specific activity increased.

The final product concentration influenced both the utility and the capital costs. For most biotechnology processes downstream processing (DSP) costs are higher than the upstream processing costs. For the two-liquid phase process the utility and capital costs of the USP were higher than those of the downstream processing DSP, because of the costs associated with using the second liquid phase. Waste – water treatment made up 68 % of the DSP utility costs. All these costs can be reduced if the final product concentration is increased.

The volumetric activity of a whole-cell oxygenase bioconversion is determined by the biomass concentration and the specific activity. The results in this thesis have shown that the oxygen transfer rate can determine the maximum volumetric activity. Therefore, if the maximum oxygen transfer rate is increased a biocatalyst with a higher specific activity can be used and therefore the media costs per kg of product will decrease.

## **Appendix 4 Eng.D elements: validation**

The purpose of validation is to expose non-conformance to design and deficiencies in operation of a process. Manufacturers must provide documented evidence that all critical and product impacting processes function reliably and comply with applicable regulations and guidelines.

The validation master plan deals with quality assurance, manufacturing, engineering, facility expansion and process scale-up during the life of the process. It should include a comprehensive description of the entire project including: a description of the layout of the facilities, utilities and equipment and their function.

A prerequisite of validation planning is that the process is well defined and will be operated without major modifications: the objectives of the process must be preset and the limits must be predefined. However, the validation master plan should be written during the point in process design that it is often incomplete or ill-defined. Process validation may be done at small scale and but has to be repeated at large scale after all support and process equipment and facilities have been installed and validated.

To facilitate the validation of whole – cell oxygenase processes the effect of scale-up on hydrodynamic and transport processes should be considered. The design of these processes requires an understanding of the kinetics, the biocatalyst concentration, the oxygen transfer rate, and if a second liquid phase is used, the substrate and product transfer rates. The results obtained at production scale might differ from those obtained at laboratory scale if the hydrodynamics and transport processes are different. This could mean that the pre-defined limits specified in the validation master plan are not met.

Problem that could arise upon scale-up because of the existence of oxygen concentration gradients include:



- If the DOT was below zero in some parts of the fermenter the volumetric and specific activity could be lower than expected.
- If the activity was reduced, and the substrate was fed to the aqueous phase it could begin to accumulate to toxic concentrations.
- The stability of the biocatalyst could decrease if metabolites produced during mixed-acid fermentation accumulated.
- A significant change in the final product concentration or the accumulation of the substrate could impact on downstream processing.